

**PLATELET-DERIVED GROWTH FACTOR RECEPTOR ALPHA OVEREXPRESSION
COOPERATES WITH INK4A/ARF LOSS TO PROMOTE GLIOMAGENESIS—ROLES
OF SHP-2 AND PI3K PATHWAYS**

by

Kun-Wei Liu

B.S., National Tsing Hua University, Taiwan, 2004

Submitted to the Graduate Faculty of
the School of Medicine in partial fulfillment
of the requirements for the degree of
Doctor of Philosophy

University of Pittsburgh

2011

UNIVERSITY OF PITTSBURGH
SCHOOL OF MEDICINE

This dissertation was presented

by

Kun-Wei Liu

It was defended on

April 27, 2011

and approved by

Committee Chair: Monga, Satdarshan P.S. (Paul), MD
Associate Professor, Department of Pathology

Bowser, Robert, PhD
Associate Professor, Department of Pathology

Li, Luyuan, PhD
Associate Professor, Department of Pathology

Sobol, Robert W., PhD
Associate Professor, Department of Pharmacology and Chemical Biology

Dissertation Advisor: Cheng, Shi-Yuan, PhD
Associate Professor, Department of Pathology

Copy Right © by Kun-Wei Liu

2011

**PLATELET-DERIVED GROWTH FACTOR RECEPTOR ALPHA OVEREXPRESSION
COOPERATES WITH INK4A/ARF LOSS TO PROMOTE GLIOMAGENESIS—ROLES
OF SHP-2 AND PI3K PATHWAYS**

Kun-Wei Liu, B.S.

University of Pittsburgh, 2011

BACKGROUND: Human gliomas account for the most common and malignant tumors in the central nervous system (CNS). Despite optimal treatments, survival of patients with high-grade glioblastoma multiforme (GBM) remains poor. Recent coordinated genomic analyses of a large cohort of clinical GBM specimens identified frequent co-alterations of genes in three core pathways—the P53, retinoblastoma (RB), and receptor tyrosine kinase (RTK) pathways that are crucial in gliomagenesis. Further multi-institutional efforts have sub-classified GBMs into four clinical relevant subtypes based on their signature genetic lesions. Among them, *PDGFRA* overexpression is concomitant with a loss of *CDKN2A* locus (encoding P16INK4A and P14ARF) in a large number of tumors within one subtype of GBMs. To better understand and design therapeutic strategies against gliomas driven by abnormal platelet-derived growth factor (PDGF) signaling, functional studies using human or mouse models are needed.

MAJOR FINDINGS: In order to establish a model that allows us to assess contributions of different signaling pathways to PDGFR α -induced glioma formation, we generated *Ink4a/Arf-*

deficient primary mouse astrocytes (referred to as mAst hereafter) and human glioma cells that overexpress PDGFR α and/or PDGF-A. We found that activation of PDGFR α confers tumorigenicity to *Ink4a/Arf*-deficient mAst and human glioma cells in the brain. Restoration of p16INK4a but not p19ARF by retroviral transduction suppresses PDGFR α -promoted glioma formation. Mechanistically, abrogation of signaling modules in PDGFR α that lost capacity to bind to SH-2-containing phosphotyrosine phosphatase SHP-2 or Phosphoinositol 3'-Kinase (PI3K) significantly diminished PDGFR α -promoted tumorigenesis. Furthermore, inhibition of SHP-2 by shRNAs or pharmacological inhibitors disrupted the interaction of PI3K with PDGFR α , suppressed downstream AKT/mTOR activation, and impaired tumorigenesis of *Ink4a/Arf*-null cells, whereas expression of an activated PI3K mutant rescued the effect of SHP-2 inhibition on tumorigenicity. In clinical glioblastoma specimens, PDGFR α and PDGF-A are co-expressed and such co-expression is linked with activation of SHP-2/AKT/mTOR-signaling. Our data thus suggest that in glioblastomas with *Ink4a/Arf* deficiency, overexpressed PDGFR α promotes tumorigenesis through the PI3K/AKT/mTOR-mediated pathway regulated by SHP-2 activity.

SIGNIFICANCE: We expect these findings will improve our understanding of the formation of the gliomas with *PDGFRA* and *INK4A/ARF* aberrations. There were studies that predicted SHP-2/*PTPN11* as one of the linker genes in clinical GBMs that interact with multiple commonly altered genes. Our results functionally validate this hypothesis and identify SHP-2 as a converge point of several signaling pathways such as PDGFR, EGFR, PI3K, and mTOR that are frequently deregulated in GBMs. It thus represents a promising target for treatments against this fatal disease.

TABLE OF CONTENTS

PREFACE.....	xxi
1.0 INTRODUCTION.....	1
1.1 MALIGNANT GLIOMAS	1
1.1.1 Classical Subtype.....	4
1.1.2 Mesenchymal Subtype	4
1.1.3 Proneural Subtype.....	5
1.1.4 Neural Subtype	5
1.1.5 <i>IDH1</i> Mutations.....	5
1.1.6 Current Treatments and Future Prospects	6
1.2 THE <i>CDKN2A</i> LOCUS IN MALIGNANT GLIOMAS.....	7
1.2.1 P16INK4A.....	7
1.2.2 ARF.....	8
1.2.3 INK4A/ARF in cellular senescence and aging.....	10
1.2.4 INK4A/ARF in malignant gliomas and other cancers.....	11
1.3 PLATELET-DERIVED GROWTH FACTOR (PDGF) SIGNALING.....	13
1.3.1 Structures of PDGFs and PDGFRs.....	13
1.3.2 Activation and Downstream Signaling of PDGFRs	15
1.3.2.1 PI3K.....	17
1.3.2.2 PLC- γ	18
1.3.2.3 SFK.....	18

1.3.2.4 SHP-2.....	18
1.3.2.5 Crk.....	19
1.3.3 PDGFR Mutation Studies	19
1.4 PDGF SIGNALING IN NORMAL CNS DEVELOPMENT AND REPAIR	20
1.4.1 PDGF-A in Oligodendrocyte Development.....	20
1.4.2 PDGF-C and -D in CNS Development	23
1.5 PDGF SIGNALING IN HUMAN GLIOMAS	24
1.5.1 Pre-Cancer-Genomic Studies	24
1.5.2 Cancer Genomics Studies.....	25
1.5.3 Constitutively Active <i>PDGFRA</i> mutations in Gliomas	27
1.5.4 PDGF-C and -D in Human Gliomas.....	28
1.5.5 Animal Models of PDGF-induced Gliomagenesis.....	29
1.5.5.1 Transgenic Mice.....	29
1.5.5.2 Virus-induced GEMs.....	31
1.5.5.3 Other Model Systems	33
1.5.5.4 PDGF Downstream Signaling and Gliomagenesis Revealed by Animal Models	34
1.6 PDGF SIGNALING IN OTHER BRAIN TUMORS.....	35
1.6.1 Pediatric Gliomas.....	35
1.6.2 CNS Primitive Neuroectodermal Tumors.....	36
1.6.3 Ependymal Tumors.....	37
1.6.4 Meningeal Tumors.....	37
1.7 PDGF-TARGETED THERAPIES.....	38
1.7.1 Imatinib mesylate.....	39

1.7.2 Sunitinib malate.....	42
1.7.3 Cediranib maleate	43
1.7.4 Vatalanib	44
1.7.5 Sorafenib	44
1.7.6 Pazopanib hydrochloride.....	45
1.7.7 Tandutinib	45
1.7.8 Other PDGF-targeted Agents	45
1.7.9 Lessons Learned From Clinical Trials.....	46
1.7.10 Future Directions.....	48
2.0 PDGFRA OVEREXPRESSION COOPERATES WITH P16INK4A LOSS TO PROMOTE GLIOMA FORMATION FROM MOUSE ASTROCYTES OR HUMAN GLIOMA CELLS	50
2.1 INTRODUCTION AND RATIONALE	50
2.2 MATERIALS AND METHODS	52
2.2.1 Cell Lines and Reagents	52
2.2.2 Retroviral and Lentiviral Constructs and Infections	53
2.2.3 Reverse Transcriptase Polymerase Chain Reaction (RT-PCR).....	54
2.2.4 Mouse Glioma Transplantation/Xenograft.....	55
2.2.5 Immunohistochemistry	56
2.2.6 Immunoblotting.....	56
2.2.7 Soft Agar Colony Formation Assay	57
2.2.8 Cell Proliferation Assay.....	57
2.2.9 Cell Viability Assay	58

2.2.10 Statistical Analyses.....	58
2.3 RESULTS.....	59
2.3.1 <i>PDGFRA</i> and <i>Ink4a/Arf</i> aberrations in mouse astrocytes in vitro	59
2.3.2 <i>PDGFRA</i> and <i>Ink4a/Arf</i> aberrations in transplanted mouse astrocytes in vivo.....	61
2.3.3 Mouse astrocytes with <i>PDGFRA</i> and <i>Ink4a/Arf</i> aberrations express markers of neural progenitor cells	65
2.3.4 <i>PDGFRA</i> and <i>Ink4a/Arf</i> aberrations in human glioma cells in vitro	66
2.3.5 Overexpression of PDGF-A conferred tumorigenicity to <i>Ink4a/Arf</i> -deficient but not -wildtype human glioma cells.....	69
2.3.6 p16 ^{INK4a} but not p19 ^{ARF} attenuates PDGFR α -induced tumorigenesis of <i>Ink4a/Arf</i> -deficient mouse astrocytes and human glioma cells.....	71
2.4 SUMMARY AND CONCLUSION.....	76
3.0 PDGFRA-INDUCED GLIOMAGENESIS DEPENDS ON DOWNSTREAM PI3K PATHWAY THAT IS REGULATED BY SHP-2/<i>PTPN11</i> ACTIVITY	77
3.1 INTRODUCTION AND RATIONALE	77
3.2 MATERIALS AND METHODS	78
3.2.1 Cell Lines and Reagents	78
3.2.2 Retroviral and Lentiviral Constructs and Infections	79
3.2.3 Immunoprecipitation and Immunoblotting.....	80
3.2.4 RNA Interference	81
3.2.5 Other Experiments.....	81
3.2.6 Statistical Analyses.....	81
3.3 RESULTS.....	82

3.3.1	Generation of Ink4a/Arf ^{-/-} mouse astrocytes overexpressing various PDGFR α mutants that are not able to activate specific downstream pathways.....	82
3.3.2	Disruption of SHP-2 and PI3K pathways downstream to PDGFR α suppresses tumor growth of Ink4a/Arf ^{-/-} mouse astrocytes	83
3.3.3	Pharmacological inhibition of SHP-2 or PI3K abrogates PDGF-promoted tumorigenesis of Ink4a/Arf ^{-/-} mouse astrocytes or human glioma cells	87
3.3.4	SHP-2 ablation disrupts PI3K/AKT activation by interfering with PI3K association with PDGFR α	91
3.3.5	SHP-2 ablation attenuates the enhanced anchorage-independent growth of PDGFR α -overexpressing cells which can be rescued by constitutively active PI3K signaling..	94
3.3.6	SHP-2 ablation disrupts mTORC1/S6K activation and mTOR inhibitor rapamycin treatment suppresses growth of PDGFR α - or EGFRvIII-overexpressing cells.....	96
3.4	SUMMARY AND CONCLUSION.....	100
4.0	PDGFRA/PDGF-A EXPRESSION IN CLINICAL GLIOMA TISSUES IS CONCOMITANT WITH ACTIVATION OF SHP-2 AND PI3K/AKT/MTOR SIGNALING PATHWAYS.....	102
4.1	INTRODUCTION AND RATIONALE	102
4.2	MATERIALS AND METHODS	103
4.2.1	Antibodies	103
4.2.2	Histology and IHC of Clinical Human Glioma Tissues	103
4.2.3	Immunoblotting.....	104
4.3	RESULTS	105

4.3.1 Analysis of PDGFR α /PDGF-A, SHP-2, and PI3K/AKT/mTOR pathway activation status by immunohistochemistry on paraffin-embedded human glioma tissues.	105
4.3.2 Analysis of PDGFR α /PDGF-A, SHP-2, and PI3K/AKT/mTOR pathway activation status by immunoblotting using snap-frozen human glioma tissues.	108
4.4 SUMMARY AND CONCLUSION.....	110
5.0 GENERATION OF GENETICALLY MODIFIED MICE USING THE SLEEPING BEAUTY TRANSPOSON SYSTEM—A POTENTIAL PLATFORM FOR PRE-CLINICAL TESTING OF PDGF/SHP-2 TARGETED THERAPIES.....	111
5.1 INTRODUCTION AND RATIONALE	111
5.1.1 Animal Model Systems For Malignant Gliomas	111
5.1.2 Sleeping Beauty Awakens!	112
5.2 MATERIALS AND METHODS	113
5.2.1 Animal Care and Mating	113
5.2.2 SB DNA Plasmid Vectors.....	114
5.2.3 Intracranial SB DNA Injection Using Polyethylenimine (PEI) In-Vivo Transfection	114
5.2.4 Bioluminescence Detection and Histology.....	115
5.3 RESULTS	117
5.3.1 Monitoring real-time tumor growth by luciferase bioluminescence	117
5.3.2 Histological analyses of SB tumors reveal characteristics corresponding to those observed in human gliomas.....	121
5.4 SUMMARY AND CONCLUSION.....	125
6.0 DISCUSSION AND FUTURE DIRECTIONS	126

6.1 DISCUSSION	126
6.2 FUTURE DIRECTIONS	133
7.0 BIBLIOGRAPHY	137

LIST OF TABLES

Table 1. Summary of Animal Models of PDGF-induced Spontaneous Brain Tumor Formation	32
Table 2. Summary of PDGF-targeted Therapies.....	41
Table 3. Human Glioma Cell Lines Used in This Study.....	67
Table 4. Summary of Immunohistochemical Analyses on Clinical Human Glioma Tissues	107
Table 5. Histological and immunohistochemical analyses of SB-induced gliomas.....	124

LIST OF FIGURES

Figure 1. Progression and genetic alterations in human malignant gliomas.	3
Figure 2. The CDKN2A locus.....	9
Figure 3. The Structures of PDGFRs and PDGFs.....	14
Figure 4. Specific Binding between PDGF receptors and ligands.....	15
Figure 5. The PDGFR α /PDGF-A signaling.....	17
Figure 6. The PDGFR α and/or PDGF-A overexpression in <i>Ink4a/Arf</i> ^{-/-} mAst.....	60
Figure 7. <i>In vitro</i> characterization of <i>Ink4a/Arf</i> ^{-/-} mouse astrocytes overexpressing PDGF-R α and/or PDGF-A.....	60
Figure 8. <i>In vivo</i> growth of <i>Ink4a/Arf</i> ^{-/-} mouse astrocytes overexpressing PDGFR α and/or PDGF-A.....	61
Figure 9. Orthotopic growth in the mouse brain of <i>Ink4a/Arf</i> ^{-/-} mouse astrocytes overexpressing PDGFR α and/or PDGF-A.....	62
Figure 10. <i>In vivo</i> proliferation and apoptosis of <i>Ink4a/Arf</i> ^{-/-} mouse astrocytes overexpressing PDGFR α and/or PDGF-A.....	63
Figure 11. <i>Ink4a/Arf</i> ^{-/-} mouse astrocytes overexpressing PDGFR α and PDGF-A retained high expression of both the receptor and the ligand <i>in vivo</i>	64
Figure 12. <i>Ink4a/Arf</i> ^{-/-} mouse astrocytes overexpressing PDGFR α and PDGF-A retained high expression of both the receptor and the ligand <i>in vivo</i>	66
Figure 13. PDGF-A overexpression in <i>INK4A/ARF</i> -deficient and <i>INK4A/ARF</i> -wt human glioma cells.	68

Figure 14. PDGF-A overexpression enhances anchorage-independent growth of <i>INK4A/ARF</i> -deficient but not <i>INK4A/ARF</i> -wt human glioma cells <i>in vitro</i>	69
Figure 15. Exogenous PDGF-A expression enhances growth of <i>Ink4a/Arf</i> -null LN444 but not <i>Ink4a/Arf</i> -WT LN-Z308 tumors in the flanks of mice.....	70
Figure 16. Exogenous PDGF-A expression enhances growth of <i>Ink4a/Arf</i> -null LN444 but not <i>Ink4a/Arf</i> -WT LN-Z308 tumors in the brain of mice.	71
Figure 17. Re-expression of p16INK4a but not p19ARF suppresses the anchorage-independent growth of mAst expressing PDGFR α /-A <i>in vitro</i>	72
Figure 18. Re-expression of p16INK4a suppresses the <i>in vivo</i> tumor growth of mAst expressing PDGFR α /-A.....	72
Figure 19. P16INK4A knockdown in <i>INK4A/ARF</i> -wt human glioma cell LN319 potentiates PDGF-A- promoted anchorage-dependent growth <i>in vitro</i>	73
Figure 20. P16INK4A knockdown in <i>INK4A/ARF</i> -wt human glioma cell LN319 potentiates PDGF-A- promoted anchorage-dependent growth <i>in vitro</i>	74
Figure 21. Cisplatin induces p53 expression and cell death in <i>Ink4a/Arf</i> ^{-/-} PDGFR α -expressing mAst in the presence of p19ARF.....	75
Figure 22. Impacts of PDGFR α mutations on downstream signaling of PDGFR α	83
Figure 23. Impacts of PDGFR α mutations on downstream signaling of PDGFR α and anchorage-independent growth in soft agar of <i>Ink4a/Arf</i> ^{-/-} mAst.....	84
Figure 24. Impacts of individual mutations of PDGFR α in mAst on brain tumorigenesis.	85
Figure 25. Impacts of individual mutations of PDGFR α in mAst on <i>in vivo</i> proliferation in the mouse brain.....	86

Figure 26. Impacts of individual mutations of PDGFRα in mAst on <i>in vivo</i> apoptosis in the mouse brain.	86
Figure 27. Inhibition of PI3K or SHP-2 activity suppresses PDGFRα-stimulated signaling and cell transformation in <i>Ink4a/Arf</i>^{-/-} mAst.	88
Figure 28. Inhibition of PI3K or SHP-2 activities suppresses PDGFRα-stimulated signaling and cell transformation in LN444 cells.	89
Figure 29. Effects of SHP-2 inhibitors on <i>Ink4a/Arf</i>^{-/-} mAst and LN444 cell viability.....	90
Figure 30. SHP-2 recruits PI3K to activate AKT pathway and is important for PDGF-A-stimulated growth.	91
Figure 31. The impacts of SHP-2 knockdown in NIH3T3, <i>Ink4a/Arf</i>^{-/-} EGFRvIII mAst, LN444/EGFRvIII, and U87MG/EGFRvIII cells.....	93
Figure 32. SHP-2 knockdown suppresses PDGF-A-stimulated soft agar growth of <i>Ink4a/Arf</i>^{-/-} mAst overexpressing PDGFRα.	94
Figure 33. Constitutively activated PI3K rescued the inhibitory effect of SHP-2 inhibition on blocking PDGFRα-mediated cell transformation.	95
Figure 34. SHP-2 is required for activation of mTOR/S6K pathway stimulated by PDGF-A in PDGFRα-overexpressing mAst.....	96
Figure 35. Rapamycin inhibits PDGFRα-promoted cell transformation.....	97
Figure 36. Rapamycin inhibits EGFRvIII-promoted cell transformation.....	98
Figure 37. Rapamycin treatment does not lead to feedback AKT activation in PDGF-A-stimulated cells.	99
Figure 38. SHP-2-regulated PI3K/AKT/mTOR pathway in the PDGFRα/PDGF-A-mediated gliomagenesis.....	101

Figure 39. PDGFRα and PDGF-A are co-expressed in clinical glioma specimens with activated SHP-2 and PI3K/AKT/mTOR pathways.	106
Figure 40. Representative images of PDGF-A IHC staining showing grading of clinical glioma tissues according to PDGF-A positivity.....	108
Figure 41. PDGFRα and PDGF-A are co-expressed in clinical glioma specimens with activated SHP-2 and PI3K/AKT/mTOR pathways.	109
Figure 42. Kaplan-Meier survival curve for mice injected with SB transposase and NRAS/SV40-LgT-encoding transposons.....	118
Figure 43. Luciferase imaging for mice injected with SB transposase and NRAS/SV40-LgT-encoding transposons.....	119
Figure 44. SB-induced spontaneous gliomas exhibit characteristics of human gliomas..	123
Figure 45. SB-induced spontaneous gliomas showed high positivity for Ki67 and CD31 staining.	124

LIST OF ABBREVIATIONS

2-HG	2-Hydroxyglutarate
bFGF	Basic Fibroblast Growth Factor
BBB	Blood-Brain Barrier
CHI3L1	Chitinase-3-like protein 1
CSC	Cancer Stem Cell
CNS	Central Nervous System
CDK	Cyclin-Dependent Kinases
EGFR	Epidermal Growth Factor Receptor
EGL	External Germinal Layer
ECM	Extracellular Matrix
ERBB2	Erythroblastic Leukemia Viral Oncogene 2
ERK	Extracellular Signal-Regulated Kinase
GEM	Genetically Engineered Mouse
GFAP	Glial Fibrillary Acidic Protein
GBM	Glioblastoma Multiforme
GFP	Green Fluorescent Protein
GAP	GTPase Activating Protein
HSC	Hematopoietic Stem Cell
IB	Immunoblotting
IHC	Immunohistochemistry
IP	Immunoprecipitation
I.P.	Intraperitoneal
IDH1	Isocitrate Dehydrogenase 1
LOH	Loss of Heterozygosity
mTOR	Mammalian Target of Rapamycin
MAPK	Mitogen-Activated Protein Kinases
mAst	Mouse Astrocyte
NFκB	Nuclear Factor Kappa-light-chain-enhancer of Activated B cells
NSC	Neural Stem Cell
MGMT	O6-Methylguanine-DNA Methyltransferase
NF1	Neurofibromatosis 1
OPC	Oligodendrocyte Progenitor Cell
O-2A	Oligodendrocyte-type-2 Astrocyte
OS	Overall Survival
PTEN	Phosphatase and Tensin Homolog
PI3K	Phosphoinositol 3'-Kinase

PLC-γ	Phospholipase C-γ
PDGFR	Platelet-Derived Growth Factor Receptor
PNET	Primitive Neuroectodermal Tumors
PFS	Progression-Free Survival
RTK	Receptor Tyrosine Kinase
RB	Retinoblastoma
SHP-2	SH2-containing Phosphotyrosine Phosphatase
STAT	Signal Transducers and Activators of Transcription
Shh	Sonic hedgehog
SFK	Src Family of Tyrosine Kinases
SH2	Src Homology 2
S.C.	Subcutaneous
SVZ	Subventricular Zone
TMZ	Temozolomide
TNF	Tumor Necrosis Factor
VEGFR	Vascular Endothelial Growth Factor Receptor
WT	Wild Type
α-KG	α-Ketoglutarate

ACKNOWLEDGEMENT

Projects in this dissertation were performed in collaboration with Dr. Robert Bachoo at University of Texas Southwestern Medical Center (for isolation of primary Ink4a/Arf^{-/-} mouse astrocytes); Dr. Andrius Kazlauskas at Harvard Medical School, Dr. Erin M. Smith and Karen Symes at Boston University (for generation of PDGFR α point mutation constructs); Dr. Ronald L. Hamilton at University of Pittsburgh (for GBM clinical specimens used for immunoblotting); Dr. Motoo Nagane at Kyorin University and Dr. Ryo Nishikawa at Saitama Medical University (for clinical glioma specimens used for immunohistochemistry staining); Dr. John R. Ohlfest at University of Minnesota (for providing *Sleeping Beauty* constructs and protocols); Dr. Okada Hideho and Dr. Mitsugu Fujita (for establishment of *Sleeping Beauty* mouse model), Dr. Haizhong Feng (for generation of human glioma LN444 intracerebral mouse model) and Dr. Bo Hu (for generation of PDGF-A-overexpressing human glioma cells) at the University of Pittsburgh Cancer Institute. We also would like to thank Dr. Carl-Henrik Heldin at Uppsala University in Sweden for PDGFR α and PDGF-A cDNAs, Dr. Russell O. Pieper at University of California San Francisco for pMXI-*gfp* retroviral vector, Dr. Lynda Chin at Dana-Farber Cancer Institute for the cDNA of p16INK4a, Dr. Yi Zheng at Cincinnati Children's Hospital Medical Center for cDNA of p19ARF, and Dr. Tao Cheng at University of Pittsburgh for pMSCV retroviral vectors. This work was supported by grants from the NIH (CA102011, CA130966), American Cancer Society (RSG CSM-107144), a grant with the Pennsylvania Department of Health, and Innovative Research Scholar Awards of the Hillman Foundation to S.-Y. Cheng and B. Hu; NIH (EY012509) to A. Kazlauskas and (CA87375) to K. Symes.

PREFACE

Nearly five years of graduate school have transformed me into a half-scientist from a scientifically naïve student that just got out of college. During this long journey, I have met numerous wonderful mentors and scientists who helped me along the way and learned a lot from them how to become an independent scientist. And now here I am, writing the last part, the most important part of my dissertation. Without you, I would not have had this opportunity to sit here and write at this quiet night right now.

There are so many I want to thank. The most GIGANTIC THANK is of course given to my dissertation advisor, Dr. Shi-Yuan Cheng, who has not only assisted me enormously in trouble-shooting my experiments, but also been generous with his time and wisdom to guide me in a way that continuously invigorated my enthusiasm in science. Thank you for always being there and sharing with me your interesting stories and experiences. An enormous THANK-YOU to all of my dissertation committee members, Drs. Robert Bowser, Luyuan Li, Paul Monga, and Robert Sobol (in alphabetical order). Every one of you has played an important role during my graduate years. I would like to specifically mention Dr. Bowser, whose knowledge on CNS pathology has always provided invaluable insights into the designing of my project; Dr. Li, for his expertise in tumor angiogenesis has guided me through thinking of alternative explanations of my results; Dr. Monga, the committee Chair and also a great mentor, whose knowledge in PDGF signaling and tumor biology/development has constantly stimulated brainstorming of novel ideas for my project; last but not least, Dr. Sobol, who has provided very helpful advices in every step toward the completion of my project and in postdoctoral position searching as well.

Also, thanks to all the current and previous Cheng lab members and colleagues. I can't imagine what it would be like to work in a lab without you. I would like to especially thank Dr. Bo Hu, a great mentor and a lab manager in the lab, who has offered a lot of help in guiding me through the project and taking care of all the lab supply ordering and management. And special thanks to every current and former postdoctoral in the lab, Drs. Haizhong Feng, Irina Abecassis, Jia-Jean Yiin (Jackson), and Michael Jarzynka. All of you have been very helpful to me. Also, I am particularly grateful to my collaborators from around the world (listed in author line and acknowledgement section in my publication in JCI and also in this dissertation). The works in my dissertation would not have been possible without the invaluable resources from all of you. Moreover, I would like to thank all the colleagues working in the Room 2.19 of Hillman Cancer Center Research Pavilion, for accompanying me every minute during my graduate years. Thanks also to all the colleagues working in the FACS core facility and the DLAR animal facility, for offering me with technical advices and helps.

Finally, HUGE thanks to my dear family in Taiwan, my dad Laurence Liu, mom Jennifer Chou, and younger brother James Liu, for always being there caring about every little bit of my life. We have been so far away apart for almost five years (though they came visit me every year), but I still can feel the unreserved love from every one of you. A gigantic THANK-YOU is certainly belong to my dear girl friend, Yangyang Wang, an M.D. from China, who has given me enormous support and unconditional love during both my good times and bad times, and who not only provided novel ideas of what to eat for dinner, but also great suggestions in how to design and perform my animal experiments and surgeries.

Three chapters of this dissertation contain a published manuscript:

Liu, K. -W., Feng, H., Bachoo, R., Kazlauskas, A., Smith, E. M., Symes, K., Hamilton, R. L., Nagane, M., Nishikawa, R., Hu, B., Cheng, S. Y. SHP-2/*PTPN11* mediates gliomagenesis driven by *PDGFRA* and *INK4A/ARF* aberrations in mice and humans. *J Clin Invest.* 2011;121(3):905-917.

1.0 INTRODUCTION

1.1 MALIGNANT GLIOMAS

Malignant tumors in the brain are relatively rare but deadly due to their insidious location and highly invasive capacity rendering them inaccessible to surgery or therapeutic drugs (1, 2). Clinically, these tumors are classified based on the predominant cell type as determined by histological approaches (3). Among them, malignant gliomas that originate from the glial cells in the brain represent the most common and aggressive type of tumor in the CNS (2, 4). Malignant gliomas in adults can be classified, based on histological features, into astrocytomas, oligodendrogliomas, and mixed oligoastrocytomas, and further within each type divided into 4 grades corresponding to their malignancy and genetic alterations (WHO grade I-IV) (Figure 1). Grade I gliomas (pilocytic astrocytomas) were primarily found in childhood and young adults, and can mostly be surgically removed. Grade II gliomas (diffuse astrocytomas or oligodendrogliomas) are diffusely infiltrative and thus complete removal is nearly impossible. These tumors showed minimal nuclear atypia and low cellularity; Grade III gliomas (anaplastic astrocytomas or oligodendrogliomas) display marked anaplasia and tend to progress to Grade IV within a short period of time. These tumors are characterized by high cellularity, marked mitotic activity and nuclear atypia; Grade IV glioblastoma multiforme (GBM) is incurable and characterized by additional features such as robust microvascular proliferation and frequent

necrosis when compared to lower-grade tumors (3). Despite intensive treatments including maximal surgical resection, combined with radiotherapy and concurrent or adjuvant chemotherapies, the median survival of patients with GBMs remains 13-16 months after diagnosis (5). Clinical GBMs are composed of poorly differentiated glial cells with features such as uncontrolled growth, resistance to apoptosis, diffuse infiltration, cellular pleomorphism, nuclear atypia, mitotic abnormalities, microvascular proliferation, and focal necrosis (2, 3). Based on genetic and clinical presentation, GBM has been classified into two subtypes. The primary GBMs, which arise *de novo* with very short or no clinical history, mostly occur in older patients, whereas the secondary GBMs develop from lower-grade gliomas in younger patients (2, 4) (Figure 1). Over the past decade, a plethora of data has accumulated on genetic alterations in human gliomas, including activation of oncogenes and inactivation of tumor suppressor genes (2, 4, 6-8). It appears that in human gliomas, these genetic alterations occur in a pattern corresponding to distinct histological subtypes and different grades of tumors. For example, it is believed that low-grade astrocytomas and oligodendrogliomas may develop from common glial progenitor cells that acquire features of astrocytic tumors in the presence of *TP53* mutations and oligodendrocytic tumors in the presence of *1p/19q* chromosomal loss (Figure 1)(7). Additionally, *PDGFRA/PDGF-A* overexpression and *IDH1* mutations are some of the major genetic alterations found in low-grade gliomas as well as secondary GBMs. When the low-grade tumors progress toward the high-grade secondary GBMs, additional changes such as *CDKN2A/CDKN2B* deletion are acquired (Figure 1). In the primary GBMs, however, a distinct set of genetic changes were observed, such as *EGFR* amplification/mutation, *PTEN* mutations/deletion, and *MDM2* overexpression (Figure 1), suggesting that a different cell of origin of these tumors is responsible for generating primary GBMs (2, 4, 6-8).

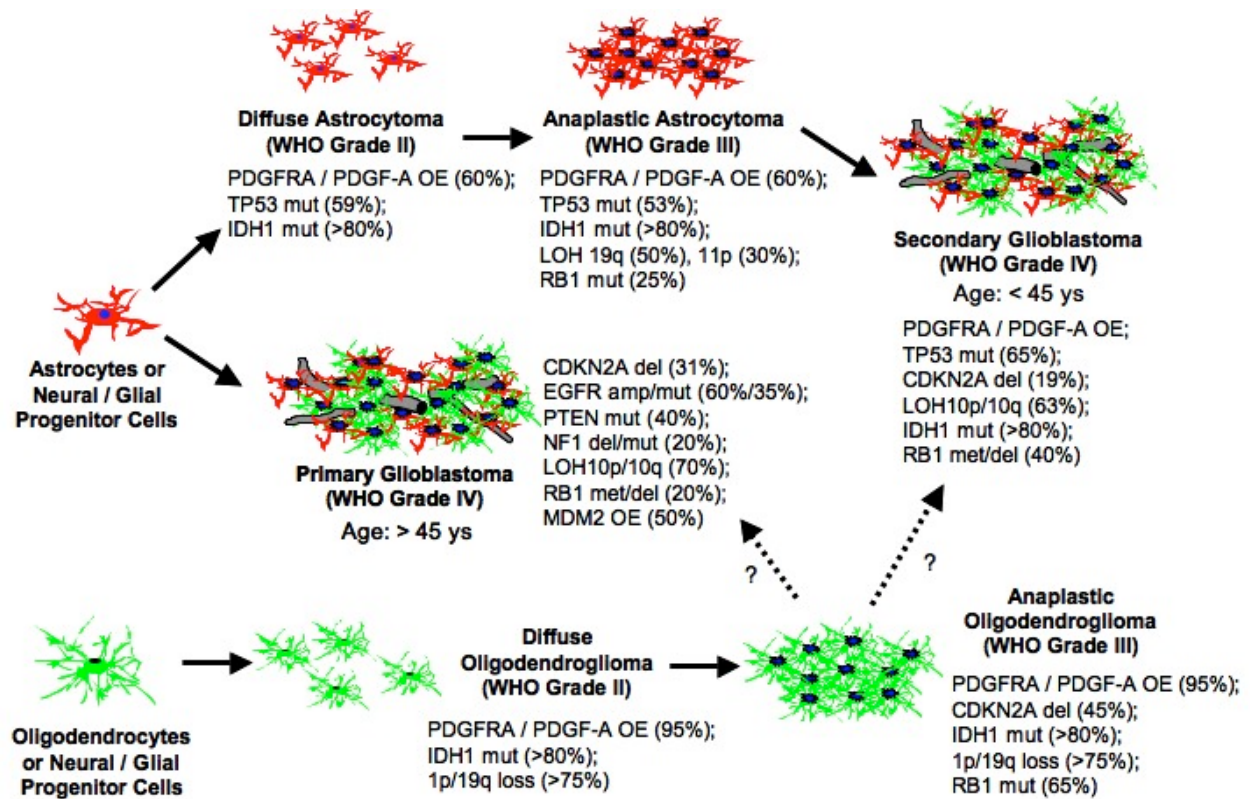


Figure 1. Progression and genetic alterations in human malignant gliomas.

The astrocytomas may originate from astrocytes or progenitor cells that accumulate genetic alterations and become transformed. IDH1 and TP53 mutations were believed to be the very first alterations that occur in these tumors. Oligodendrogliomas can come from the same progenitor cells or mature oligodendrocytes that acquire distinct set of genetic changes. The earliest changes that occur include IDH1 mutations and 1p/19q loss. Representative genetic changes are illustrated in this schematic with the estimated frequency of occurrence within each type of tumors (2, 4, 6-8). OE, overexpression; mut, mutation; del, deletion; met, promoter methylation; amp, amplification.

Recently, coordinated genomic analyses of a large cohort of clinical GBM specimens identified frequent co-alterations of genes in three core pathways—the P53, RB, and RTK (9) pathways that are crucial in gliomagenesis (10). Further analysis classified these GBMs into four clinically relevant subtypes based on gene expression profiles (11): Classical, Mesenchymal, Proneural, and Neural subtypes.

1.1.1 Classical Subtype

Classical subtype of GBMs are characterized by the presence of signature genetic aberrations such as chromosome 7 amplification and chromosome 10 loss (100%), *EGFR* amplification (95%) and mutation (55%), *CDKN2A/CDKN2B* deletion (95%), *PTEN* deletion (100%), as well as predominant expression of neural stem cell markers such as *NES* (encoding Nestin), and Notch and Shh pathways signaling molecules (11).

1.1.2 Mesenchymal Subtype

Mesenchymal subtype of GBMs are characterized by the presence of signature genetic alterations such as *NF1* deletion (38%) and mutation (37%), *PTEN* mutation (32%), and predominant expression of mesenchymal markers such as *CHI3L1*, *MET*, *CD44*, and *MERTK*, and TNF superfamily and NF- κ B pathways signaling molecules (11).

1.1.3 Proneural Subtype

Proneural subtype of GBMs are characterized by the presence of genetic alterations such as *PDGFRA* amplification (35%) and mutation (11%), *TP53* mutation (54%), *IDH1* mutation (30%), *PI3K (PIK3R1/PIK3CA)* mutation (27%), *CDKN2A/CDKN2B* deletion (56%), *EGFR* amplification (17%) and mutation (19%), and predominant expression of oligodendrocyte markers such as *PDGFRA*, *NKX2-2*, and *OLIG2*, and proneural development genes such as *SOX*, *DCV*, *DLL3*, *ASCL1*, and *TCF4*. The Proneural GBMs are the most resistant among all subtypes to standard intensive radio-/chemotherapy (11).

1.1.4 Neural Subtype

Neural subtype of GBMs are characterized by the presence of genetic alterations such as *ERBB2* mutation (16%), *EGFR* amplification (67%), and mutation (26%), *PTEN* deletion (96%) and mutation (21%), *CDKN2A/CDKN2B* deletion (71%), *PI3K (PIK3R1/PIK3CA)* (16%) and *IDH1* mutations (5%), and predominant expression of neuron markers such as *NEFL*, *GABRA1*, *SYT1*, and *SLC12A5*, and genes involved in neuron projection, axon and synaptic transmission (11).

1.1.5 IDH1 Mutations

The newly identified mutation in the *IDH1* gene emerged as the first metabolic gene mutation found in the GBMs (12). *IDH1* mutation was originally identified in a high-throughput

sequencing analysis and was later found to be present in as much as 70% of the grade II/III astrocytomas, oligodendrogliomas and secondary GBMs (13). Moreover, GBM patients with *IDH1* mutations often had significantly better prognosis, and these alterations were frequently found in patients without most of the common genetic lesions, indicating IDH1 mutations as early events during the initiation of glioma development (13). However, the facts that *IDH1* mutations mostly occur in the Arginine 132 (R132) of the IDH1 protein and that there is a lack of LOH associated with *IDH1* mutations indicate that these mutations may result in a gain- rather than loss-of-function of the *IDH1* gene product (13). Indeed, accumulation of a putative onco-metabolite 2-HG was found in the *IDH1*-mutated tumors instead of the WT IDH1 product α -KG (14). In a series of attempts to identify the mechanisms by which 2-HG initiates gliomagenesis, 2-HG was suggested to confer a genome-wide histone and DNA methylation phenotype to a subgroup of gliomas by its inhibitory activity against certain α -KG-dependent dioxygenases such as histone demethylases and 5-methylcytosine (5mC) hydroxylases (15, 16). These studies suggest that IDH1 mutations are responsible for altering a large number of genes that are important for gliomagenesis through its capacity of modulating the epigenetic controls of these genes. However, whether therapies targeting this specific genetic alteration will benefit patients with gliomas that have already undergone significant genetic and epigenetic changes conferred by the putative initiator *IDH1* mutation warrants further investigations.

1.1.6 Current Treatments and Future Prospects

Standard treatment for newly diagnosed malignant gliomas includes maximal surgical resection, followed by radiotherapy, and concomitant or adjuvant chemotherapy with TMZ (4). The

introduction of TMZ into the therapy regimen improves the OS and the PFS of GBM patients (5). However, the presence of DNA repair enzymes such as MGMT in the tumor cells significantly reduces the efficacy of TMZ, and GBMs that recur after these first-line treatments generally are resistant to TMZ or radiotherapy (4). Consequently, treatment options for patients with recurrent gliomas remain limited. Many of the common genetic alterations in gliomas have been identified for years. However, none of them has substantially impacted the current treatment of this deadly disease. Large-scale genomic profiling has brought our understanding of glioma molecular pathogenesis to a new era, and other new findings will keep amassing our knowledge even more. Moreover, cancer genome profiling may enable early detection and prevention of tumor progression, and prediction of prognosis and responses to therapies. However, more challengingly, the current task is to transform these genomic data into better therapeutic strategies and eventually into personalized medicine (17-19).

1.2 THE *CDKN2A* LOCUS IN MALIGNANT GLIOMAS

1.2.1 P16INK4A

Mitogens such as PDGFs trigger cell cycle progression through G1 phase to S phase, a process regulated by several CDKs, whose activities are in turn modulated by CDK inhibitors (CKIs) (20). One of the CKIs, P16INK4A, belongs to the INK4 family, and binds only to CDK4/6/Cyclin D complex, restricting their capacity to phosphorylate RB protein. Phosphorylation of RB is required for release of E2F transcription factor and the subsequent

expression of various DNA synthesis and S phase entry genes (20). P16INK4A is encoded by *CDKN2A* locus in the genome that also encodes an unrelated protein ARF. Expression of *Ink4a* and *Arf* uses different promoters and the first exons (*E1 α* and *E1 β* , respectively) that are spliced to a common second exon *E2* and third exon *E3* (21).

1.2.2 ARF

By using an alternative reading frame (9), the *CDKN2A* locus also encodes a protein, P14ARF (p19ARF in mouse), with an entirely different amino acid sequence from that of P16INK4A (22, 23). The primary tumor suppressor activity of ARF protein has been shown to be its ability to antagonize the E3 ubiquitin ligase activity of MDM2, which inhibits p53 by mediating proteasomal degradation of p53, despite the presence of putative p53-independent tumor suppressor functions of ARF (24). P14ARF thus can stabilize p53 by sequestering MDM2 in the nucleolus, preventing its ubiquitin activity on the p53 (25). In normal tissues, expression of ARF is nearly undetectable, whereas under oncogenic stress such as Myc and Ras expression, ARF level is elevated (26). This regulation of ARF level is to ensure that normal cells have low level of p53 and when exposed to oncogenic damages, they undergo growth arrest or apoptosis to retain homeostasis of the tissue.

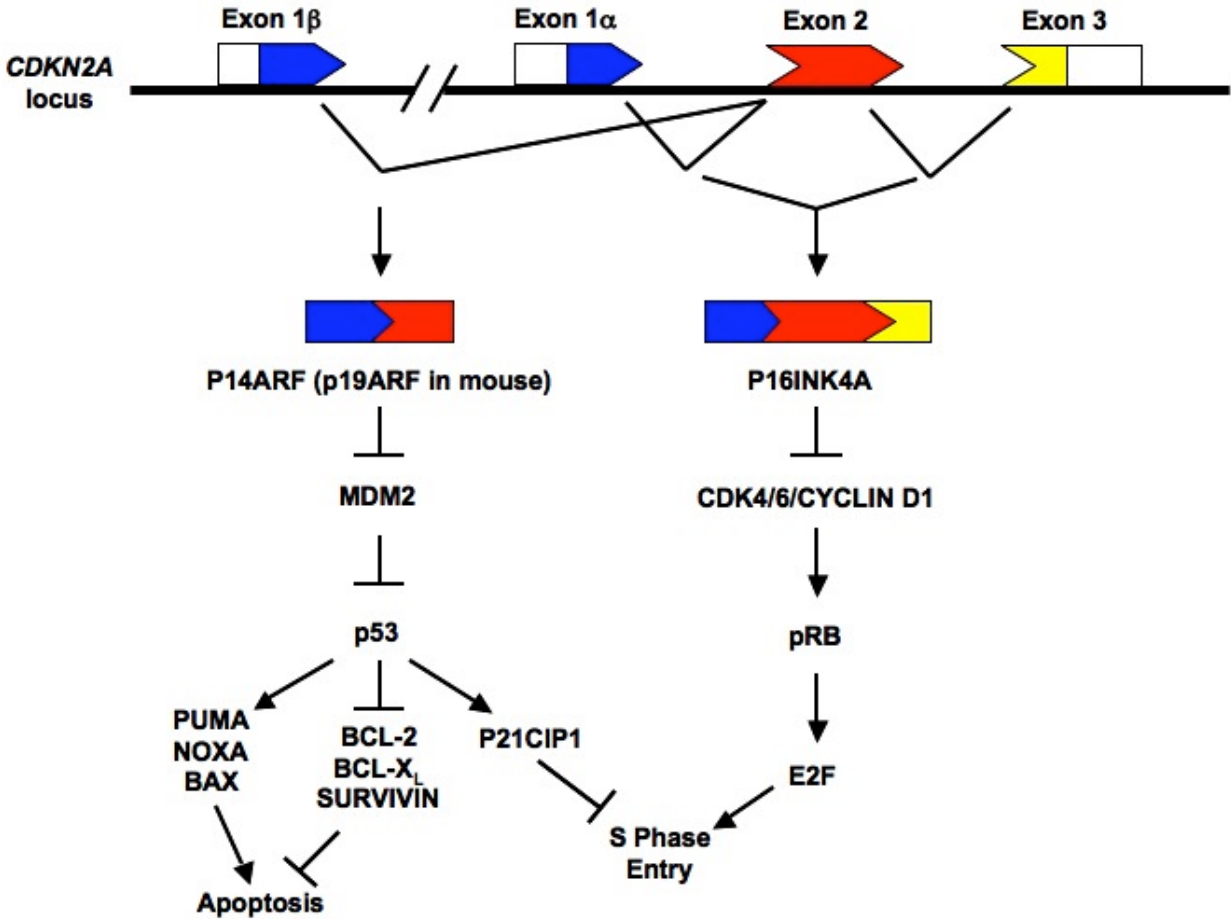


Figure 2. The CDKN2A locus.

The CDKN2A locus on human chromosome 9p21 encodes two tumor suppressors with distinct amino acid sequences and biological functions by using alternative first exons spliced to common exons 2 and 3. P16INK4A is involved in pRB pathway in which it suppresses S phase entry in the cell cycle and induces senescence of cells. P14ARF (p19ARF is the mouse homolog) is involved in p53 pathway in which it promotes apoptosis and senescence by stabilizing the p53 protein.

1.2.3 INK4A/ARF in cellular senescence and aging

The first indication that *in-vitro* cultured cells undergo cellular senescence after serial passages came from the observations in normal human fibroblasts by Hayflick and colleagues in 1961 (27). They proposed that factors within these cells dictate the cell senescence and these factors may be lost in cancer cells to confer immortality to them. The so-called “Hayflick factors” were later found to be telomere loss, accumulation of DNA damages, and derepression of the *INK4A/ARF* locus (27). Several studies have shown that p16INK4a and ARF mRNA and protein levels significantly increased with aging in rodents (28, 29) and human tissues (9, 30). The levels of the transcription regulators of p16INK4a, Polycomb group (PcG) member Bmi1 (9) and transcription factor Ets1 (29), have been associated with the increased p16INK4a level in aging. The age-related increase of reactive oxygen species (ROS) is also another contributor to the increase of p16INK4a during aging (27). P16INK4a has also been implicated in stem/progenitor cell aging. Tissue stem/progenitor cells in the fetus are important for generation of tissues and organs, and in the adults they are responsible for tissue maintenance and regeneration (31). The tissue stem cell is a double-edged sword in that the aging of stem cells may have detrimental effects on tissue repairs, while the uncontrolled proliferation of them may also contribute to hyperplasias (31). Indeed, an increase in p16INK4a level was shown to result in decreased forebrain NSC number in the SVZ (32, 33) and in the cerebellum (33). Additionally, an increase in the p16INK4a repressor Bmi1 has also been linked to increased self-renewal of HSCs (34), and a decrease in p16INK4a activity to enhanced repopulating capacity of HSCs in serial bone marrow transplantation experiments (35). These results indicate that one of the mechanisms by which p16INK4a promotes aging may be its ability to limit stem cell self-renewal/proliferation.

Surprisingly, mice with increased *Ink4a/Arf* expression showed normal life span and aging (36), suggesting that p16^{INK4a}-induced stem cell defects may not have impacts on the long-term longevity of the animals. Another explanation to this observation is that the anti-aging activity of p53 resulted from increased *Arf* negates the pro-aging activity of *Ink4a* expression. Intriguingly, mice that harbored two additional alleles of *Arf* gene present an extended life span and delayed aging (37), further suggesting an anti-aging effect of *Arf* or p53 overexpression.

1.2.4 INK4A/ARF in malignant gliomas and other cancers

The implication that the INK4A/ARF locus is involved in development of various types of human cancers came from the observation that this genomic region is frequently altered in human malignancies (38-40), including gliomas, lung cancers, prostate cancers, melanomas, head and neck cancers, pancreatic cancers, renal cell carcinomas, breast cancers, bladder carcinomas, and leukemias (41). Mice lacking the *Cdkn2a* locus developed spontaneous tumors and were more prone to carcinogenesis (42). Mice deficient in *Ink4a* (*Ink4a*^{-/-}) (43) or *Arf* (*Arf*^{-/-}) (23) alone were less tumor-prone than the *Ink4a/Arf*^{-/-} or p53^{-/-} mice, and displayed distinct spontaneous tumor spectra from each other and the double-knockout animals (44). Whereas no spontaneous tumors were found in the brain of the *Ink4a/Arf*-deficient mice, astrocytes and NSCs from these mice formed high-grade gliomas in the brain upon EGFR activation (45). Consistently, the *Ink4a/Arf* loss cooperates with constitutively active EGFRvIII expression targeted to either glial progenitor or astrocytes to generate gliomas in the mouse brain (46). Additionally, K-Ras activation was shown to cooperate with loss of *Ink4a* and *Arf* in mAst or neural progenitor cells to generate GBMs (47). On the other hand, expression of an additional

transgenic copy of the entire *Ink4a/Arf* locus in mice rendered these animals resistant to oncogenic transformation (36). Re-introduction of p16INK4A into *INK4A*-null human glioma cell lines led to significant suppression of cell growth (48, 49). Clinically, deregulation of P16INK4A/CDK4/6/RB pathway frequently occurs with alterations in P14ARF/MDM2/P53 pathway in both low- and high-grade gliomas (50). Recent coordinated efforts have also identified these two pathways as the core pathways that are altered in clinical GBM tissues (10, 11). The homozygous deletion of the *CDKN2A* locus at chromosome 9p21, thus eliminating both *INK4A* and *ARF* genes, concomitantly deregulates two major tumor suppressor pathways, the RB and P53 pathways (26). In gliomas without *INK4A/ARF* alteration, there are often other genetic changes within the RB and P53 pathways to achieve the disruption of these two core pathways, such as *CDK4/6* amplification, *RB* mutations, *TP53* mutations, and *MDM2/4* amplification (10, 51), further demonstrating the importance of abrogation of the RB and P53 pathways for gliomagenesis. In addition to allelic deletion (52), *CDKN2A* locus can also be inactivated by promoter hypermethylation (53, 54) or point mutations (55) in some cases. Given the role of p16INK4A in normal aging of NSCs (32), this molecule is important in maintaining a balance between aging and oncogenesis.

1.3 PLATELET-DERIVED GROWTH FACTOR (PDGF) SIGNALING

1.3.1 Structures of PDGFs and PDGFRs

PDGF was identified and purified more than 35 years ago as a molecule released by platelets into the whole blood serum that stimulates proliferation of various mesenchymal cells (56-58), as well as glial cells in the brain (59, 60). The mitogenic effect of this growth factor requires the target cells express the receptors for PDGF (PDGFR) (61). The PDGF family consists of four ligands, PDGF-A, -B, -C, and -D, and two receptors, PDGFR α and β (Figure 3). The structures of PDGF-A and -B are largely similar, consisting of a PDGF/VEGF core domain with conserved cysteine residues called the cysteine knot motif, and a N-terminal propeptide region that is removed intracellularly for their activation prior to its secretion (Figure 3) (62). Additionally, in PDGF-B and a membrane-bound, long alternative splice form of PDGF-A, there is a C-terminal basic “retention motif” that can interact with heparan sulfate proteoglycans of the ECM (Figure 3)(63). The retention motif needs to be cleaved prior to secretion of the ligands. Expression of long or short form of PDGF-A results from alternative splicing of the exon 6 of *PDGFA* gene and is cell-type specific. Human glioma cells produce mainly the long form (64), while normal human endothelial cells express the short form of PDGF-A. Interestingly, the differential alternative splicing of PDGF-A might determine its mitogenic capacity in these cells (64). The two novel PDGFs, PDGF-C and PDGF-D, contain a distinct N-terminal domain called CUB domain (Figure 3). It is cleaved extracellularly after secretion of the growth factors and this cleavage is important for their activity (65). PDGFRs shared a common structure including five extracellular immunoglobulin (Ig) loops and a split intracellular tyrosine kinase (TK) domain

separated by a kinase insert region (Figure 3) (62, 66). Similar structures can be also found in other RTKs such as VEGFRs, c-Kit, c-Fms, and Flt-3 (66).

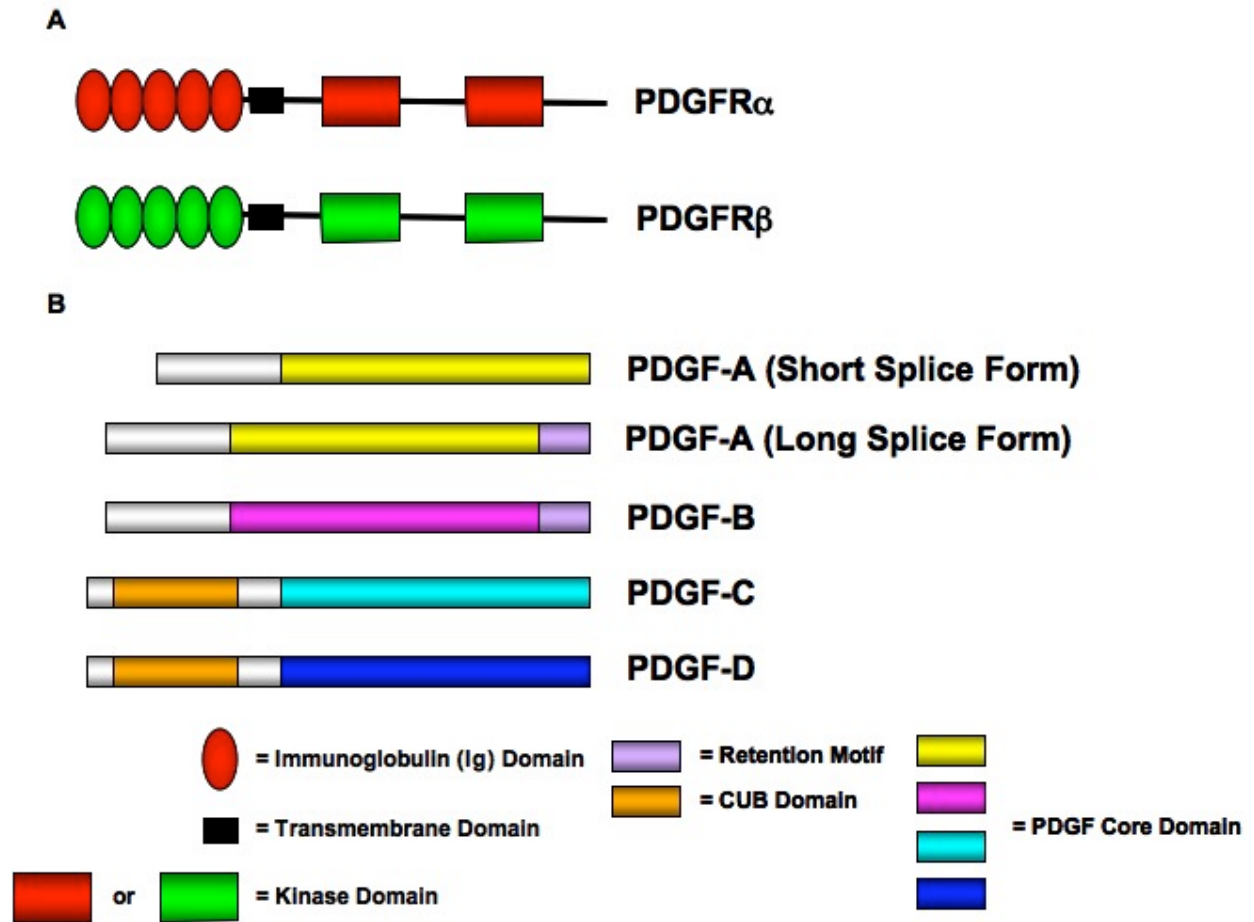


Figure 3. The Structures of PDGFRs and PDGFs.

1.3.2 Activation and Downstream Signaling of PDGFRs

The PDGF ligands function as disulfide-linked homo- or hetero-dimers, PDGF-AA, PDGF-AB, PDGF-BB, PDGF-CC, and PDGF-DD (65). These dimeric isoforms are capable of binding to two structurally related RTKs with different specificities (PDGFR α and PDGFR β) (Figure 4) (65, 67).

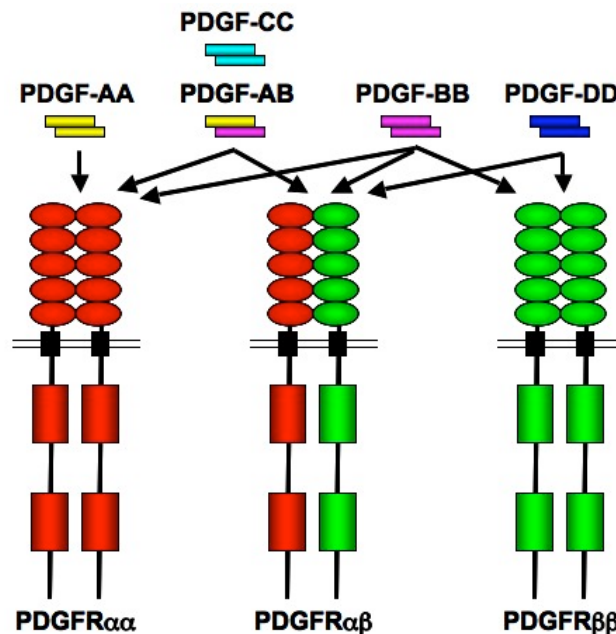


Figure 4. Specific binding between PDGF receptors and ligands.

The binding of PDGF ligands induces dimerization of the PDGFRs and juxtaposition of their intracellular tyrosine kinase domains, leading to *trans*-autophosphorylation of multiple tyrosine residue sites (68). The subsequent association between different SH2 domain-containing signaling molecules and the phosphorylated tyrosine residues engages various downstream signaling cascades (Figure 5), gene transcription events, and various cellular behaviors, such as

cell proliferation, apoptosis, actin reorganization, and chemotaxis (62, 69). The SH2 domain-containing signaling effectors include PI3K, PLC- γ , SFK, phosphotyrosine phosphatase SHP-2, GAP for Ras, STATs, as well as adaptor proteins such as Grb2, Grb7, Shc, Nck, and Crk (69). PDGFR α and β bind to distinct but overlapping sets of these signaling molecules upon ligand stimulation. Allelic series of mutant PDGFRs have been generated and it appears that, compared to PDGFR β , PDGFR α relies more on activation of specific signaling pathways to function properly in specific stages and organs during animal development (70, 71). For example, PI3K signaling is indispensable for PDGFR α during early animal development, while for PDGFR β , disruption of PI3K alone had little effect on normal development (66). Cytoplasmic domain swapping experiments further revealed that in contrast to PDGFR β , it is not the intrinsic properties of the receptor but the ability of PDGFR α to engage specific signaling molecules that determines the activity and functions of receptor signaling (72, 73). In this dissertation, we focus on the downstream SH2 domain-containing signaling effectors of PDGFR α (Figure 5).

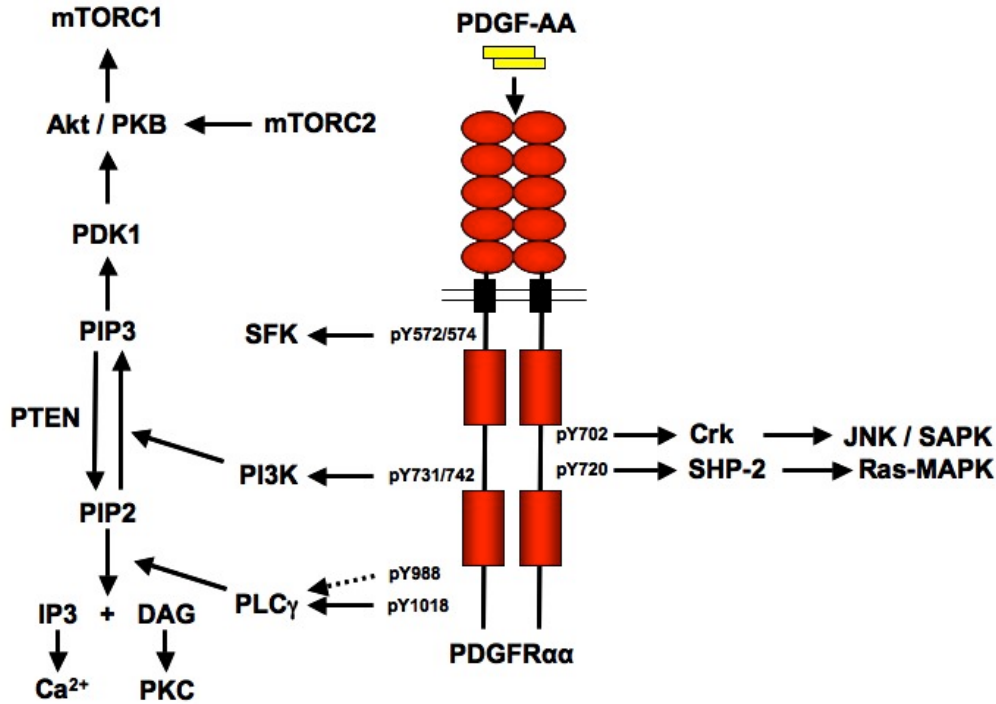


Figure 5. The PDGF-A/PDGFR α signaling.

The PDGF-AA homodimers bind and induce dimerization, autophosphorylation of PDGFR α homodimer receptor. Various SH 2 domain-containing signaling effectors are then recruited to the receptor by binding to specific phosphorylated tyrosine residues and initiate downstream signaling cascades.

1.3.2.1 PI3K

Members of the PI3K family consist of a regulatory p85 subunit and a catalytic p110 subunit. Upon association with the phosphorylated tyrosine residues 731 and 742 (Tyr-731/42) of PDGFR α intracellular domain (62), PI3K is activated and phosphorylates its preferred target phosphatidylinositol 4,5-bisphosphate [PI(4,5)P₂ or PIP₂] to produce phosphatidylinositol 3,4,5-triphosphate [PI(3,4,5) P₃ or PIP₃] in the plasma membrane. The PIP₃ then recruits several downstream effectors such as Akt/PKB, p70 S6 kinase, c-Jun N-terminal kinase (JNK), and small GTPase of the Rho family to the plasma membrane (62, 69). The activation of PI3K

pathway leads to several cellular effects including cell growth, survival, chemotaxis, and actin reorganization (Figure 5) (62, 69).

1.3.2.2 PLC- γ

PLC- γ shares the same substrate as PI3K. Upon association to Tyr-988 and -1018, it phosphorylates PIP₂ to generate inositol 1,4,5-trisphosphate (IP₃) and diacylglycerol (DAG), which then mobilize intracellular Ca²⁺ and activate the PKC family, respectively (Figure 5) (62, 69). PDGF-induced PLC- γ activation is responsible for cellular effects such as cell motility and growth. Full activation of PLC- γ , however, is dependent on the PIP₃ generated by PI3K, since recruitment of PLC- γ requires association of its pleckstrin homology (PH) domain with the PIP₃ in the plasma membrane (62, 69).

1.3.2.3 Src Family Kinases (SFKs)

The SFK represents a family of tyrosine kinases including Src. Their binding sites on PDGFR α autophosphorylated tyrosine sites are Tyr-572 and -574. PDGFR α -mediated Src activation appears to be unnecessary for mitogenic responses in some cell types (Figure 5) (62, 69).

1.3.2.4 SHP-2

SHP-2 is an SH2-containing phosphotyrosine phosphatase that binds to phosphorylated Tyr-720 of activated PDGFR α . Its phosphatase activity can potentially dephosphorylate the RTK and downstream effectors, leading to inactivation of these proteins. However, it has also been shown

that SHP-2 is involved in up-regulation of several effectors such as Ras/MAPK and Src pathways, possibly through its role as an adaptor (Figure 5) (62, 69).

1.3.2.5 Crk

Crk is an adaptor that binds to phosphorylated Tyr-702 of PDGFR α . Upon binding, it then activates the nucleotide exchange protein C3G and the subsequent activation of the JNK/SAPK pathway (Figure 5) (62, 69).

1.3.3 PDGFR Mutation Studies

An allelic series of *PDGFRA* tyrosine-to-phenylalanine mutations disrupting association between the RTK with different downstream effectors and signaling pathways have been generated (74). This study demonstrated that PDGF-AA-induced DNA synthesis was strictly dependent on PI3K signaling only, while Src, PI3K, and PLC- γ are required for PDGF-mediated mediated chemotaxis, with Src being the most important effector for cell motility (74). Surprisingly, all PDGFR α mutants in the “add-back panel” that can only initiate one of the five downstream pathways were not able to restore the PDGF-induced chemotaxis to the level achieved by WT PDGFR α , indicating that activation of multiple effectors are required for full activity of the receptor to mediate certain cellular responses (74). Using similar strategy, PI3K and PLC- γ were shown to play predominant roles in preventing apoptosis of mesoderm cells during early *Xenopus* embryo development (75). These studies suggest that distinct downstream effectors of PDGFR may be required for different cell types, species, and stages of development. To further

dissect the contribution of signaling pathways emanating from the PDGFR α , Klinghoffer and colleagues further generated knockin mice that harbored one of the three mutants, PDGFR α -F7, PDGFR α -F731/42, or PDGFR α -F572/74 (70). Interestingly, mice that homozygously harbored PDGFR α -F731/42, as well as PDGFR α -F7, displayed phenotypes comparable to PDGF-A- or PDGFR α -null animals, including growth retardation, skeletal and lung developmental abnormalities (70). However, Src association with PDGFR α was only required for oligodendrocyte development, possibly due to the role of Src in promoting progenitor cell migration (70). These experiments suggest that PI3K is the major effector of PDGFR α signaling during embryogenesis.

1.4 PDGF SIGNALING IN NORMAL CNS DEVELOPMENT AND REPAIR

1.4.1 PDGF-A in Oligodendrocyte Development

The developmental functions of PDGFRs and PDGFs have been unveiled mainly through genetic studies in mice [reviewed in (76) and (66)]. The role of closely related PDGF/VEGF superfamily in neural and glial development is evolutionarily conserved: in *Caenorhabditis elegans*, the VERs, which are structurally similar to vertebrate VEGFRs, are expressed in neurons and glial cells (77); in *Drosophila melanogaster*, the PDGFR/VEGFR homologue PVR (and its ligand, PVF) is required for ventral midline glia cell survival (78). In the mammalian CNS, messenger RNA (mRNA) and protein expression of PDGF ligands and receptors were found throughout various brain regions (79). In rodents, the PDGFR α -positive OPCs (80)

originate at the ventricular surface near the floor plate of spinal cord in embryonic day 12.5 (E12.5) of mice (E14 for rats) (81). Neurons and astrocytes throughout the CNS produce PDGF-A that acts as a mitogen for OPCs (82-85). Early studies showed that PDGF-A knockout mice developed tremor caused by severe hypomyelination on neuronal projections throughout the CNS (86, 87); PDGFR α -null mice died prenatally and the OPC isolated from the pre-mortem animals showed proliferation and differentiation defects (88). Subsequent studies using PDGFR α mutant knockin mice showed that downstream SFK and PI3K were important for normal myelination of the CNS (70). Further analyses revealed that PDGF-A, but not PDGF-B, is required for proliferation, migration, and normal differentiation of PDGFR α -positive OPCs (83, 84, 89, 90), and that over-production of PDGF-A in the CNS neurons or astrocytes induced hyper-proliferation of the PDGFR α -positive O-2A progenitor cells in a paracrine manner (87, 91). The mitogenic effect of PDGF-A appears to rely on various environmental cues endowed by the ECM, which activate various integrins (92) and chondroitin sulfate proteoglycan NG2 (93). The proliferation rate and the amount of PDGF-A available are proportional and the OPC population continues to grow until the concentration of PDGF-A becomes limiting, that is, the rate of PDGF-A consumption exceeds the rate of its production due to the increased number of OPCs (94). The OPCs may also be able to sense the amount of PDGF-A by the “rheostat-like” PDGFR α function, switching downstream signaling from PI3K pathway to PLC- γ under higher PDGF-A concentration (88). Whereas in an autocrine situation, in which the PDGF ligand is over-expressed in PDGFR α -positive progenitor cells, the rate of PDGF-A production increases together with the number of the progenitor cells, theoretically rendering these cells capable of proliferating indefinitely (76). Thus in an autocrine situation, the growth factor sensing mechanism of OPCs might be lost. Similar mitogenic function of PDGFR α /PDGF-A signaling

has also been demonstrated during CNS injury. After experimental demyelination, the ensuing remyelination often involves increased proliferation of PDGFR α - and NG2-positive OPCs (95). A decrease in PDGFR α dosage in genomic level, as shown in heterozygous PDGFR α ^{+/-} mice (96), resulted in impaired remyelination after myelin damage to the CNS (97).

Besides its role as a mitogen for OPCs, PDGF-A acts as a lineage specification factor that direct the differentiation of embryonic neural progenitor cells into oligodendrocytes (98, 99). In cultured O-2A progenitor cells isolated from rat optic nerves, PDGF-A and bFGF are also capable of maintaining the proliferation and self-renewal potential of these cells, and preventing their terminal differentiation into oligodendrocytes (100). Interestingly, the effect of these growth factors on OPC proliferation and differentiation appear to be reserved in the adult CNS in that following demyelinating damage, PDGF-A and bFGF levels are increased in order to promote OPC proliferation and subsequent differentiation into mature oligodendrocytes for remyelination (101). The observation that PDGF and bFGF convert the adult rat O-2A cells to their perinatal counterparts after injury to the adult brain (102) implied their capacity of reprogramming OPCs to earlier progenitors (103).

In addition to the role of PDGF-A in the glial-restricted progenitor cell development, PDGF-A is also capable of stimulating proliferation of the PDGFR α -positive NSCs residing in the SVZ of the adult murine brain, which are capable of differentiating into both neurons and oligodendrocytes (104). The presence of the neuron/oligodendrocyte common progenitor has been appreciated long ago, which can be identified in embryonic mouse spinal cord by expression of basic helix-loop-helix transcription factor Oligs (105). By observations obtained in *Olig2*-null animals, one of the *Olig* genes, *Olig2*, was found to be important for oligodendrocyte development (105). In-situ hybridization experiments further revealed that expression of *Olig2*

gene precedes that of PDGFR α in mouse embryonic oligodendrocyte precursors (105, 106), suggesting a possible link between these two genes during glial development. Indeed, ectopic expression of *Olig2* gene *in vivo* induces expression of transcription factor Sox10, which, together with Sox9, control transcription of the gene encoding PDGFR α (107, 108). Intriguingly, in mouse embryos, the *Olig* gene expression is regulated by Shh (106) that is also required for self-renewal of the embryonic forebrain progenitors induced by PDGF-A and bFGF (109), evincing a complex interaction of Shh, Sox, Olig, and PDGF in oligodendrocyte development. Surprisingly, normal astrocytic development does not seem to be affected in *Olig2*-null animals (105). Exactly which cell type (glial-restricted O-2A cells or neuron/oligodendrocyte common progenitor cells) do OPCs come from is still an open question (109). However, these findings suggest the existence of distinct PDGF-responsive neural progenitor cells, each of which is spatiotemporally responsible for generating various neural cells during CNS development. These observations in normal CNS development may not only help elucidate the identity of the long pursued cells-of-origin of the malignant gliomas, but also raise such questions as whether these intrinsic developmental and physiological properties and functions are preserved after cell transformation.

1.4.2 PDGF-C and -D in CNS Development

The roles of the two new members of the PDGF family, PDGF-C and PDGF-D, in CNS development remain relatively elusive. PDGF-C was first found in the spinal cord of chick embryo, thus it was originally named spinal cord-derived growth factor (SCDGF) (110). In rats, PDGF-C is expressed predominantly in embryonic brain and spinal cord, while PDGF-D

expression is evident in the adults than in the embryos (111). In addition, PDGF-C was detected by IHC in developing brain and spinal cord in mouse embryos (112). Interestingly, PDGF-C expression was also found in the transient EGL cells of the cerebellum in mouse E13 embryo (113). The requirement of PDGF-C for normal spinal cord development was further demonstrated by using PDGF-C knockout mice (114). These mice displayed a range of abnormalities and died perinatally due to difficulties in breathing and eating. Examination of the mouse embryos revealed the development of spina bifida occulta, an incomplete closure and deformation of the vertebrae (114). PDGF-D knockout animals have not been reported yet, and studies on its role in normal CNS development still fall behind. However, PDGF-D has been shown to stimulate blood vessel formation and wound healing processes (115), suggesting that PDGF-D might impact on tumor angiogenesis. The roles of PDGF-C and PDGF-D in brain tumor development will be discussed in the following sections of this chapter.

1.5 PDGF SIGNALING IN HUMAN GLIOMAS

1.5.1 Pre-Cancer-Genomic Studies

The first implication that PDGF autocrine signaling can contribute to cell transformation came from the discoveries of amino acid sequence similarity between simian sarcoma virus (SSV) oncogene *v-sis* and PDGF-B chain gene (116, 117). In human glioma, a glioma cell line was shown to secrete a growth-promoting factor (118-120) that was later found to be three disulfide-linked dimers, PDGF-AA, PDGF-AB, and PDGF-BB (121-123). Each of these dimers had

distinct binding affinities to receptors α and β (67). Subsequent studies revealed that mRNAs for PDGF ligands and receptors were expressed in a series of established glioma cell lines (124, 125). *In situ* hybridization and IHC analyses further demonstrated that in human glioma tissues, tumor cells express PDGF-A, -B, and PDGFR α , while the surrounding hyperplastic endothelial cells express PDGF-B and PDGFR β , suggesting the presence of autocrine and paracrine PDGF stimulation in glioma development (126-129). Overexpression/gene amplification of PDGFR α occurred mostly in lower-grade gliomas as well as secondary GBMs (2, 4, 130-132), representing a distinct subtype from those with EGFR overexpression (Figure 1) (133). In a study of IHC staining on 103 grade II astrocytomas, PDGFR expression was found to be an independent prognostic factor for these patients (134). Overexpression of PDGF ligands, however, varies among gliomas of different grades, with PDGF-A being expressed in all grades and PDGF-B only in higher-grade GBMs (135), suggesting PDGF-B may be involved in the conversion of low- to high-grade gliomas. In fact, it has been shown that in human oligodendroglioma tissues (136) and in a mouse glioma model (137), the level of PDGF signaling may predict the grade and malignancy of these tumors.

1.5.2 Cancer Genomics Studies

Cancer is a disease of genomic alterations. For the past decade, high-throughput approaches such as microarrays and comparative genomic hybridization (CGH) arrays have been introduced and it was thus possible to profile gliomas in a whole-genome scale (12, 138-140). The most comprehensive and reliable analysis of genomic alterations in primary GBM tissues has been conducted by The Cancer Genome Atlas Network (TCGA), a project team funded by the

National Cancer Institute (NCI) (10). This multi-institutional effort provides invaluable resources for gene expression and mutation, DNA copy number alterations (CNA), and DNA methylation data for GBMs. Most of the previously appreciated genetic aberrations such as alterations in the RB, TP53, and RTK pathways were re-captured in the initial TCGA studies. However, an unexpected higher frequency (~13%) of focal amplifications of the 4q12 locus harboring *PDGFRA* was reported for primary GBMs in the TCGA collection than that published previously (10, 141). Further classification of these GBMs by the gene expression signatures revealed that *PDGFRA* overexpression occurs together with *TP53* and *IDH1* mutations in the Proneural subtype of GBMs, which also express oligodendrocyte lineage genes such as *OLIG2* and *SOX* (11). Interestingly, within this subtype of GBMs, *PDGFRA* amplifications and the *PIK3CA/PIK3R1* mutations (leading to constitutively active PI3K subunits p110 and p85, respectively) mostly occur in a mutually exclusive manner (11), signifying an overlapping functionality between these two alterations in gliomagenesis. Indeed, analyses in different cohorts of gliomas of different grades using other methods such as single nucleotide polymorphism array (SNP-Chip) (142) or a western blot-based proteomic analysis (143) confirmed the importance of PI3K/AKT/mTOR pathway activation in *PDGFRA*-amplified gliomas.

The Proneural subtype of GBMs that harbor *PDGFRA* amplification from the TCGA dataset shares similar gene expression profile with the previously reported pro-neural (*PN*) subclass (139). Nearly all WHO grade III tumors including astrocytomas, oligodendrogliomas, and mixed oligoastrocytomas were classified as *PN* subclass, as well as secondary GBMs (11, 139). Patients with *PN* tumors were younger with better survival. A comparison of the *PN* tumors signature also revealed that they resemble the fetal and adult brain, as well as cultured

NSCs, indicating a possible cell of origin of this subclass of gliomas being the neural stem/progenitor cells (139). Indeed, putative NSCs residing in the adult mouse SVZ are PDGFR α -positive and responded to PDGF-A stimulation by forming a glioma-like lesion (104), suggesting the potential susceptibility of adult NSCs to oncogenic transformation by *PDGFRA* alterations.

1.5.3 Constitutively Active *PDGFRA* mutations in Gliomas

EGFR is the most frequently amplified RTKs in human gliomas (2, 6). It mainly occurs in a mutually exclusive manner with *PDGFRA* amplification in a distinct subclass of GBMs (11), although there were cases in which co-alteration of both RTKs were observed. Approximately 50% of the EGFR-overexpressing GBMs also harbor an *EGFR* mutant allele with deletion of exons 2-7 (EGFR Δ III or Δ EGFR), leading to a constitutively active RTK (144, 145). Among PDGFR α -overexpressing gliomas, similar to the EGFR-overexpressing tumors, several mutations in the RTK also have been reported: an in-frame deletion in the extracellular domain of PDGFR α (146), a frameshift deletion (147), and a gene fusion product between kinase insert domain receptor (*KDR/VEGFR-2*) and *PDGFRA* (148). In particular, the complete deletion of exons 8 and 9 in the gene encoding PDGFR α (PDGFRA Δ 8,9), leading to a constitutively active and transforming RTK (149), was recently found to be more prevalent than was previously thought (148). In this study, Ozawa and colleagues demonstrated that the mutant PDGFRA Δ 8,9 was capable of transforming mouse fibroblasts *in vitro* and *in vivo*, stimulating downstream Akt/Erk phosphorylation/activation, and responding to anti-PDGFR treatments (148). However, the fact that PDGFRA Δ 8,9 was not able to transform Ink4a/Arf $^{-/-}$ mouse glial cells (148) is

seemingly contradictory to the observation that *PDGFRA* overexpression can cooperate with *Ink4a/Arf* deletion to induce glioma growth from mAst, as shown in the recent publication from our lab (150). Therefore, it is possible that concomitant overexpression of WT *PDGFRA* is necessary for the *PDGFRA*^{Δ8,9} mutant to be oncogenic, which also explains the fact that mutant *PDGFRA* occurs only within the *PDGFRA*-overexpressing GBMs (144, 148).

1.5.4 PDGF-C and -D in Human Gliomas

The two novel PDGF ligands, PDGF-C and PDGF-D, were first implicated in glioma development by a study that examined expression of PDGF ligands and receptors in glioma cell lines and primary glioma tissues (151, 152). Lokker and colleagues found that PDGF-C and -D were expressed at high levels in tumor tissues as compared with those in the normal brain control. Additionally, autocrine loops that involve PDGF-C/PDGFR α and PDGF-D/PDGFR β exist in all tumors they examined. However, the pathological consequences of PDGF-C and -D over-expression and whether they compensate PDGF-A and -B functions or merely initiate redundant signaling cascades remain elusive. Interestingly, in an s.c. tumor model, PDGF-C was associated with tumor resistance to anti-VEGF therapies. The resistant tumors tend to up-regulate the level of PDGF-C after anti-VEGF treatment, possibly compensating the function of the inhibited VEGF in stimulating angiogenesis (153). Indeed, in patients with recurrent GBMs after anti-VEGF therapy, PDGF-C, together with c-Met, was expressed at high levels, especially in the center of the tumor mass (154). The mechanism of resistance to anti-VEGF therapy may involve the capacity of PDGF-C to alter the structure of blood vessels by recruiting perivascular cells (155), thus stabilizing the vessels and rendering them insensitive to anti-VEGF treatment.

The function of the PDGF-D/PDGFR β autocrine remains unknown despite its presence in several GBM cell lines and primary tissues (151, 152). However, it has been shown that PDGF-D was responsible for inducing chemotactic tropism of PDGFR-positive stem cells toward glioma cells in the mouse brain (156). This observation is likely important for development of therapeutic strategies using stem cells as a drug carrier.

1.5.5 Animal Models of PDGF-induced Gliomagenesis

1.5.5.1 Transgenic Mice

Despite decades of intensive research, the prognosis for patients diagnosed with high-grade gliomas remains dismal. One of the major hurdles to the progress is the lack of animal models that can accurately recapitulate the behaviors and the neuropathological features of the tumors in humans (157). Several GEM models of spontaneous glioma formation have been reported, by generating mice with astrocyte-specific transgenic expression of *v-src* (158) or *H-ras* (159), and with concomitant loss of *NFI* and *p53* tumor suppressors (160, 161). Recently, transgenic mice that harbor an astrocyte-specific expression of PDGF-B (hGFAPpPDGFB mice) were generated and assessed for spontaneous glioma formation (Table 1) (162). Neither loss of p53 nor overexpression of PDGF-B alone was able to induce brain tumor growth. However, when Hede and colleagues crossed the hGFAPpPDGFB mice with the p53-null mice, the resultant hGFAPpPDGFB/p53-null mice developed an aggressive GBM-like tumor with characteristics comparable to human GBMs (162). The researchers further showed that PDGFR α was highly expressed in tumor cells, while PDGFR β was expressed in the tumor vasculature, and that the

tumor expressed a series of lineage markers indicating presence of various cell types including neurons, astrocytes, and oligodendrocytes, especially in tumors of large size.

More recently, spontaneous gliomas have been found to develop in transgenic mice overexpressing the long isoform of PDGF-A, PDGF-A_L (Figure 3), under control of a GFAP promoter (Table 1) (163). Unlike hGFAPpPDGFB mice, hGFAPpPDGFA_L mice did not require additional genetic aberrations such as *p53* deletion in order to develop spontaneous tumors. These mice were further found to harbor neoplastic cells positive for PDGFR α , Olig2, and NG2 in the SVZ, corpus callosum, hippocampus, and cerebellum (163), suggesting that the resident OPCs in these areas of the brain were likely the target of transformation in these mice. Alternatively, GFAP-positive neural stem cells could also be the cell of origin for PDGF-induced gliomas in the hGFAPpPDGFA_L mice since PDGF-A has been reported to be capable of biasing the cell fates of stem cells residing in the SVZ toward OPC-like cells (104). Histologically, the spontaneous gliomas formed in hGFAPpPDGFA_L mice showed characteristics of both astrocytes and oligodendrocytes and thus were determined to be WHO grade III oligoastrocytomas (Table 1). Although it is difficult to assess the tumor-promoting potentials of PDGF-B, short- and long-form PDGF-A by comparing the transgenic mice generated by overexpression of these genes, due to the differences in promoter strength and transgenic copy numbers among these mice, these studies have suggested that the glioma-specific long-form PDGF-A may exert its tumorigenic effects through distinct signaling pathways than that stimulated by the PDGF-B and short-form PDGF-A (163).

1.5.5.2 Virus-induced GEMs

Other GEM models of PDGF-induced glioma development have also been reported, most of which involved a single intracranial injection of retroviruses expressing PDGF-B ligand (Table 1) (164-168), targeted either nonspecifically, or to astrocytes (GFAP-positive) or neural progenitor cells (Nestin-positive) using cell type-specific promoters. In these studies, PDGF-B overexpression alone induces glioma growth from various cell types including glial progenitor cells, astrocytes, and neural progenitor cells, and the tumors frequently exhibited characteristics of oligodendrogliomas or mixed oligoastrocytomas (Table 1). These two models, the germ-line transgenic and retrovirus induction models, differ in many ways such as the incidence of tumorigenesis and histological features. The discrepancies may be due to different time of stimulation during animal development, different targeted cells, or retroviral-mediated insertional mutagenesis in genes that cooperate with PDGF to induce tumorigenesis (169). Additionally, the local injection of various agents including cells or viruses into the brain of mice may induce proliferation of VEGF-expressing Olig2-positive glial cells and a local increase of angiogenesis (170, 171). These factors may contribute to the differential tumor induction potentials observed in these models where PDGF-B alone was targeted to GFAP-positive cells in the brain. Despite the differences between the transgenic and the virus-mediated models, an increase in tumor malignancy by concomitantly introducing a loss of p53 function or *Ink4a/Arf* locus was evident in all studies (Table 1) (162, 165, 168, 172), demonstrating a cooperative effect of PDGF overexpression and disruption of p53 or RB pathway in glioma tumorigenesis.

Table 1. Summary of Animal Models of PDGF-induced Spontaneous Brain Tumor Formation

Method	Vector	PDGF	Strain	Age	Target	Histology	Ref
Virus Sup I.C. Inj	MoMuLV	PDGF-B	C57BL/6	Neonatal	Non-specific	GBM / PNET	(164)
Virus Sup I.C. Inj	MoMuLV	PDGF-B	p53 ^{-/-}	Neonatal	Non-specific	GBM / PNET	(172)
Virus Sup I.C. Inj	MoMuLV	PDGF-B	Ink4a/Arf ^{-/-} ,	Neonatal	Non-specific	GBM / PNET	(172)
Packaging Cell I.C. Inj	RCAS	PDGF-B	Ntv-a	Neonatal	nestin+	Low-grade Oligo	(165)
Packaging Cell I.C. Inj	RCAS	PDGF-B	Ntv-a, Ink4a/Arf ^{-/-}	Neonatal	nestin+	Anaplastic Oligo	(163, 165)
Packaging Cell I.C. Inj	RCAS	PDGF-B	Gtv-a	Neonatal	gfap+	Low-grade Oligo / Oligoastro	(165)
Packaging Cell I.C. Inj	RCAS	PDGF-B	Gtv-a, Ink4a/Arf ^{-/-}	Neonatal	gfap+	Anaplastic Oligo / Oligoastro	(165)
Packaging Cell I.C. Inj	RCAS	PDGF-B	Gtv-a, p53 ^{-/-}	Neonatal	gfap+	Low-grade Oligo / Oligoastro	(165)
Packaging Cell I.C. Inj	RCAS	ACC-PDGF-B-HA	Ntv-a	Neonatal	nestin+	High-grade Oligo	(137)
Virus Sup C.C. Inj	pQ (Retroviral)	PDGF-B	Sprague Dawley Rat	Adult	Non-specific	GBM	(166)
Virus Sup L.V. Inj	pQ (Retroviral)	PDGF-B	Sprague Dawley Rat	Neonatal	SVZ	GBM	(173)
Packaging Cell L.V. Inj	pCEG (Retroviral)	PDGF-B	C57BL/6	E14	SVZ	High-grade Oligo	(99) (167)
Protein L.V. Infusion	NA	PDGF-A	CD-1	Adult	SVZ	Low-grade Glioma	(104)
Zygote Pronuclear Inj	IRES β GEO	PDGF-B	Transgenic hGFAPPDGFB, p53 ^{-/-}	E0	gfap+	GBM / High-grade Oligo	(162)
Zygote Pronuclear Inj	IRES β GEO	PDGF-A _(L)	Transgenic hGFAPPDGFA	E0	gfap+	Grade III Oligoastro	(163)

Abbreviations: I.C., intracerebral; C.C., corpus callosum; L.V., lateral ventricle; Inj., injection; Oligo, oligodendroglioma; Oligoastro, oligoastrocytoma; PDGF-A_(L), PDGF-A long form.

1.5.5.3 Other Model Systems

Sleeping Beauty Animal Model—A relatively new mouse model of generating *de novo* brain tumors using stereotactic injection of non-viral plasmid DNA into the brain of neonatal mice has been developed (174). In this model, a single injection of DNA plasmids encoding a Sleeping Beauty (SB) (175) transposable element, gene(s) of interest, and SB transposase into the lateral cerebral ventricle is performed on newborn mice. The tumors generated in this model can then be monitored by bioluminescent imaging of luciferase expression and the differences in tumor incidence in various mouse strains appear to be minimal (174). This approach, combined with the use of Cre-loxP system, is possible to restrict expression of various genes in a cell type-specific manner (176). However, as in virus-mediated models, transposon-mediated mutagenesis and injection-induced reactive gliosis will also complicate the use of this system for pre-clinical testing. Whether PDGF overexpression via the SB transposon system in the mouse brain generates gliomas comparable to those in other animal models has not been determined yet.

Xenograft Model—The traditional and most commonly used model of tumor formation is transplantation of human or mouse tumor cells into the immuno-deficient mice. Most of the evidence of interactions between specific signaling molecules and the PDGF pathway have been obtained from the human or mouse cell line models. Despite their limitation in recapitulating the human cancers, these models still play an important role in understanding the molecular mechanisms of tumor development and activity of therapeutic anti-cancer agents (177, 178). In fact, studies have shown that in many aspects human tumor cell line xenograft model may better predict the tumorigenesis processes that occurred in humans than do various mouse models (179, 180), owing to the dramatic differences between mouse and human in genetics, tumor

susceptibility, and tumor microenvironment. A combination of human and mouse models to understand brain tumors and to design better therapeutic strategies might be necessary in the post-cancer-genomic era (181).

1.5.5.4 PDGF Downstream Signaling and Gliomagenesis Revealed by Animal Models

Using RCAS/*tv-a* system, Dai and colleagues have shown that combined activation of Akt and K-Ras generated astrocytomas while PDGF-B overexpression led to mostly oligodendrogliomas (182). They further showed that blockade of mTOR pathway converted PDGF-B-induced oligodendrogliomas into astrocytoma-like tumors (183). Thus it appears that, in the RCAS/*tv-a* system, PDGF-B and Ras/Akt/mTOR signaling pathways promote formation of distinct histological types of tumors in the mouse brain. However, in human gliomas, as shown by a proteomic study, activation of mTOR and RAS/ERK pathways frequently co-occurred in the PDGF-B-enriched subgroup (143), and two out of four oligodendrogliomas in this study were of the PDGF-B/mTOR/RAS activation subtype, suggesting that in human gliomas, a more complex connection between PDGF signaling and tumor cell lineage specification may exist than that found in the mouse models. Additionally, since there was no concomitant overexpression of PDGFR α in tumors generated from RCAS/*tv-a*-mediated PDGF-B expression, it will be interesting to determine whether targeted co-overexpression of PDGFR α and PDGF-B in the mouse brain will generate gliomas with same histopathological characteristics, as does PDGF-B alone.

1.6 PDGF SIGNALING IN OTHER BRAIN TUMORS

1.6.1 Pediatric Gliomas

Gliomas in children differ from those in adults in terms of location, frequency, and progression patterns, which may result from distinct cell of origin, genetic susceptibility, or tumor microenvironment present in relatively immature developing brain (3). However, focal amplification of *PDGFRA*, together with deletion of *CDKN2A* locus, was also found in high frequency in childhood gliomas, especially in pediatric high-grade gliomas (HGGs) (184), whereas other common alterations in the adults such as *EGFR* amplification/mutation and *PTEN* mutations are less frequent in pediatric HGGs (185), suggesting different cell of origin in pediatric from adult tumors. It is likely that the developing brain harbors more PDGF-responsive cells, which in the presence of additional genetic alterations such as *TP53* mutations or *CDKN2A* deletion, are responsible for gliomagenesis in the childhood brain. The most common childhood glioma is the lower-grade juvenile pilocytic astrocytoma. Studies have suggested that the cell of origin of this type of brain tumor is likely the human counterpart of the O-2A progenitor cells in the rat brain (80, 186, 187), which express both NG2 and PDGFR α . The presence of these lineage markers is reminiscent of the adult oligodendrogliomas (187). Whether these adult and childhood gliomas share the same or closely related cell of origin warrants further investigation.

1.6.2 CNS Primitive Neuroectodermal Tumors

Primitive neuroectodermal brain tumors (PNETs), including medulloblastomas (cerebellar PNET), are the most common malignant brain tumor of childhood (3). They are highly invasive and often metastasize within the CNS prior to diagnosis. The cell of origin of medulloblastomas are likely multipotential cells residing in the EGL of cerebellum that can generate both neurons and glial cells (188). Studies on normal CNS development often enlighten understanding of the tumor initiation and progression. In normal neurogenesis, PDGF was reported to play an important role in the differentiation of premature neuroepithelial cells into neuronal lineage cells (189). In medulloblastoma tissues and cultured cell lines, PDGF ligands and receptors are also expressed at high levels (190-193). In particular, aberrant PDGFR α activation/expression was associated with abnormal neuronal development and likely the cause of medulloblastoma formation (107, 191, 193). Interestingly, microarray profiling of clinical medulloblastoma specimens revealed that *PDGFRA* expression levels corresponded to the degree of tumor metastasis (192), suggesting that PDGF signaling is responsible for the mobility of medulloblastoma cells within the CNS. Indeed, *in vitro* studies also showed that migration of cultured medulloblastoma cells relied on the PDGFR/ERK signaling cascade (194). The activation of PDGFR α in the medulloblastoma cells, however, appears to be largely associated with PDGF-C expression (193). In the CNS of mouse embryo, PDGF-C was exclusively expressed in the EGL of the cerebellum (113). Therefore, a PDGFR α /PDGF-C autocrine loop is most likely the driving force for medulloblastoma formation from premature neuronal precursors in the cerebellum, although further studies using animal models are required to test this hypothesis.

1.6.3 Ependymal Tumors

Ependymomas are derived from ependymal cells lining the ventricular system in the CNS. The infratentorial ependymomas (in the brain) occur mostly in younger adults and children (3). Early studies using northern blot analysis has detected PDGFR α and PDGF-A mRNAs expression in human ependymoma tissue (195). Little is known about the significance of PDGF signaling in the development of these tumors. A large-scale genomic analysis of gene expression signature in clinical ependymomas suggested that the ependymoma initiating cells are embryonic radial glia (RG)-like cells (196, 197). In mouse embryos, RG cells are important for migration of PDGFR α /NG2-positive glial progenitor cells as well as neurons (198). Whether PDGF signaling plays a role in malignant transformation of these ependymoma stem cells is unknown.

1.6.4 Meningeal Tumors

Meningiomas are slow-growing intracranial tumors and mostly benign. However, the higher-grade meningiomas are more aggressive and frequently recur after surgical removal of the primary tumors, and may be fatal upon relapse (3). Early studies showed that PDGF-A, PDGF-B, and PDGFR β , but not PDGFR α , mRNAs and proteins were detected in high levels on human meningioma tissues (199-201). Subsequent study further demonstrated the presence of phosphorylated/activated PDGFR β in meningiomas, indicating that autocrine stimulation of PDGF signaling is responsible for proliferation of this tumor (202). More recently, high throughput IHC-based tissue array identified PDGFR β as a useful biomarker for high-grade anaplastic meningiomas (203). Several *in vitro* studies also complemented these observations by

showing that PDGF-BB can stimulate downstream signaling and growth of the cultured meningioma cells (204). In particular, MAPK (205) and PI3K/AKT/S6K (206) pathways likely represent the major transducers of PDGF signaling in inducing the growth of human meningiomas. Interestingly, in some rare cases of patients with concurrent GBM and meningioma at adjacent sites, PDGFR α and PDGFR β were highly expressed in both tumor types, implying a possible causal role of paracrine PDGF that induces formation of one type of tumor by another (207).

1.7 PDGF-TARGETED THERAPIES

Decades of research performed on malignant gliomas have provided a better picture of the molecular alterations that frequently occurred in the tumor cells. The large-scale genomic profiling of GBMs such as the TCGA project identified *PDGFRA* as one of the most frequently altered genes in GBMs (10, 11). And the Proneural subtype of GBMs that frequently harbor *PDGFRA* alterations are the most resistant to standard chemo-/radiotherapy (11). Molecular therapies targeting PDGFR have been under intensive investigation both in preclinical animal models and in clinical trials (208). Most of the anti-PDGF therapies under investigation involve the use of small molecule tyrosine kinase inhibitors, which bind to the ATP-binding pocket of the PDGFR kinase domain. However, there is no kinase inhibitor that specifically binds to PDGFR α or β . Various tyrosine kinase inhibitors in development that are able to cross-target PDGFRs as well as a PDGFR α -specific neutralizing monoclonal antibody will be discussed here.

1.7.1 Imatinib mesylate

Imatinib mesylate (Gleevec, formally STI-571) blocks the ATP binding site of tyrosine kinases and is a multiple tyrosine kinase inhibitor targeting PDGFRs, c-Kit, c-Fms, and Bcr-Abl. It was initially developed for treatment of Philadelphia chromosome-positive chronic myeloid leukemia (CML) with constitutive activation of Bcr-Abl (209), and was later investigated for its anti-tumor activity against other types of cancers including malignant gliomas. In preclinical models using human glioma-derived cell lines implanted into brain of nude mice, imatinib dramatically decreased the size of tumor and prolong survival of mice (210, 211). However, several phase II clinical trials of imatinib monotherapy for recurrent gliomas have been disappointing (Table 2) (212-214). In one study with 55 patients, the 6-month PFS (PFS-6) was 3% for GBMs and 10% for anaplastic gliomas (212); in another one that enrolled 112 patients, PFS-6 was 16% for GBMs, 4% for oligodendrogliomas, and 9% for anaplastic astrocytomas (213). The minimal responses of gliomas to imatinib were not likely due to the poor accessibility of the tumor mass to the drug, since intact imatinib was detected in post-treatment tissue specimens (214). IB analyses performed on pre- and post-imatinib treatment biopsies revealed that p-Akt and p-Erk levels were not decreased in most of the specimens. However, cautions should be taken in interpreting these results since most of the pre-treatment tumors in this study expressed low or undetectable levels of PDGFR α by IB analysis (214). Interestingly, in one of the tumors with decreased PDGFR β level after imatinib treatment, there were concomitant increases of EGFR, Akt, and Erk activation (214), suggesting that inhibition of one RTK may activate another, and the same set of downstream effectors may be activated by redundant RTK signaling (215). In addition, intratumoral hemorrhage observed in some of the glioma patients that received imatinib

treatment was another factor that may affect the interpretation of the efficacy of imatinib (212). The cause of the hemorrhage was believed to be the off-target inhibition of PDGFR β in the normal perivascular cells in the brain (212). Based on these studies, the efficacy of imatinib as a single agent appears to be limited, at least in unselected patients with recurrent GBMs. Imatinib treatment of pre-selected glioma patients with PDGFR expression, however, yielded promising results, with a PFS-6 of 32.4% (18).

Due to the disappointing results from imatinib monotherapy, new clinical trials have been focusing on testing the efficacy of imatinib in combination with chemotherapy drugs. The strategy is promising in that imatinib was shown to modulate the tumor interstitial hypertension (216), multidrug resistance transporter ABCG2 (217), and angiogenesis processes (218), conferring higher drug uptake into tumor cells. In initial phase II trials using a combination of imatinib and hydroxyurea (219, 220) for patients with recurrent grade III gliomas or GBMs, the efficacy of imatinib plus hydroxyurea were encouraging. However, the following phase II and III studies on unselected recurrent GBM patients again did not show clinical meaningful anti-tumor activity (Table 2) (221, 222). To improve the delivery of TMZ into the tumor, imatinib was also used in combination with TMZ in a clinical trial. *In vitro*, imatinib plus TMZ elicited a synergistic anti-tumor effect on cultured human glioma cell lines (223). In the phase I clinical trial, dose-intensive imatinib plus TMZ were well tolerated and showed durable anti-tumor activity in some of the glioma patients (Table 2) (224), although more definitive results need to be obtained from the subsequent phase II study. Imatinib has also been investigated for its anti-tumor activity against other brain tumors. *In vitro* imatinib was able to inhibit PDGF-B-mediated Akt and Erk activation, and tumor cell migration and invasion of human medulloblastoma cell lines (225), whereas the effect of imatinib on clinical medulloblastomas is unknown. Also in a

phase I trial, imatinib doses have been determined for pediatric newly diagnosed brainstem gliomas and recurrent HGG (226). The efficacy of imatinib in treating childhood gliomas will necessitate design of a subsequent phase II study.

Table 2. Summary of PDGF-targeted Therapies (Updated 4/14/2011)

Generic Name	Other Names	Targeted Molecules	Combination Drugs	Completed and Ongoing Clinical Trials	References
Imatinib Mesylate	Gleevec Glivec STI-571 CGP 57148	PDGFRs c-Kit c-Fms Bcr-Abl	Monotherapy	Unsatisfactory (Low PFS in Phase II)	(212), (213), (214)
			Monotherapy	Ongoing Phase I/II trial on recurrent brain tumor	clinicaltrials.gov
			Hydroxyurea	Unsatisfactory (Low anti-tumor activity in Phase II/III)	(219), (221), (221), (222)
			Hydroxyurea	Ongoing Phase II trial on low-grade gliomas	clinicaltrials.gov
			Hydroxyurea + Zactima TMZ	Ongoing Phase I trial on recurrent gliomas Encouraging (Durable anti-tumor activity in Phase I)	clinicaltrials.gov (224)
Sunitinib Malate	SU11248 Sutent	PDGFR β VEGFR2 c-Kit FLT3	Monotherapy	Unsatisfactory (Low anti-tumor activity in Phase II)	(227)
			Monotherapy	Several ongoing Phase II trials on recurrent AAs and GBMs	clinicaltrials.gov
			Cilengitide	Pilot feasibility study on GBMs	clinicaltrials.gov
Cediranib Maleate	AZD2171 Recentin	PDGFRs VEGFRs c-Kit	Monotherapy	Encouraging (high PFS but with aggressive recurrences in Phase II)	(228)
			RO4929097	Ongoing Phase I trial on advanced brain tumors	clinicaltrials.gov
			Lomustine	Ongoing Phase III trial on recurrent GBMs	clinicaltrials.gov
			Bevacizumab	Ongoing Phase I trial on GBMs	clinicaltrials.gov
			Gefitinib	Ongoing Phase II trial on recurrent or progressive GBMs	clinicaltrials.gov
			TMZ + X-ray Cilengitide	Ongoing Phase II trial on newly diagnosed GBMs Ongoing Phase I trial on recurrent or progressive GBMs	clinicaltrials.gov clinicaltrials.gov
Vatalanib	PTK878 ZK 222584 CGP-79787	PDGFRs VEGFR1 and 2 c-Kit c-Fms	TMZ + Radiation	Encouraging (Phase I/II with high PFS but discontinued)	(229)
			TMZ + Radiation Imatinib + Hydroxyurea	Ongoing Phase I trial on newly diagnosed GBMs Well-tolerated in Phase I	clinicaltrials.gov (230)

Table 2 (Continued)

Sorafenib Tosylate	Nexavar BAY 43-9006	PDGFR β VEGFR2 c-Kit FLT Raf	Monotherapy	Ongoing Phase I trial on recurrent or progressive GBMs	clinicaltrials.gov
			TMZ	Unsatisfactory (Low anti-tumor activity in Phase II)	(231), (232)
			TMZ + Radiation Temozolimus	Several ongoing Phase I/II trial on newly diagnosed GBMs Ongoing Phase I/II trial on recurrent GBMs	clinicaltrials.gov clinicaltrials.gov
			Erlotinib + Temozolimus + Tipifarnib	Ongoing Phase I/II trial on recurrent GBMs	clinicaltrials.gov
Pazopanib hydrochloride	Votrient GW786034	PDGFRs VEGFR1, 2, 3 c-Kit	Monotherapy	Unsatisfactory (Low PFS in Phase II)	(233)
			Lapatinib	Ongoing Phase II trial on relapsed malignant gliomas	clinicaltrials.gov
Tandutinib	MLN-518 CT53518	PDGFRs FLT3 c-Kit	Monotherapy	Ongoing Phase I/II trial on recurrent or progressive GBMs	clinicaltrials.gov
			Bevacizumab	Ongoing Phase II trial on recurrent brain tumors	clinicaltrials.gov

Abbreviations: FLT, c-Fms-like tyrosine kinase; AA, astrocytoma.

1.7.2 Sunitinib malate

Sunitinib malate (SU11248 or Sutent) is a potent multiple tyrosine kinase inhibitor that targets PDGFR β , VEGFR2, c-Kit, Fms-like tyrosine kinase 3 (FLT3), and several other kinases (234). Like imatinib, sunitinib showed significant anti-tumor and anti-angiogenic activities in cultured human glioma cell lines *in vitro* as well as orthotopic mouse model *in vivo* (235). However, in a phase II study in patients with recurrent high-grade gliomas, sunitinib showed minimal efficacy as a monotherapy (Table 2) (227). Neither the gene copy number nor the protein expression of PDGFR α , VEGFR, or c-KIT was able to predict the response to sunitinib treatment. In medulloblastomas, sunitinib was also shown to display a potent activity against tumor cell

migration and survival *in vitro* (236). Whether this observation reflects its anti-tumor activity in the clinical medulloblastomas is not known.

1.7.3 Cediranib maleate

Cediranib maleate (AZD2171 or Recentin) is a potent inhibitor for PDGFR α and β , VEGFRs, and c-Kit (237). A phase II study of cediranib in patients with recurrent GBMs has been performed (Table 2) (228). The results were encouraging with a PFS-6 of 25.8%. However, a recent finding suggested that potentially more aggressive tumors were able to recur after cediranib treatment of GBM patients (154). These recurrent tumors expressed increased oncoproteins such as PDGF-C and c-Met, harbored more tumor-infiltrating myeloid cells (TIMs), and were potentially more aggressive than the untreated tumors (154). Thus whether cediranib monotherapy is a viable treatment option for GBM patients needs further investigations.

The abnormal tumor vasculature is one of the cause of poor drug delivery to the tumor mass. The ability of cediranib or similar VEGFR/PDGFR inhibitors to normalize the tumor vessels (238) thus suggests that cediranib may potentially increase the efficacy of chemotherapy using cytotoxic drugs. A phase I/II clinical trial is currently being conducted using this regimen in patients with newly diagnosed GBMs (Table 2) (see <http://clinicaltrials.gov/> for more information).

1.7.4 Vatalanib

Vatalanib (or PTK878/ZK 222584) is an inhibitor for PDGFRs, VEGFR1 and 2, c-Kit, and c-Fms (237). In preclinical models, vatalanib effectively suppressed PDGF- or VEGF-induced tumor growth (239, 240). The initial phase I/II trial using concomitant and adjuvant TMZ and radiotherapy with vatalanib showed promising results, with a PFS-6 of 63.2% (Table 2) (229). Although the initial trial was discontinued, a separate phase I trial using the similar regimen on newly diagnosed GBM patients have been initiated (Table 2) (see <http://clinicaltrials.gov/> for more information).

1.7.5 Sorafenib

Sorafenib tosylate (or Nexavar/BAY 43-9006) is multiple kinase inhibitor against PDGFR β , VEGFR2, c-Kit, FLT, and Raf (237). Sorafenib was shown to exhibit significant anti-tumor activity in human glioma- or medulloblastoma-derived cell lines both *in vitro* and *in vivo* in orthotopic xenograft transplantation models, mechanisms of which were likely due to the inhibition of STAT3 activity in these cells (241-243). However, phase II studies using sorafenib with TMZ in newly diagnosed GBM or recurrent GBM patients were discouraging (Table 2) (231, 232). Several phase I/II studies are being conducted using either in monotherapy or in combination with other treatment modalities (Table 2) (see <http://clinicaltrials.gov/> for more information).

1.7.6 Pazopanib hydrochloride

Pazopanib hydrochloride (Votrient or GW786034) is a multi-targeted inhibitor for PDGFRs, VEGFR1, 2, 3, and c-Kit (237). It has been approved for treatment of advanced or metastatic renal cell carcinomas (8). In recurrent GBMs, a phase II trial of single-agent pazopanib did not show a dramatic improvement in these patients, with a PFS-6 of only 3% (Table 2) (233). More studies are needed to test whether combination therapy using pazopanib can exert a better anti-tumor effect.

1.7.7 Tandutinib

Tandutinib (formally MLN-518) is an orally active inhibitor of FLT3, PDGFRs, and c-Kit (244). Several phase I/II trials are being conducted using tandutinib mono- or combination therapy (Table 2) (see <http://clinicaltrials.gov/> for more information). However, toxicity to the neuromuscular junctions has been reported and may discourage the use of this drug in certain patients (245).

1.7.8 Other PDGF-targeted Agents

There are numerous other tyrosine kinase inhibitors that are under development or in clinical trials to determine their efficacy against malignant brain cancers. Dasatinib (or Sprycel) is a potent multiple tyrosine kinase inhibitor that targets PDGFRs, c-Kit, Bcr-Abl, and SFKs (234).

Due to its potent activity against Src phosphorylation, it may be effective in treatment of patients with p-Src positive tumors (246). A novel multiple tyrosine kinase inhibitor, SU14813, inhibits phosphorylation of VEGFR-2, PDGFR β , and FLT3, and exerted a potent anti-tumor effect in a pre-clinical xenograft glioma model (247). Clinical evaluations of its efficacy in glioma patients are underway. SU6668 is an inhibitor of Flk-1, FGFR, and PDGFR β . Preclinical studies of SU6668 in human xenografts of gliomas yielded promising results, with significant inhibition of growth of C6 glioma cells and suppression of angiogenesis (248). It is currently under investigation for its clinical performance in various solid tumors. PDGF-targeted monoclonal antibodies have also been developed for treatment of various cancers including gliomas. One fully human neutralizing monoclonal antibody that targets specifically PDGFR α but not PDGFR β was developed and showed significant anti-tumor effect against human GBM cell line xenograft (249). A phase II trial using this antibody for treating patients with recurrent GBMs is being conducted to evaluate its clinical efficacy (250) (also see <http://clinicaltrials.gov/> for more information).

1.7.9 Lessons Learned From Clinical Trials

Although PDGF targeted therapies using various tyrosine kinase inhibitors have been extensively studied over the past few years, the results were generally disappointing and have yet to shift the standard clinical treatment of GBMs, which encompasses maximal surgical resection, followed by TMZ and radiation (251). Several factors might be contributing to the failure of these PDGF-targeted inhibitors in GBM treatment. First, delivery of drugs to the tumors in the brain was limited or insufficient to mount an effective anti-tumor response. The specialized structure of

BBB is one of the impediments that restrict the penetration of therapeutic drugs into the brain parenchyma (252). Second, brain tumor, especially malignant glioma, cells are highly infiltrative (2). Perhaps tumor cells were disseminated throughout the brain parenchyma prior to the administration of various PDGF inhibitors. Third, tumors in the patients of clinical studies might not respond to PDGF inhibition due to a lack of PDGFR expression/activation in the tumors. Thus, pre-selection of enrolled patients that will potentially benefit from anti-PDGF treatment should be performed in each clinical trial to more accurately determine the efficacy of anti-PDGF treatments. A personalized treatment options should be provided for each individual in the future studies. Fourth, as suggested by its name, GBM is a disease of mixed cell types and genetic alterations. Heterogeneity of GBMs is another major factor that significantly decrease the efficacy of targeted therapies. Additionally, inhibition of one pathway may activate another one to either compensate (215) or substitute for (154, 253) the inhibited signaling molecules. The relapsed tumors are potentially more aggressive, resistant to the original therapies, and often lead to a rapid death of the patients. Fifth, the efficacy of PDGF-targeted therapies might also be reduced by multiple off-target effects of these agents on normal brain cells. One example is the intratumoral hemorrhage caused by off-target inhibition of PDGFR β expression in normal perivascular cells observed in some of the glioma patients that received imatinib treatment (212). Lastly, the small population of CD133-positive CSC (254) identified in the brain tumor may represent another source of tumor recurrence after anti-PDGF treatment. Targeted therapies such as anti-PDGF inhibitors are expected to eliminate the tumor cells that are “addicted” to the targeted signaling pathways for survival and proliferation, but might leave the relatively dormant CSCs intact. These CSCs were later able to self-renew and differentiate into tumor cells that may acquire distinct properties and genetic aberrations from those of the primary tumors. All these

and other factors make the PDGF-targeted therapy an even more challenging issue than was previously thought.

1.7.10 Future Directions

Despite significant anti-tumor effect of various PDGF-targeted therapies in pre-clinical animal model testing, the results of subsequent clinical trials were often disappointing. In order to design therapeutic strategies that can benefit patients with brain tumors driven and maintained by PDGF signaling, more thorough pre-clinical studies are required. Various animal models that are candidates for this purpose have been proposed (255). Additionally, identification of new potential molecular targets in tumors induced by PDGF signaling is also important. The application of systems biology to the genomic data obtained from patient samples is expected to aid in this process (207). To generate a network of genes that share a regulatory program, the commonly altered genes in GBM were grouped into several functional “modules.” The interactions between each cancer-altered gene and other non-altered “linkers” can be identified within and among different modules (143). The *SHP-2/PTPN11* was identified in this network approach as one of the six linkers, and was also shown to be important in the PDGF-driven gliomagenesis in our model (150). Molecules such as *SHP-2/PTPN11* that are not commonly overexpressed or mutated in GBMs and are often understudied. However, several signaling pathways may converge on these molecules to exert downstream functions. Besides its involvement in regulating the PDGFR α /PI3K/Akt pathway in gliomas (150), SHP-2 has also been known to mediate EGFR/PI3K/Akt signaling (256) and downstream of Ras/MAPK pathway (257). Thus it represents one of the molecules loss of which may lead to disruption of

multiple signaling cascades involved in tumorigenesis. As tumors are now considered to be rather “network-addicted” than single “oncogene-addicted” (258), perhaps strategies targeting such a molecule in monotherapy or in combination with other cytotoxic drugs will prove more efficient than targeting multiple upstream RTKs. With the recent advances in the large-scale whole-genome profiling of GBMs, we expect that more promising targets like these can be uncovered. However, preclinical studies of various targeted pharmacological drugs require a more stringent selection of animal models that can most accurately re-capitulate the human tumors in every aspect. Additionally, personalized medicine should be given to each individual exploiting data gained from genomic profiling and systems biology.

2.0 PDGFRA OVEREXPRESSION COOPERATES WITH P16INK4A LOSS TO PROMOTE GLIOMA FORMATION FROM MOUSE ASTROCYTES OR HUMAN GLIOMA CELLS

2.1 INTRODUCTION AND RATIONALE

GBM is the most common and malignant tumor in the CNS. The prognosis of patients with this cancer remains dismal despite intensive treatments and care. A better understanding of the mechanisms of tumorigenesis is necessary to design more efficient therapeutic strategies. The recent advance in high-throughput genomic analysis technology has made possible to analyze GBM genomes in large scale (10). Although cancer genomics is still in its infancy and yet to impact the standard clinical treatments, studies have been underway to functionally validate the knowledge we gained from these genomic data in the hope that it will ultimately be routine to characterize the GBM genomes of each patient, and provide patients with personalized medications.

Notably among the most frequently altered genes in GBMs, the gene encoding PDGFR α was amplified in ~13% of the total GBMs analyzed, and deletion of the tumor suppressor *CDKN2A* locus was frequently found in these PDGFR α amplified GBMs (10) (11). Most of the animal models of PDGF-induced gliomagenesis involve overexpression of PDGF-B chain in the mouse brain. The potential of PDGF-A chain, however, was relatively unexplored despite its

frequent co-overexpression with the *PDGFRA* gene and important role in glial progenitor cell development. The PDGFR α -positive progenitor cells that respond to PDGF stimulation can be found in various parts of the adult brain (104, 162, 166). Exogenous PDGF-A infusion into the adult SVZ induces the PDGFR α -positive neural progenitor cells to generate glioma-like lesion in the mouse brain (104). Compared with PDGF-B homodimer, PDGF-A only binds to PDGFR α but not PDGFR β , making it a less potent tumor inducer than PDGF-B. Indeed, mouse transplanted with PDGF-B overexpressing *Ink4a/Arf*-null astrocytes developed tumors with shorter latency and increased malignancy (by our lab, unpublished data). These tumors also displayed high angiogenic characteristics with a high degree of microvascular proliferation, further demonstrating the role of PDGF-B/PDGFR β in tumor angiogenesis (66, 69), one mechanism of which may involve modulation of VEGF expression in the tumor microenvironment by PDGF-B in a paracrine manner (259). In order to determine which signaling pathway(s) downstream of PDGFR α is necessary for its oncogenic capacity, our lab chose PDGF-A instead of PDGF-B in that PDGF-A can only stimulate PDGFR α but not PDGFR β . To investigate how PDGF-A-mediated PDGFR α activation contributes to glioma formation, we utilized an orthotopic transplantation model, in which we implanted various PDGF receptor or ligand overexpressing human or mouse cells into the brain of mice to assess their tumorigenic potentials (150). Furthermore, we utilized cells harboring another frequently co-altered genetic lesion, the *Ink4a/Arf* deletion, to demonstrate cooperation between this and the *PDGFRA* amplification during the glioma development.

2.2 MATERIALS AND METHODS

2.2.1 Cell Lines and Reagents

Primary *Ink4a/Arf*^{-/-} mAst were derived and propagated as previously described (45). Human glioma cell lines, LN444, LN443, LN-Z308, and LN319, were obtained from American Cell Type Culture Collection (Manassas, VA) or from our own collection (260). Unless otherwise mentioned, all glioma cell lines and primary mAst were routinely maintained in 5% CO₂ at 37°C, in DMEM (Invitrogen) containing 10% FBS (Hyclone), 100 units/ml penicillin, and 100 µg/ml streptomycin (Invitrogen).

The following antibodies and reagents were used in this study: rabbit anti-PDGFR α (sc-338, 1:500 for IB; 1:50 for IHC), rabbit anti-PDGF-A (sc-128, 1:500 for IB; 1:50 for IHC), rabbit anti-p16 (sc-759, 1:500), and goat anti- β -actin (sc-1616, 1:500) antibodies were from Santa Cruz Biotechnology Inc., Santa Cruz, CA; a rabbit anti-phospho-RB (Ser807/811, #9308, 1:1000) antibody was from Cell Signaling Technology, Danvers, MA; mouse anti-nestin (MAB353, 1:100), rabbit anti-GFAP (AB5804, 1:500), rabbit anti-NG2 (AB5320, 1:100), and mouse anti-phosphotyrosine (clone 4G10, #05-321, 1:1000) antibodies were from Millipore, Temecula, CA; a mouse anti-neuronal class III β -tubulin (clone TUJ1, MMS-435P, 1:250) antibody was from Covance, Richmond, CA; a mouse anti-SHP-2 (610621) antibody was from BD Biosciences, San Jose, CA; a mouse anti-p14/ARF (P2610, 1:500) antibody was from Sigma-Aldrich, St. Louis, MO; a mouse anti-p53 (OP33, 1:500) antibody was from EMD Chemicals, Gibbstown, NJ; a rabbit anti-Ki67 antigen (NCL-Ki67p, IHC, 1:200) antibody was

from Leica Microsystems Inc., Bannockburn, IL; MatrigelTM Basement Membrane Matrix, Growth Factor Reduced (GFR) (#356230) was obtained from BD Biosciences, San Jose, CA; CDK inhibitor PD0332991 (S1116) was from Selleck Chemicals, Houston, TX; Cisplatin (C3374) was from LKT Laboratories, Inc., St. Paul, MN. All secondary antibodies were from Vector Laboratories (Burlingame, CA) or Jackson ImmunoResearch Laboratories (West Grove, PA). All other reagents were from Invitrogen, Sigma-Aldrich, or Fisher Scientific.

2.2.2 Retroviral and Lentiviral Constructs and Infections

The retroviral vector pMXI-*gfp* was a gift from Dr. R. Pieper at the University of California, San Francisco (261). The cDNA insert encoding WT PDGFR α (a gift from Dr. Carl-Henrik Heldin at Uppsala University, Uppsala, Sweden) was excised from a pcDNA3 vector and subcloned into a BamHI site of the pMXI-*gfp* retroviral vector. To generate retroviral vectors encoding PDGF-A, cDNA insert encoding PDGF-A was excised from pcDNA3 vector and subcloned into a BamHI-NotI site of pMXI-*gfp* or into an EcoRI site of a pMSCV (Murine Stem Cell Virus)-dsred2 retroviral vector (a gift from Dr. T. Cheng at the University of Pittsburgh, Pittsburgh). For experiments of p16INK4a (a gift from Dr. L. Chin, Dana-Farber Cancer Institute, Boston) and p19ARF (a gift from Dr. Y. Zheng, Cincinnati Children's Hospital Medical Center, Cincinnati) re-expression, retroviral vectors pBabe-Puro-*p16INK4a* and pMIEG3-*egfp-p19ARF* were used. For shRNA experiments, the lentiviral vectors pLKO.1-sh*CDKN2A* (6 clones) were purchased from Thermo Scientific, Huntsville, AL.

Retroviruses and lentiviruses were produced by co-transfecting various cDNA and packaging plasmids (pKat and pVSV-g for retrovirus; pMDL-RRE, pRSV-REV, and pVSV-g

for lentivirus) into 293T or PhoenixTM (Orbigen Inc., San Diego, CA) cells using Lipofectamine 2000TM reagent according to manufacturer's instruction (#52758, Invitrogen). Forty-eight hours after transfection, the supernatants containing viruses were filtered by a 0.45- μ m syringe filter (5) and added into the culture media supplemented with 8 μ g/ml polybrene. Forty-eight hours after the infection, transduced human glioma cells or primary astrocytes were harvested and replated in DMEM containing 10% FBS and 2 μ g/ml puromycin or 300 μ g/ml hygromycin for drug selection or sorted by Fluorescence-activated Cell Sorting (FACS) for GFP expression. Expression of exogenous PDGFR α in the resultant cell populations was validated by IB and GFP expression by FACS analysis.

2.2.3 Reverse Transcriptase Polymerase Chain Reaction (RT-PCR)

Total RNAs from various human glioma cell lines were extracted using RNeasy Mini Kit (Qiagen). Approximately 5 μ g of total RNAs were used to synthesize the first strand cDNA by SuperscriptTM II Reverse Transcriptase (Invitrogen). The following primers were used for the PCR reactions: p16INK4a forward, 5'-CAA CGC ACC GAA TAG TTA-3'; reverse, 5'-AGC ACC ACC AGC GTG TC-3'; actin forward, 5'-CGG GAA ATC GTG CGT GAC AT-3'; reverse, 5'-GGA GTT GAA GGT AGT TTC GTG-3'. The resulting PCR products were then analyzed using 2% agarose gel electrophoresis.

2.2.4 Mouse Glioma Transplantation/Xenograft

Experiments of glioma xenografts were performed as previously described (262). For intracranial glioma xenograft experiments, human glioma cells or mAst were harvested and re-suspended at 1×10^5 cells / μ l in PBS solution and placed on ice until injection. Anesthetized 6-week-old female athymic *nu/nu* mice (Taconic Farms Inc., Hudson, NY) were placed on a stereotactic frame with ear bars. A burr hole was drilled 2 mm lateral and 1.5 mm anterior to the Bregma. Approximately 3×10^5 cells in a 3 μ l volume (for mAst) or 5×10^5 cells in a 5 μ l volume (for human glioma cells) were then injected 3 mm below the skull into the striatum of the brain. Mice were then monitored every 3 days. When neuropathological symptoms developed due to tumor burdens in the brain, the mice were euthanized. Brains of mice were then removed, embedded in Optimum Cutting Temperature (OCT) compound (Tissue-Tek) at -80°C , and cryo-sectioned at 5- μ m thickness. Sections of brains were stored at -80°C until histological analysis. For s.c. tumor xenograft experiments, 5 million of various types of cells in 100- μ l PBS were mixed with equal volume of growth factor-reduced MatrigelTM and injected into flanks of mice using a 1-ml syringe with a 30-gauge needle (Bektom Dickinson). Tumor volumes were measured every 3 days with a caliper, estimated as $(a^2 \times b) / 2$, $a < b$ (263), and analyzed with GraphPad Prism version 4.00 for Windows (GraphPad Software inc., La Jolla, CA). Mice were euthanized before s.c. tumors reached 2000 mm^3 in volume or when pathological symptoms developed due to tumor burdens. All animal experiments were approved by Institutional Animal Care and Use Committee (IACUC) of University of Pittsburgh, Pittsburgh, PA.

2.2.5 Immunohistochemistry

Thin sections of harvested mouse brains with various tumors were analyzed by IHC using indicated antibodies or a TUNEL staining kit as previously described (260, 262). Briefly, 5- μ m frozen sections were fixed in pre-chilled acetone at -20°C for 5 min, rinsed with PBS, and blocked by AquaBlock (East Coast Biologics Inc.) for 1 hour at room temperature. Afterwards, various tissue sections were then incubated with a primary antibody overnight at 4°C, and blocked by Peroxidase Blocking Reagent (DAKO) for 10 minutes, followed by incubation with a biotinylated secondary antibody for 30 min at room temperature. After washed in PBS, stained tissue sections were visualized by diaminobenzidine chromophore and H₂O₂ followed by hematoxylin counterstaining. Sections were then dehydrated by graded ethanol, and mounted with Permount Solution (5).

2.2.6 Immunoblotting

For IB analysis, total cell lysates containing ~30 μ g of total proteins were separated in a SDS-PAGE gel under a reducing condition. The separated proteins were then transferred to a polyvinylidene fluoride (PVDF) membrane (Bio-Rad), blocked by 5% (w/v) nonfat dry milk (Bio-Rad) in PBS, and probed with indicated primary antibodies at 4°C overnight. Proteins of interest were then visualized by incubating the membrane with indicated peroxidase-labeled secondary antibodies at room temperature for 30 min followed by detection with enhanced chemiluminescence (ECL, Amersham Bioscience) reaction following manufacturer's instructions.

2.2.7 Soft Agar Colony Formation Assay

Colony formation assay in soft agar was performed as previously described (264). Briefly, approximately 5000 cells were seeded in a 0.5% Noble Agar top layer with a bottom layer of 0.8% Noble Agar in each of the triplicate wells of a 24-well plate. Growth factor-reduced MatrigelTM (1 mg/ml) was added into the top layer with or without indicated inhibitors. PDGF-A-expressing cells in 10% of total cells were included as a source of PDGF-AA. DMEM containing 10% FBS was added 3 days after plating and changed every 3 days thereafter. Colonies were scored after 2-3 weeks using Olympus SZX12 stereomicroscope and data were analyzed using GraphPad Software.

2.2.8 Cell Proliferation Assay

Cell proliferation and viability were determined as previously described (45). Briefly, 50,000 cells were seeded in 10% FBS / DMEM, split, counted, and re-seeded every 3 days in a 6-well plate. Population doubling was calculated by dividing the total cell number by the cells seeded (50,000 cells), using \log_2 versus the days in culture to determine the proliferation rate of each type of cells.

2.2.9 Cell Viability Assay

Cell viability was assessed by a colorimetric assay using a tetrazolium salt WST-1 (4-[3-(4-iodophenyl)-2-(4-nitrophenyl)-2H-5-tetrazolio]-1,3-benzene disulfonate) reagent (152) according to manufacturer's instruction. Briefly, 3000 cells were seeded in triplicate wells of a 96-well microplate and incubated in a serum-free medium for 48 hours at 37°C and 5% CO₂. A WST-1 reagent was then added to the media (10 µl/well) and incubated for an additional 2 hours. Light absorption of samples in each well was measured at a wavelength of 450 nm in a ThermoMax microplate reader (Molecular Devices, Sunnyvale, CA). Wells containing only culture media were used as a background control for all the samples measured. Trypan Blue Exclusion assay was performed as previously described (265). Briefly, cells were harvested and mixed with an equal volume of Trypan Blue dye. The number of live (appearing bright under light microscope) cells was then estimated from a total number of 200 cells from the harvested cells. The data were then analyzed using GraphPad Software.

2.2.10 Statistical Analyses

One-way ANOVA or an unpaired, two-tailed Student's *t* test followed by Newman-Keuls post-test was performed using GraphPad Prism software. A *P* value of 0.05 or less was considered statistically significant.

2.3 RESULTS

2.3.1 PDGFRA and *Ink4a/Arf* aberrations in mouse astrocytes *in vitro*

To determine whether activation of PDGFR α signaling in *Ink4a/Arf*^{-/-} mAst leads to increased proliferation and survival *in vitro*, we overexpressed PDGFR α and/or its ligand PDGF-A chain in a retroviral vector containing an IRES-GFP in *Ink4a/Arf*^{-/-} mAst. The IB experiment showed that the parental mAst expressed very low endogenous PDGFR α and undetectable PDGF-A (Figure 6). Overexpression of the receptor or ligand greatly increased the expression in the cells. *In vitro* growth and survival were further analyzed by using hemacytometer and WST-1 assay (an MTT-like assay that measures the number of viable cells by detecting the activity of mitochondrial dehydrogenases in the sample), respectively. As shown, the impact of PDGFR α / α -A overexpression on the growth of these cells *in vitro* was moderate (Figure 7A and 7B). The time needed for one doubling of these cells is around 12 hours for PDGFR α / α -A mAst, 15 hours for PDGF-A cells, and 20 hours for PDGFR α and GFP control cells. For survival assay, cells were plated in 96-well for 48 hours in serum-deprived medium. WST-1 survival assay was then performed on these cells. As shown, PDGFR α / α -A mAst survived better than the other three cell lines in serum starvation, likely due to its capability to initiate survival pathways via PDGF autocrine signaling. Taken together, PDGFR α and/or PDGF-A overexpression exert moderate effect on *Ink4a/Arf*^{-/-} mAst growth and survival only when both the receptor and ligand are co-transfected into the cells, whereas overexpression of PDGFR α or PDGF-A alone did not markedly affect these processes.

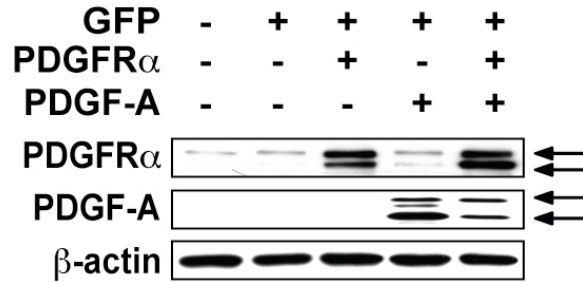


Figure 6. The PDGFR α and/or PDGF-A overexpression in *Ink4a/Arf^{-/-}* mAst.

IB analysis of exogenous expression of PDGFR α and/or PDGF-A in mAst. Arrows, PDGFR α and PDGF-A proteins run as doublet bands. β -actin was used as a loading control.

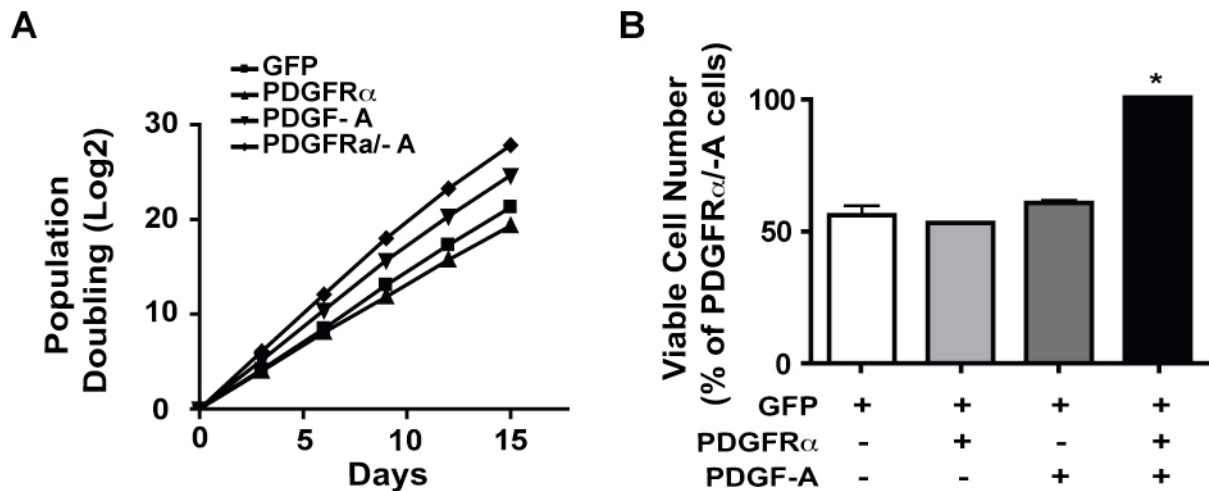


Figure 7. *In vitro* characterization of *Ink4a/Arf^{-/-}* mouse astrocytes overexpressing PDGFR α and/or PDGF-A.

(A) Growth of *Ink4a/Arf^{-/-}* mAsts *in vitro*. 50,000 of various cells with similar passage numbers were seeded in triplicate wells of 6-well plates, counted every three days, and re-seeded. Population doubling was calculated by dividing the total cell number by 50,000 and converting it to a \log_2 value. No significant difference in cell proliferation was found among these cells. (B) Viability of *Ink4a/Arf^{-/-}* mAsts *in vitro*. 3,000 of various cells were seeded in triplicate wells of a 96-well plate, followed by a 48-hour serum starvation. The number of viable cells was estimated using the WST-1 reagent and presented as a percentage to the number of viable

PDGFR α /-A cells. Data are shown as mean \pm s.d. *, $P < 0.001$, one-way ANOVA followed by Newman-Keuls post hoc test.

2.3.2 PDGFRA and *Ink4a/Arf* aberrations in transplanted mouse astrocytes *in vivo*

To assess the effect of PDGF activation on *in vivo* tumor growth of *Ink4a/Arf*^{-/-} mAst, we transplanted these cells into two different anatomic sites in the nude mice, the flanks and the brain. When mAsts expressing PDGFR α and/or PDGF-A were transplanted into the flanks of mice, significant s.c. tumor growth was evident in mice that separately received *Ink4a/Arf*^{-/-} mAst expressing PDGFR α , PDGF-A, or PDGFR α /-A, whereas minimal or no tumor formation was seen in control mice that received *Ink4a/Arf*^{-/-} mAst expressing GFP (Figure 8).

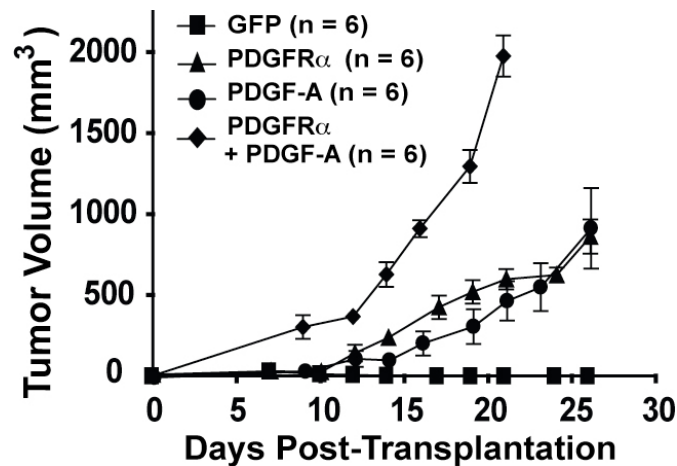


Figure 8. *In vivo* growth of *Ink4a/Arf*^{-/-} mouse astrocytes overexpressing PDGFR α and/or PDGF-A.

Subcutaneous tumor growth of various mAst. Tumor volumes were measured with a caliper, and estimated as $(a^2 \times b) / 2$, $a < b$. n, the number of mice used for each group. Data are shown as mean \pm s.d.

To determine tumorigenicity of these cells in the brain, various mAst were separately implanted into the brain of mice. Notably, mice that received GFP mAst did not show active tumor growth up to 42 days post-implantation, while PDGFR α , PDGF-A, or PDGFR α /-A mAst started to form tumors in the brain as early as 8-11 days, majority of tumors reached a volume of ~25 to 30 mm³ in 25 to 35 days. Moreover, mice that separately received PDGFR α - or PDGF-A-expressing mAst survived up to 2 months post-implantation. On the other hand, all mice received autocrine PDGFR α /-A-expressing mAst developed large and invasive tumors by 20 days with an average survival time of 25 days post-implantation. As shown in Figure 9, significant larger and highly invasive gliomas formed in the brains of mice that received *Ink4a/Arf*^{-/-} mAst overexpressing PDGFR α , PDGF-A, or PDGFR α /-A, whereas only small tumor lesions were found in the brain of mice that received control mAst (Figure 9A to 9J).

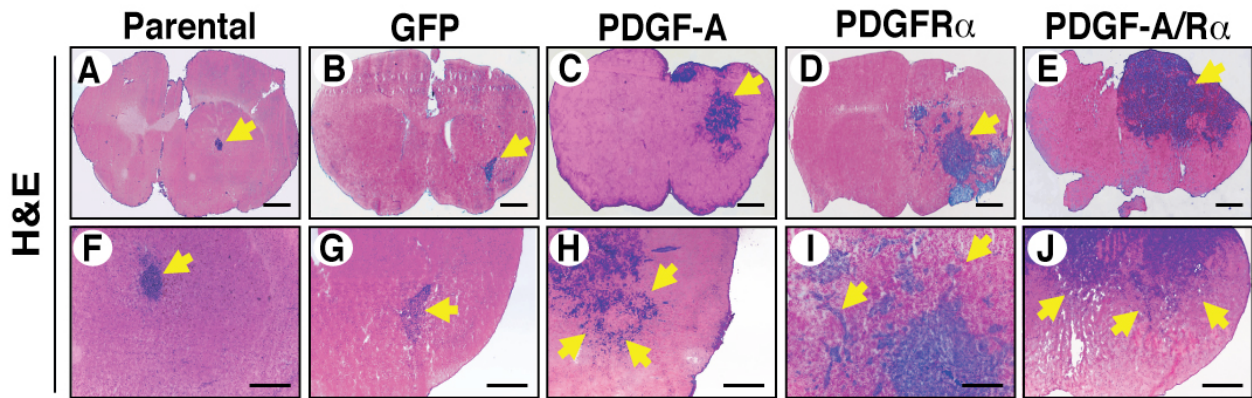


Figure 9. Orthotopic growth in the mouse brain of *Ink4a/Arf*^{-/-} mouse astrocytes overexpressing PDGFR α and/or PDGF-A.

Representative H&E staining images of various brain sections from two independent experiments with at least 3-5 mice per group with similar results. Brains were harvested 25-30 days post-transplantation for (A)-(D), and 20 days for (E). Bars, 1 mm for (A)-(E); 200 μ m for (F)-(J).

Significantly, a ~10-fold increase in the cell proliferation index was found in gliomas derived from PDGFR α -activated mAst compared to control tumors (Figure 10A to F), whereas a ~10-fold decrease of cell apoptosis was seen in PDGFR α -A expressing tumors (Figure 10G). Of note, in established s.c. or brain tumors, exogenous expression of PDGFR α or PDGF-A was maintained at the end of the experiments (Figure 11 and data not shown). Taken together, these results indicate that expression of PDGFR α and/or PDGF-A confers tumorigenicity to *Ink4a/Arf*-deficient mAst in the brain.

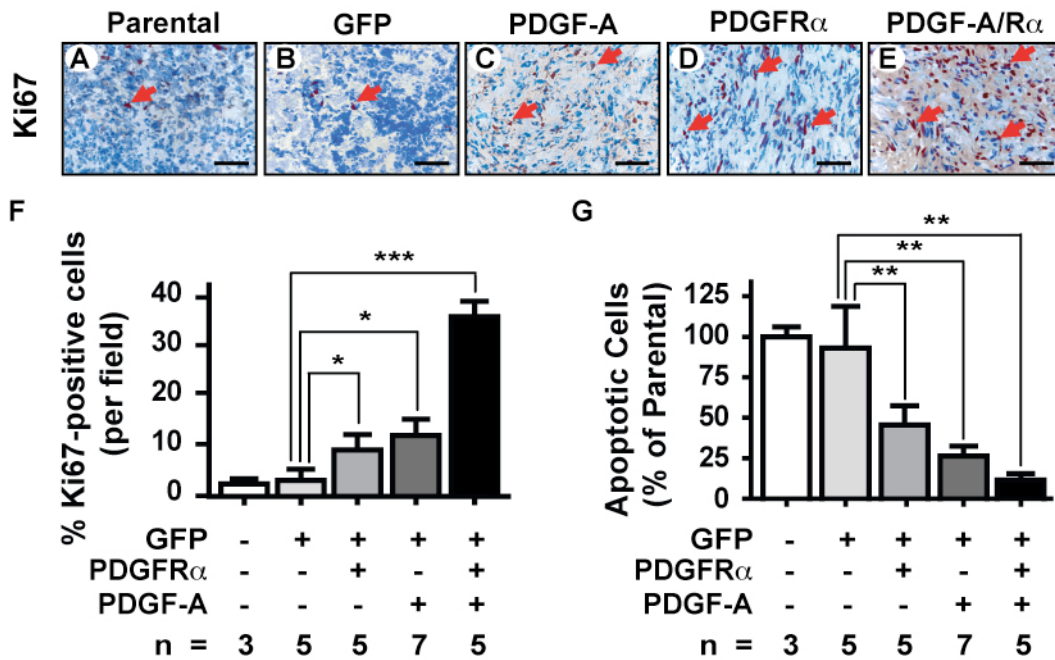


Figure 10. *In vivo* proliferation and apoptosis of *Ink4a/Arf*^{-/-} mouse astrocytes overexpressing PDGFR α and/or PDGF-A.

(A)-(E) Ki-67 staining of the corresponding brain sections in Figure 10(A)-(E). Yellow arrows, tumor mass or invading tumor cells. Red arrows, Ki-67-positive cells. Bar, 50 μ m. Quantification of (F) Ki-67 staining and (G) TUNEL staining of various brain sections. Data are presented as percentage to parental controls (mean \pm s.d.). n, the number of mice used for each group. *, $P < 0.05$; **, $P < 0.01$; ***, $P < 0.001$.

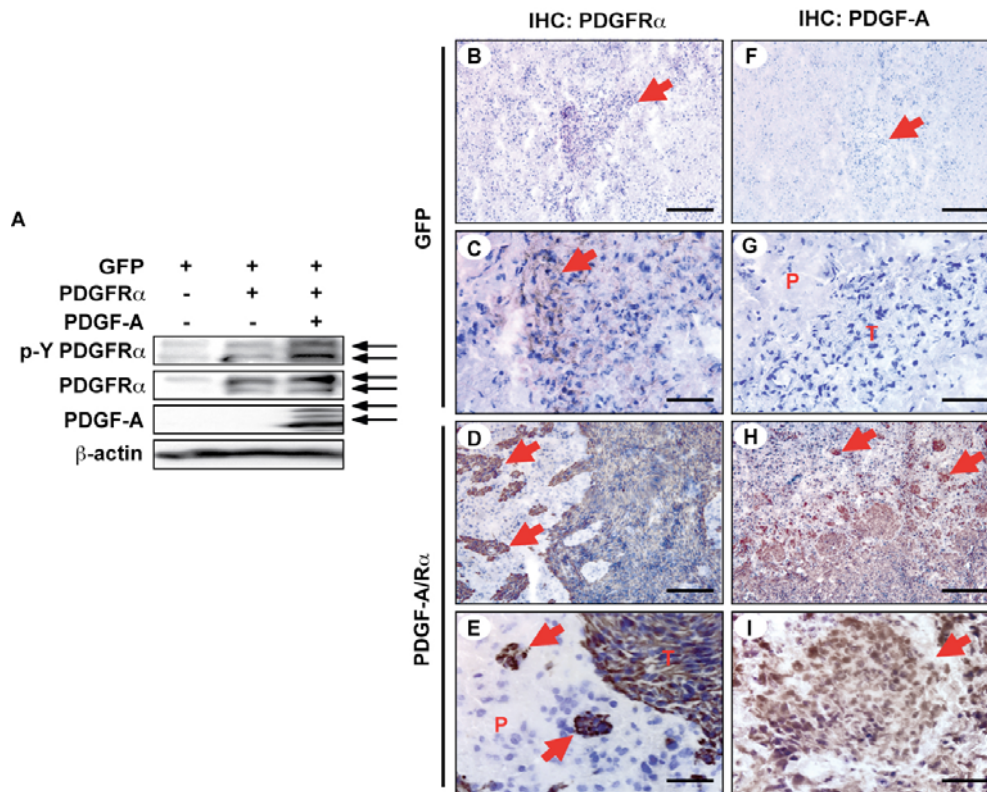


Figure 11. *Ink4a/Arf^{-/-}* mouse astrocytes overexpressing PDGFR α and PDGF-A retained high expression of both the receptor and the ligand *in vivo*.

(A) IB analysis of tissue lysates from s.c. tumors derived from *Ink4a/Arf^{-/-}* GFP control, PDGFR α , and PDGFR α /-A mAst. Various s.c. tumors were snap-frozen, weighed, homogenized, and lysed in lysis buffer before IB analysis. Arrows, PDGFR α and PDGF-A proteins run as doublet bands. β -actin was used as a loading control. (B)-(I) Immunohistochemical (IHC) staining of brain tumors derived from *Ink4a/Arf^{-/-}* GFP or PDGFR α mAst using anti-PDGFR α (panels B-E) and anti-PDGF-A (panels F-I) antibodies. PDGFR α was weakly expressed (panels B and C) whereas PDGF-A proteins (panels F and G) were not detected in the *Ink4a/Arf^{-/-}* GFP control tumor. In contrast, high levels of expression of PDGFR α (panels D and E) and PDGF-A (panels H and I) were maintained in the *Ink4a/Arf^{-/-}* PDGFR α /-A tumor in the brain of mice. Arrows in panels B and C, GFP control tumor lesions; the arrow in C indicates low level of endogenous PDGFR α staining. Arrows in panels D, E, H, and I, positive staining of PDGFR α (D and E) and PDGF-A (H and I) in tumor cell clusters invading the brain parenchyma. T, tumor mass; P, normal brain parenchyma. Scale bars represent 200 μ m in panels B, D, F, and H; 50 μ m in panels C, E, G, and I.

2.3.3 Mouse astrocytes with *PDGFRA* and *Ink4a/Arf* aberrations express markers of neural progenitor cells

To further characterize the tumors derived from *Ink4a/Arf*^{-/-} PDGFR α mAst, we examined molecular markers of various cell lineages in the CNS development. As shown in Figure 12, tumors derived from PDGFR α -expressing mAst were highly positive for the neural progenitor marker nestin which was distributed along the processes of individual cells (Figure 12A and B). As expected, most of tumor cells showed expression of the progenitor/mature astrocyte marker GFAP (Figure 12C and D) whereas they were negative for the neuronal marker class III β -tubulin (TUJ1) (Figure 12E and F). Significantly, NG2, an OPC marker (266), was expressed in a population of tumor cells that were actively invading the surrounding brain parenchyma, whereas the core of the tumor mass showed relatively low NG2 expression (Figure 12G and H). In contrast, control tumors derived from *Ink4a/Arf*^{-/-} GFP mAst lacked nestin or NG2 expression (not shown). In addition, tumors derived from *Ink4a/Arf*^{-/-} PDGFR α mAst showed negative staining for O-2A progenitor marker A2B5 and an oligodendrocyte marker CNPase (data not shown). Notably, brain tumors derived from *Ink4a/Arf*^{-/-} PDGFR α /*-A* mAst (not shown) displayed similar IHC features to tumors derived from *Ink4a/Arf*^{-/-} PDGFR α mAst, suggesting that similar dedifferentiation events also occurred in autocrine PDGFR α /*-A* co-expressing tumors.

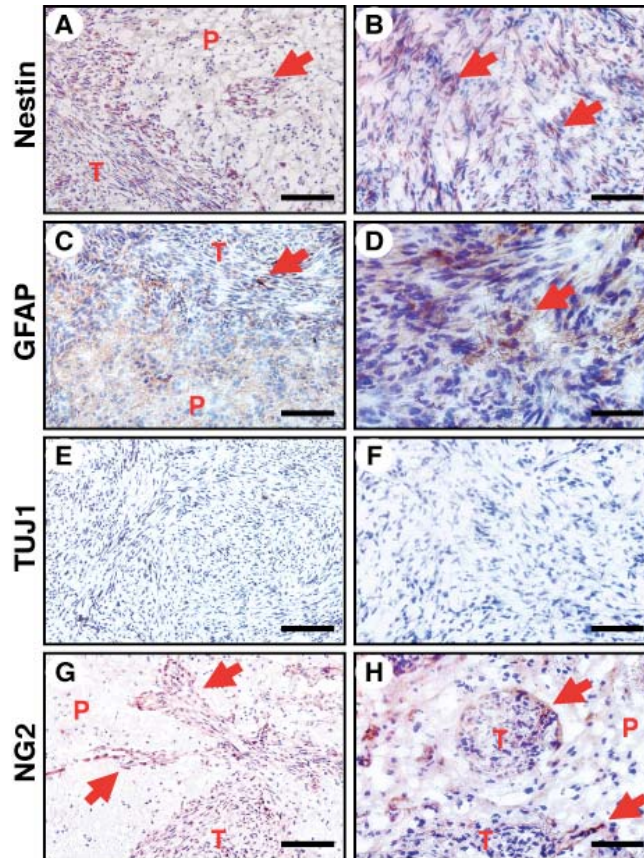


Figure 12. *Ink4a/Arf*^{-/-} mouse astrocytes overexpressing PDGFR α and PDGF-A retained high expression of both the receptor and the ligand *in vivo*.

Tumors derived from *Ink4a/Arf*^{-/-} PDGFR α mAst express markers of neural progenitor cells. Representative images of IHC staining using antibodies against nestin (A and B), GFAP (C and D), β III-tubulin (E and F), and NG2 (G and H). Arrows, positive staining of various markers. T, tumor mass; P, normal brain parenchyma. Bar, 100 μ m for (A), (C), (E), and (G); 50 μ m for (B), (D), (F), and (H).

2.3.4 PDGFRA and *Ink4a/Arf* aberrations in human glioma cells *in vitro*

Next, we utilized four human glioma cell lines that are either *INK4A/ARF*-null (LN444 and LN443) or *INK4A/ARF*-wt (LN-Z308 and LN319) (Table 3 and Figure 13A) (267) and

exogenously expressed PDGF-A in these glioma cells that express endogenous PDGFR α (Figure 13B). As shown by RT-PCR analysis, expression of p16INK4A was evident in both LN-Z308 and LN319 glioma cells, whereas LN444 and LN443 did not express any detectable p16INK4A mRNAs. IB using p16INK4A or p14ARF antibodies further confirmed that expression of both tumor suppressors is only present in LN-Z308 and LN319 but not in LN444 and LN443 cells. In order to create an autocrine stimulation loop in these cells, we overexpressed PDGF-A into each of these cells. We did not overexpress PDGFR α alone in these experiments since these cells express high level of PDGFR α endogenously. As shown in Figure 13B, exogenous PDGF-A overexpression increased the phosphorylation of the endogenous PDGFR α in these 4 cell lines.

Table 3. Human Glioma Cell Lines Used in This Study

Cell Line	Age / Sex	Type	Location	<i>PDGFRA</i>	<i>INK4A</i>	<i>ARF</i>	<i>P53</i>	<i>PTEN</i>
LN444	48 / F	Recurrent GBM	LP	+++	Del	Del	WT	Mut
LN443	66 / M	<i>de novo</i> GBM	RFT	++	Del	Del	WT	Mut
LN-Z308	65 / M	<i>de novo</i> GBM	RPO	++	WT	WT	Null	Mut
LN319	67 / M	<i>de novo</i> AA	LPO	++	WT	WT	Mut	Mut

Abbreviations: F, female; M, male; AA, astrocytoma; LP, left parietal; RFT, right frontal temporal; RPO, right parietal occipital; LPO, left parietal occipital; Del, deletion; Mut, mutation.

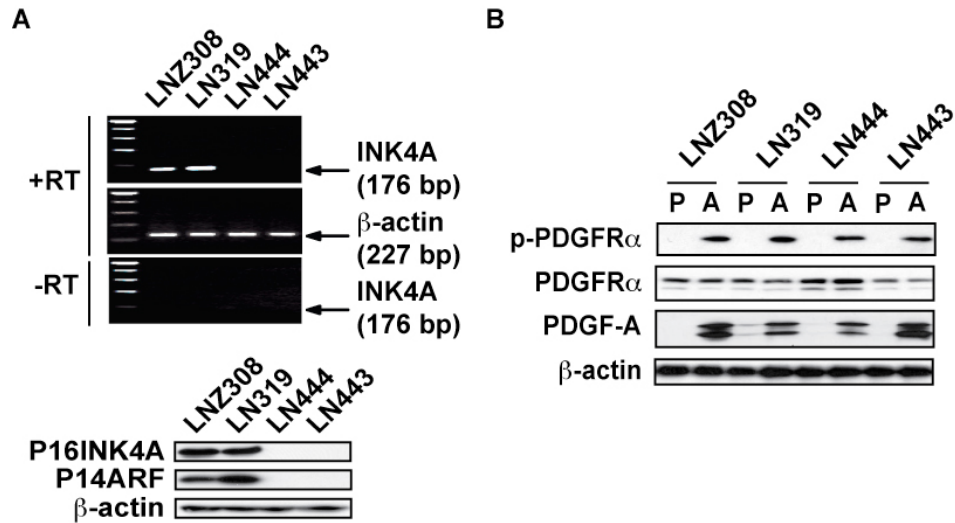


Figure 13. PDGF-A overexpression in *INK4A/ARF*-deficient and *INK4A/ARF*-wt human glioma cells.

(A) RT-PCR (upper panels) and IB analyses (lower panels) of *INK4A/ARF*-deficient LN444 and LN443, and *INK4A/ARF*-wt LN-Z308 and LN319 human glioma cells. RT, reverse transcriptase. (B) IB analysis of PDGF-A overexpression in glioma cells with endogenous PDGFR α expression. PDGFR α was phosphorylated at tyrosine residues in PDGF-A-expressing cells, but not in parental cells that have no detectable PDGF-A. Molecular weight for PDGFR α , 160-180 kD; PDGF-A, 16 and 30 kD. P, parental cells; A, PDGF-A overexpressing cells. β -actin was used as a loading control in both (A) and (B).

To assess the anchorage-independent growth of these cells *in vitro*, we utilized a soft agar colony formation assay, which can also serve as an *in vitro* cell transformation/tumorigenesis assay. As shown, expression of PDGF-A in *INK4A/ARF*-deficient LN444 cells significantly enhanced their capacity of anchorage-independent growth in soft agar, whereas a minimal effect was seen in *INK4A/ARF*-wt LN-Z308 and LN319 cells (Figure 14). Taken together from these preliminary *in vitro* analyses, PDGFR α -A autocrine signaling was able to enhance the *in vitro* tumorigenic potential of *INK4A/ARF*-deficient LN444 but not *INK4A/ARF*-wt LN-Z308 and LN319 cells.

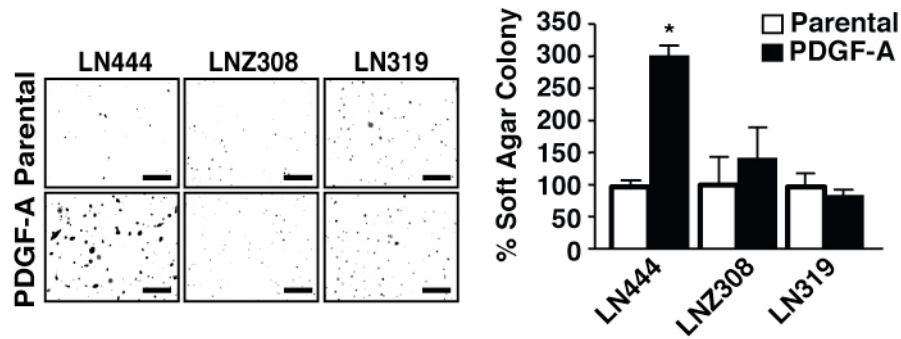


Figure 14. PDGF-A overexpression enhances anchorage-independent growth of *INK4A/ARF*-deficient but not *INK4A/ARF*-wt human glioma cells *in vitro*.

Representative images (*Left*) and quantification (*Right*) of anchorage-independent growth of various glioma cells in soft agar. Bar, 1 mm. Data are presented as percentage to the respective parental cells (mean \pm s.d.).

*, $P < 0.001$, Student's *t* test.

2.3.5 Overexpression of PDGF-A conferred tumorigenicity to *Ink4a/Arf*-deficient but not - wildtype human glioma cells

When various glioma cells were separately implanted into the brain or the flanks of mice, PDGF-A expression markedly enhanced tumor growth and invasion of *INK4A/ARF*-null LN444 and LN443 glioma cells while minimal impact of PDGF-A expression on tumorigenesis or invasion was seen in *INK4A/ARF*-wt LN-Z308 and LN319 cells in both anatomic sites (Figure 15 and 16). Mice that received LN444/PDGF-A cells in the brain had tumor onset as early as 35 days, while mice with LN443/PDGF-A cells developed invasive intracranial tumors on 25-30 days post-implantation. In contrast, LN444 and LN443 parental cells only formed small tumor lesions in the brain up to 2 to 3 months post-implantation. Mice that received LN444/PDGF-A cells survived for 75 to 80 days, while most of the mice received LN443/PDGF-A cells lived up to 3

months post-implantation. On the other hand, no significant brain tumor growth in mice that received LN308/PDGF-A or LN319/PDGF-A cells was found 2-3 months post-implantation. Thus, consistent with our findings in the *Ink4a/Arf^{-/-}* mAst, these data indicate that PDGFR α -A signaling enhances *in vivo* tumor growth and invasion of human glioma cells deficient in *INK4A/ARF*.

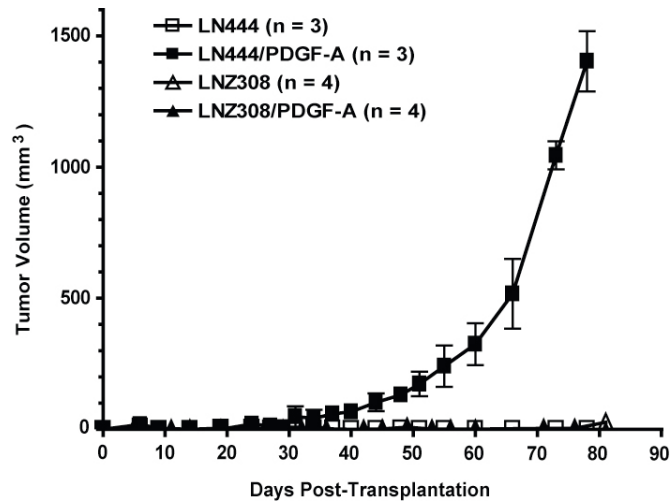


Figure 15. Exogenous PDGF-A expression enhances growth of *Ink4a/Arf*-null LN444 but not *Ink4a/Arf*-WT LN-Z308 tumors in the flanks of mice.

Parental human glioma cells were inoculated into the left flank of mice, whereas glioma cells expressing PDGF-A were implanted into the right flank of the same animals. Three to four mice were used in each group. Tumor volumes were estimated [volume = $(a^2 \times b) / 2$, $a < b$] (263) at indicated times after implantation. Data are shown as mean \pm s.e.m. and representative from two independent experiments.

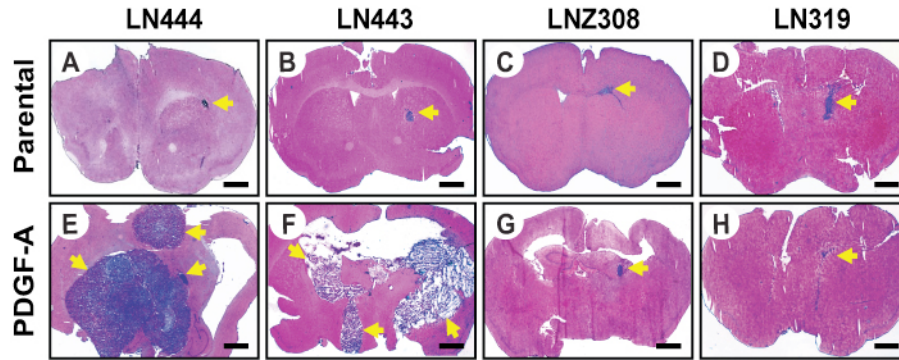


Figure 16. Exogenous PDGF-A expression enhances growth of *Ink4a/Arf*-null LN444 but not *Ink4a/Arf*-WT LN-Z308 tumors in the brain of mice.

Representative H&E staining images of various brain sections from two independent experiments with 3-5 mice per group with similar results. Brains were harvested 50-55 days post-transplantation for A and E; 75-80 days for B and F; 45-50 days for C, D, G, and H. Arrows, gliomas formed in the brain (bar, 1 mm).

2.3.6 p16INK4a but not p19ARF attenuates PDGFR α -induced tumorigenesis of *Ink4a/Arf*-deficient mouse astrocytes and human glioma cells.

To investigate whether re-expression p16INK4a or p19ARF is able to abrogate the enhanced tumorigenicity in *Ink4a/Arf*^{-/-} mAst, we separately expressed these two tumor suppressors in mAst (Figure 17A, upper and lower panels). Surprisingly, re-expression of p16INK4a but not p19ARF alone in *Ink4a/Arf*^{-/-} mAst suppressed soft agar growth of PDGFR α -expressing mAst stimulated by PDGF-A (Figure 17B). Consistently, enforced restoration of p16INK4a in *Ink4a/Arf*^{-/-} mAst significantly inhibited tumorigenesis of PDGFR α -A overexpressing mAst in the mouse brain (Figure 18).

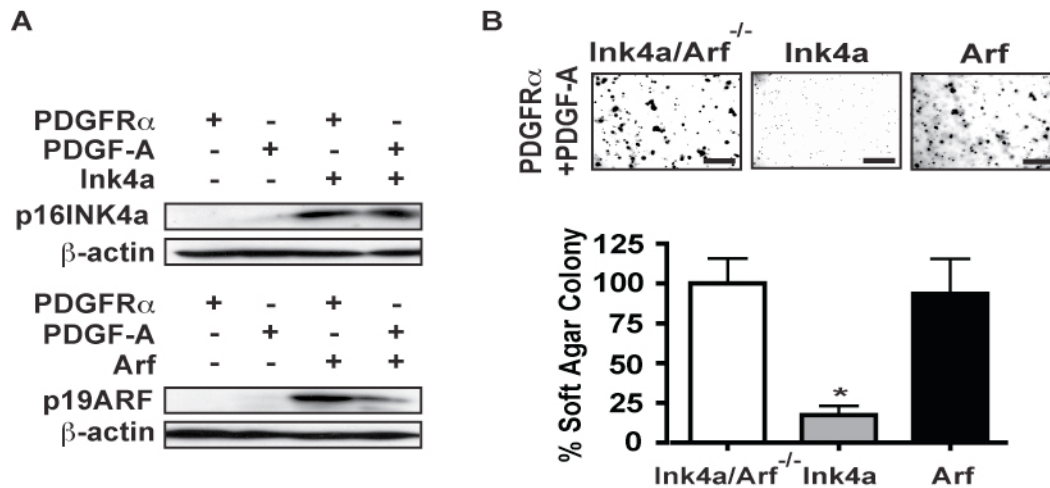


Figure 17. Re-expression of p16INK4a but not p19ARF suppresses the anchorage-independent growth of mAst expressing PDGFR α /-A *in vitro*.

(A) IB analyses of re-expression of p16INK4a or p19ARF in PDGFR α or PDGF-A overexpressing *Ink4a/Arf*^{-/-} mAst. (B) Anchorage-independent growth of p16INK4a or p19ARF expressing mAst. Bar, 1 mm. Bar graph in lower panel, quantification of soft agar assays. Data are presented as mean \pm s.d. *, $P < 0.05$.

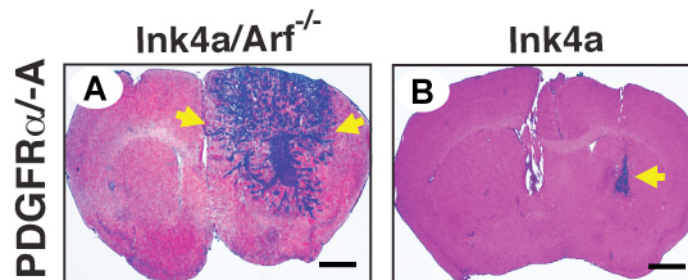


Figure 18. Re-expression of p16INK4a suppresses the *in vivo* tumor growth of mAst expressing PDGFR α /-A.

Ink4a/Arf^{-/-} mAst expressing (A) PDGFR α /-A or (B) PDGFR α /-A and p16INK4a were separately injected into brain of nude mice. Representative H&E staining images of various brain sections from two independent experiments with 3-5 mice per group with similar results. Brains were harvested 18-22 days post-implantation. Mice received either types of cells displayed similar tumor onset and survival time as described in text for mice in Figure 1. Bar, 1 mm.

To further demonstrate the cooperative effect of PDGFR α activation and loss of *Ink4a* on tumorigenesis, we knocked down endogenous p16INK4a by shRNAs targeting CDKN2A in *INK4A/ARF*-wt LN319 cells. As shown in Figure 19, significant inhibition of P16INK4A without affecting P14ARF expression by two separate shRNAs in LN319 cells (Figure 19A) resulted in a marked increase in colony formation in soft agar (Figure 19B). Since p16INK4a inhibits CDK4/6 that inactivates RB by phosphorylation and p19ARF (or P14ARF) targets MDM2 that suppresses p53 (26), we thus examined responses of modulating CDK4/6 and p53 in these cells. As shown in Figure 20, inhibition of phosphorylation of RB, the direct downstream target of CDK4/6 by a CDK4/6 inhibitor PD0332991 (268) (Figure 20A), markedly reduced PDGF-A-stimulated cell growth of *Ink4a/Arf*-deficient mAst and LN444 cells in soft agar (Figure 20B), suggesting that the tumorigenic effect of PDGFR α signaling is dependent on CDK4/6 inactivation of RB proteins (p-RB).

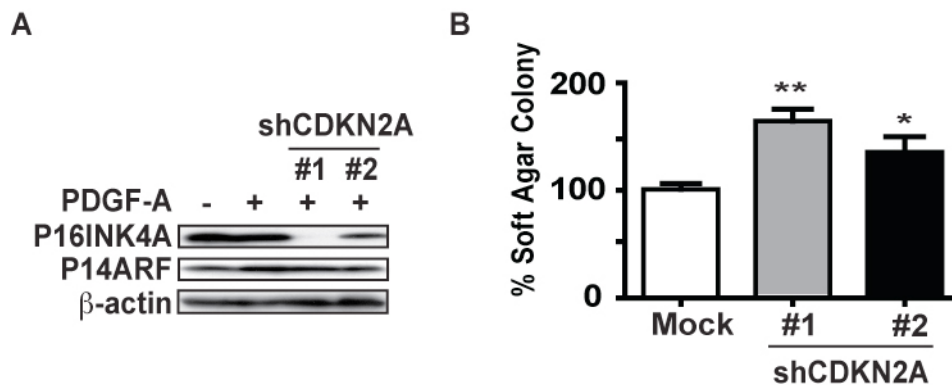


Figure 19. P16INK4A knockdown in *INK4A/ARF*-wt human glioma cell LN319 potentiates PDGF-A-promoted anchorage-dependent growth *in vitro*.

Anchorage-independent growth of *INK4A/ARF*-wt LN319 cells transfected with shCDKN2A in soft agar. (A) IB analysis. (B) Quantification of soft agar assays. Two stable cell clones with different efficiencies of P16INK4A knockdown were used. Data are mean \pm s.d. *, $P < 0.05$; **, $P < 0.01$.

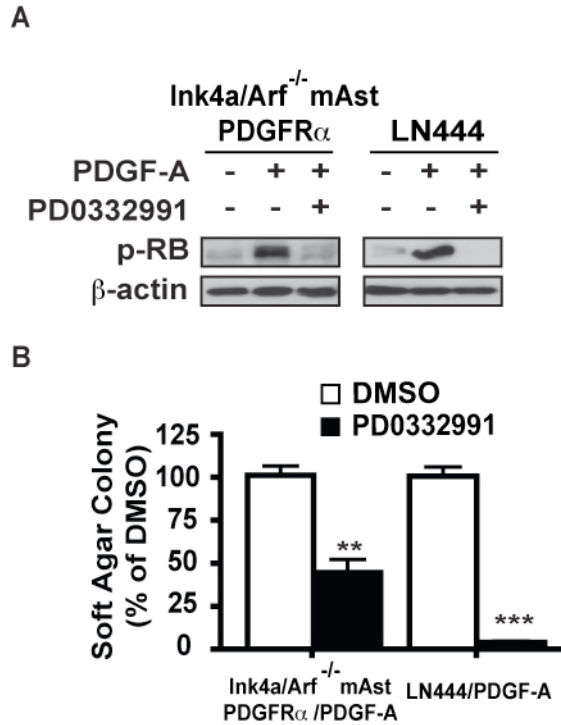


Figure 20. P16INK4A knockdown in *INK4A/ARF*-wt human glioma cell LN319 potentiates PDGF-A-promoted anchorage-dependent growth *in vitro*.

Soft agar growth of *Ink4a/Arf*-deficient mAst and LN444 cells treated with PD0332991. (A) IB analysis. (B) Quantification of soft agar assays. β -actin was used as a loading control in all IB experiments. Data are presented as mean \pm s.d. and representative of two independent experiments. **, $P < 0.01$; ***, $P < 0.001$

Since we did not observe any tumor-suppressing effect of p19ARF on *Ink4a/Arf*^{-/-} PDGFR α -expressing mAst (Figure 17B), we asked whether the downstream p53 protein was functional in these cells. When *Ink4a/Arf*^{-/-} and *Ink4a/Arf*^{-/-} p19ARF mAst were treated with cisplatin (269), p53 expression was strongly induced in *Ink4a/Arf*^{-/-} PDGFR α /p19ARF-expressing mAst, but only at a moderate level in *Ink4a/Arf*^{-/-} PDGFR α -expressing mAst (Figure 21A). The mAst expressing p19ARF were more sensitive to cisplatin inhibition of cell survival than those without p19ARF expression, indicating that p19ARF-upregulated p53 in *Ink4a/Arf*^{-/-}

PDGFR α -expressing mAst rendered sensitivity to cisplatin inhibition (Figure 21B). Collectively, these data show that p16INK4a but not p19ARF suppresses the tumorigenesis promoted by PDGFR α -A signaling, suggesting a cooperative effect of PDGFR α activation and p16INK4a inhibition during gliomagenesis. Additionally, p19ARF loss might be required for tumor survival in certain circumstances such as in the presence of DNA-damaging agents.

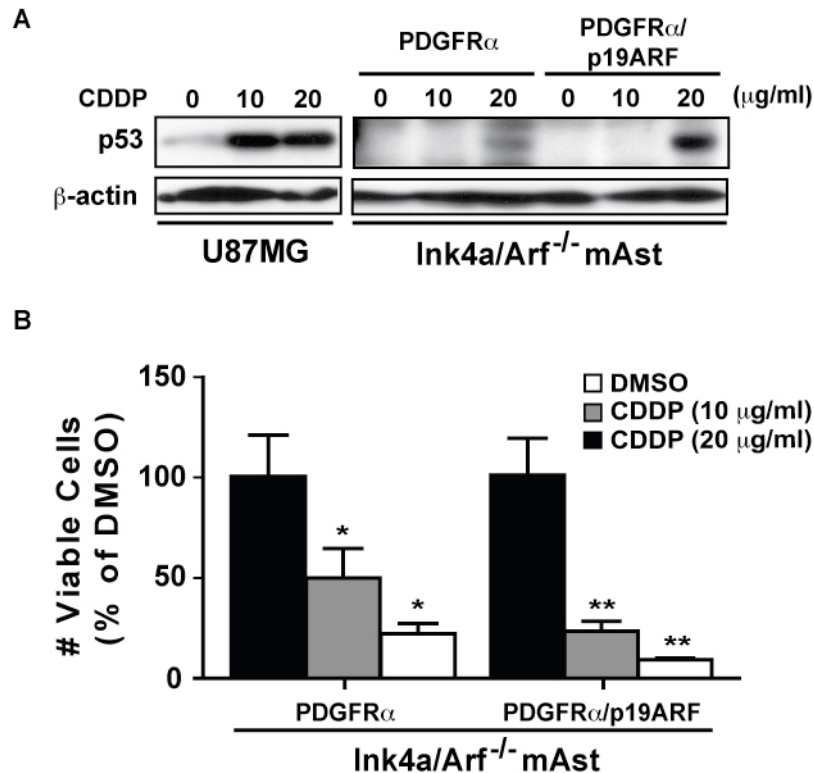


Figure 21. Cisplatin induces p53 expression and cell death in *Ink4a/Arf*^{-/-} PDGFR α -expressing mAst in the presence of p19ARF.

(A) U87MG or *Ink4a/Arf*^{-/-} mAst expressing PDGFR α or PDGFR α /p19ARF were serum-starved for 24 hours followed by incubation with cisplatin (CDDP) at indicated concentrations for an additional 24 hours. Cells were then lysed for IB analyses. Cisplatin was able to induce p53 expression at a concentration of 10 μ g/ml for U87MG and 20 μ g/ml for *Ink4a/Arf*^{-/-} mAst expressing PDGFR α /p19ARF. β -actin proteins were used as loading control. (B) An equal number of PDGFR α or PDGFR α /p19ARF-expressing *Ink4a/Arf*^{-/-} mAst were

cultured in triplicate wells in the presence of DMSO, 10 $\mu\text{g/ml}$, or 20 $\mu\text{g/ml}$ CDDP for 48 hours before Trypan Blue exclusion assay for cell viability. *, $P < 0.01$; **, $P < 0.0001$, compared with DMSO control. Data are shown as mean \pm s.d. and representative of two independent experiments.

2.4 SUMMARY AND CONCLUSION

We have demonstrated that primary murine astrocytes or human glioma cells in the *Ink4a/Arf*-null background retained the potential of responding to PDGF activation by generating gliomas, both in the brain and flanks of mice, which were significantly larger and more malignant than those formed by cells without PDGF stimulation. Moreover, we found that the PDGF-A-induced enhanced tumorigenicity only occurred in *Ink4a/Arf*-deficient but not *Ink4a/Arf*-wildtype human glioma cells. When we restored the expression of p16INK4a or p19ARF alone in the *Ink4a/Arf*^{-/-} mAst, we found a dramatic decrease of tumorigenesis only in cells expressing p16INK4a but not in those expressing p19ARF. Furthermore, in our attempt to eliminate the endogenous expression of the P16INK4A in *Ink4a/Arf*-wildtype human glioma cells, we found that these cells showed a significant increase in anchorage-independent growth in soft agar. Thus we conclude that PDGFR α /PDGF-A is able to enhance gliomagenesis in cooperation with *Ink4a/Arf* deletion, and re-expression of p16INK4a is sufficient to abrogate this induced tumorigenicity.

3.0 PDGFRA-INDUCED GLIOMAGENESIS DEPENDS ON DOWNSTREAM PI3K PATHWAY THAT IS REGULATED BY SHP-2/PTPN11 ACTIVITY

3.1 INTRODUCTION AND RATIONALE

Changes in expression or copy number of the gene *PDGFRA* have been a key feature of GBMs (2, 4). The new genomic profiling has further identified *PDGFRA* overexpression as one of the key signature genetic alterations in the Proneural subtype of GBMs, together with *TP53* and *IDH1* mutations, among many others (11). Observations obtained from *in vivo* animal models have provided invaluable insights into how PDGF over-activity can cause glioma formation from different cell types in the brain (270). However, the molecular mechanisms behind which PDGF signaling induces glioma formation remain largely unknown. In the previous sections, we showed that *PDGFRA* overexpression cooperates with loss of p16INK4A to promote gliomagenesis. In order to dissect the downstream signaling cascades mediating the PDGF-mediated enhanced tumorigenicity, we transfected a series of established PDGFR α mutants into the *Ink4a/Arf*^{-/-} mAst and assessed their tumorigenic potential by transplanting them into the mouse brain. These *in vivo* results were later confirmed by experiments using various pharmacological inhibitors that target specific signaling pathways downstream to the receptor. The subsequent biochemical studies further demonstrated how these downstream pathways interact to mediate tumor formation induced by PDGFR α overexpression.

3.2 MATERIALS AND METHODS

3.2.1 Cell Lines and Reagents

Primary *Ink4a/Arf*^{-/-} mAst were derived and propagated as previously described (45). Human glioma cell line LN444 was obtained from American Cell Type Culture Collection (Manassas, VA). Unless otherwise mentioned, LN444 and primary mAst were routinely maintained in 5% CO₂ at 37°C, in DMEM (Invitrogen) containing 10% FBS (Hyclone), 100 units/ml penicillin, and 100 µg/ml streptomycin (Invitrogen).

The following antibodies and reagents were used in this study: rabbit anti-PDGFR α (sc-338, 1:500), rabbit anti-PDGF-A (sc-128, 1:500), and goat anti- β -actin (sc-1616, 1:500) antibodies were from Santa Cruz Biotechnology Inc., Santa Cruz, CA; rabbit anti-phospho-p44/42 MAP Kinase (Thr202/Tyr204, #9101, 1:1000), rabbit anti-p44/42 MAP Kinase (#9102, 1:1000), mouse anti-phospho-Akt (Ser473, #4051, 1:1000), rabbit anti-Akt (#9272, 1:1000), rabbit anti-phospho-p70 S6 Kinase (Thr389, #9205, 1:500), rabbit anti-p70 S6 Kinase (#9202, 1:500), and mouse anti-Myc-Tag (#2276, 1:1000) antibodies were from Cell Signaling Technology, Danvers, MA; mouse anti-phosphotyrosine (clone 4G10, #05-321, 1:1000) and rabbit anti-PI3K p85 (#6-497, 1:500) antibodies were from Millipore, Temecula, CA; a rabbit anti-caspase-3 antibody was from Stressgen, Ann Arbor, MI; a rabbit anti-Ki67 antigen (NCL-Ki67p, IHC, 1:200) antibody was from Leica Microsystems Inc., Bannockburn, IL; MatrigelTM Basement Membrane Matrix, Growth Factor Reduced (GFR) (#356230) was obtained from BD Biosciences, San Jose, CA; LY294002 (#440202), InsolutionTM SU6656 (#572636), PP2

(#529573), SHP1/2 PTPase Inhibitor NSC87877 (#565851) and MEK inhibitor PD98059 were from EMD Chemicals, Gibbstown, NJ; PHP5-1 sodium salt hydrate (P0039) was from Sigma-Aldrich, St. Louis, MO. Rapamycin/Sirolimus (NSC-226080) was from NCI Developmental Therapeutic Program, National Institute of Health, Bethesda, MD. All secondary antibodies were from Vector Laboratories (Burlingame, CA) or Jackson ImmunoResearch Laboratories (West Grove, PA). All other reagents were from Invitrogen, Sigma-Aldrich, or Fisher Scientific.

3.2.2 Retroviral and Lentiviral Constructs and Infections

The cDNA's of various PDGFR α mutants were described previously (271, 272). To generate retroviral vectors encoding various PDGFR α mutants, cDNA inserts were subcloned from either pLNCX2 (for R627, F731/42, F572/74, F988, F1018, and Y720 PDGFR α mutants, gifts from Dr. Andrius Kazlauskas at Harvard Medical School, Boston) or pCS2 (for F720 and Y731/42 PDGFR α mutants, gifts from Dr. Karen Symes at Boston University School of Medicine, Boston) vectors into the NotI-SnaBI sites of the pMXI-*gfp* retroviral vector. For shRNA experiments, the lentiviral vectors pLKO.1-sh*PTPN11* (5 clones) were purchased from Thermo Scientific, Huntsville, AL.

Retroviruses and lentiviruses were produced and the mAst or LN444 cells were transduced as described in **2.2.2** (Page 51) of this dissertation.

3.2.3 Immunoprecipitation and Immunoblotting

For IP experiments, cells were serum-starved for 24-48 hours and lysed in a lysis solution (20mM Tris-HCl pH 7.4, 50mM NaCl, 0.5% Triton X-100, 2% NP-40, 1mM CaCl₂, 1mM MgCl₂, and CompleteTM EDTA-free protease inhibitor cocktail, cat# 11836170001, Roche). In some experiments, cells were pre-incubated with or without indicated inhibitors for 24 hours and then stimulated by 50 ng/ml PDGF-A for 5 min prior to lysis. The cell extracts were then centrifuged, and proteins in the supernatants were quantified. Approximately 1 µg of indicated primary antibody was added to a lysate preparation containing 1 mg total protein. The mixtures were then incubated at 4°C overnight on a rotator. The protein-antibody complex was pulled down by rProtein G Agarose beads (15920-010, Invitrogen), washed 3 times with the lysis solution, and analyzed in a SDS-PAGE. For IB analysis, immunoprecipitated proteins or total cell lysates containing ~30 µg of total proteins were separated in a SDS-PAGE gel under a reducing condition. The separated proteins were then transferred to a polyvinylidene fluoride (PVDF) membrane (Bio-Rad), blocked by 5% (w/v) nonfat dry milk (Bio-Rad) in PBS, and probed with indicated primary antibodies at 4°C overnight. Proteins of interest were then visualized by incubating the membrane with indicated peroxidase-labeled secondary antibodies at room temperature for 30 min followed by detection with enhanced chemiluminescence (ECL, Amersham Bioscience) reaction following manufacturer's instructions.

3.2.4 RNA Interference

SHP-2 specific siRNA (5'-AAG GAC AUG AAU AUA CCA AUA-3') (273) and a scrambled siRNA control were obtained from Dharmacon (Lafayette, CO). Transient transfection of siRNAs was performed using Effectene[®] Reagent (Qiagen) according to manufacturer's instructions. Cells were transfected with 100 nM siRNAs for 24 hours, recovered in 10% FBS / DMEM for 48 hours prior to further analyses. Knockdown of SHP-2 was validated by IB using a mouse anti-SHP-2 antibody.

3.2.5 Other Experiments

Experiments of glioma transplantation, IHC, soft agar assay, and cell viability assay were performed as described in sections **2.2.4** (Page 53), **2.2.5** (Page 54), **2.2.7** (Page 55), and **2.2.9** (Page 56) of this dissertation.

3.2.6 Statistical Analyses

One-way ANOVA or an unpaired, two-tailed Student's *t* test followed by Newman-Keuls post-test was performed using GraphPad Prism software. A *P* value of 0.05 or less was considered statistically significant.

3.3 RESULTS

3.3.1 Generation of *Ink4a/Arf*^{-/-} mouse astrocytes overexpressing various PDGFR α mutants that are not able to activate specific downstream pathways

Previous studies using genetic and biochemical approaches have defined the roles of signaling molecules in PDGFR α -mediated cellular functions by specific tyrosine-to-phenylalanine mutations (Y to F) (Figure 22A) (70, 74, 75). To investigate the impact of these PDGFR α mutations on tumorigenesis, we separately expressed wild-type (PDGFR α -wt) or various PDGFR α mutants in *Ink4a/Arf*^{-/-} mAst. A PDGFR α mutant R627 (PDGFR α -R627) that harbors a lysine-to-arginine (K-to-R) mutation was included as a “receptor kinase-dead” control. As shown in Figure 22B, stimulation of PDGFR α -wt by PDGF-A resulted in autophosphorylation of the receptor and promoted phosphorylation of downstream signaling molecules Erk1/2 and Akt, whereas there was an undetectable receptor tyrosine autophosphorylation in PDGFR α -R627 (Figure 22B). PDGFR α Y-to-F mutations at Y572 and Y574 (PDGFR α -F572/74; for SFK binding), Y1018 (PDGFR α -F1018; for PLC γ binding), and Y988 (PDGFR α -F988) did not result in a significant decrease in p-Akt and p-Erk levels in response to PDGF-A stimulation (Figure 22B). Moreover, the mutation at Y731 and Y742 (PDGFR α -F731/42; for PI3K binding) led to a marked decrease in PDGF-A-stimulated p-Akt and p-Erk1/2 levels (Figure 22B). In agreement with a previous report (274), p-Erk1/2 was markedly reduced in PDGF-A-stimulated mAst expressing PDGFR α -F720 (Y-to-F mutation at Y720; for SHP-2 binding), compared to PDGFR α -wt mAst (Figure 22B). Interestingly, p-Akt level was also attenuated in PDGFR α -F720 cells.

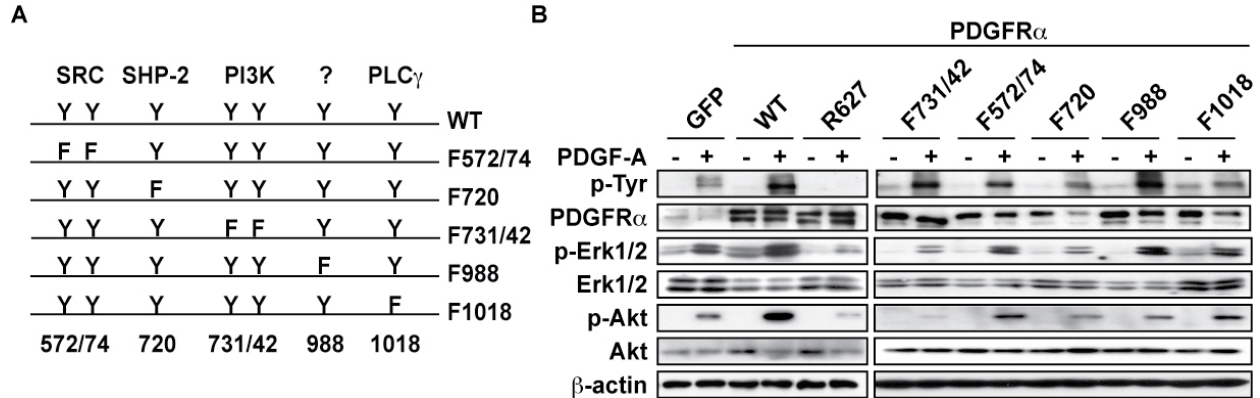


Figure 22. Impacts of PDGFR α mutations on downstream signaling of PDGFR α .

(A) Schematics of various PDGFR α mutants. (B) IB analyses of PDGF-A-stimulated *Ink4a/Arf*^{-/-} mAst overexpressing individual PDGFR α mutants. Various mAst cells were serum-starved for 48 hours before stimulation by 50 ng/ml PDGF-A for 5 min. Total cell lysates were then collected for IB experiments. Corresponding total proteins or β -actin were used as loading controls.

3.3.2 Disruption of SHP-2 and PI3K pathways downstream to PDGFR α suppresses tumor growth of *Ink4a/Arf*^{-/-} mouse astrocytes

Next, we determined the impact of these Y-to-F mutations on PDGFR α -promoted cell transformation of *Ink4a/Arf*^{-/-} mAst *in vitro*. As shown in Figure 23A, mAst expressing PDGFR α -wt, PDGFR α -F572/74, PDGFR α -F988, and PDGFR α -F1018 PDGFR α mutants showed similar capability of anchorage-independent growth in soft agar. In contrast, expression of PDGFR α -R627, PDGFR α -F731/42, or PDGFR α -F720 instead of PDGFR α -wt significantly abrogated the capacity of mAst to form colonies in soft agar (Figure 23A and B), indicating that PI3K and SHP-2 signaling were critical for cell transformation *in vitro*.

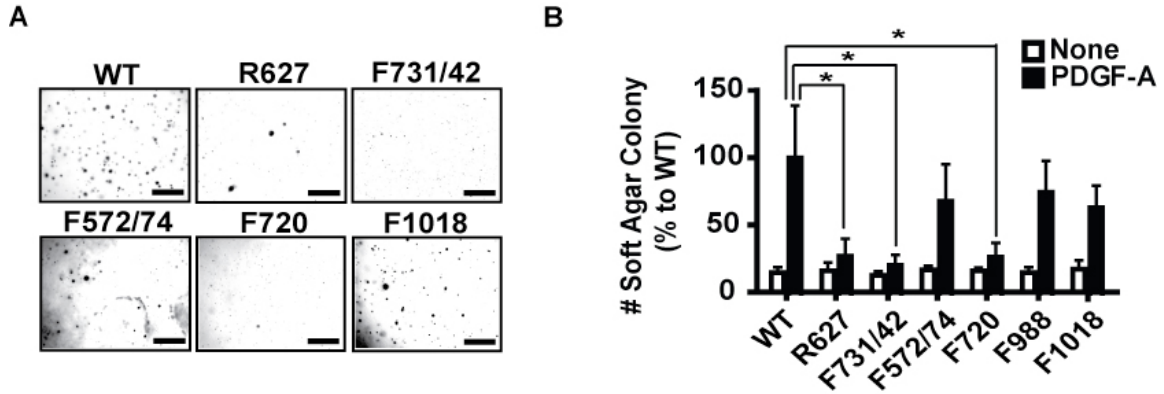


Figure 23. Impacts of PDGFR α mutations on downstream signaling of PDGFR α and anchorage-independent growth in soft agar of *Ink4a/Arf*^{-/-} mAst.

(A) Representative images of soft agar colonies. (B) Quantification of soft agar assays. Data are presented as mean \pm s.d. and representative of two independent experiments. *, $P < 0.01$. Bar, 1 mm.

When various *Ink4a/Arf*^{-/-} mAst were separately implanted into the brains of mice, compared to PDGFR α -wt (Figure 24A), PDGFR α -R627, PDGFR α -F731/42, PDGFR α -F720, and PDGFR α -F988 significantly impaired PDGFR α -promoted tumorigenesis and invasion (Figure 24B, C, E and F). However, mAst expressing PDGFR α -F572/74 or PDGFR α -F1018 displayed comparable tumorigenicity to PDGFR α -wt tumors (Figure 24D and G, compared to 24A), but with markedly reduced tumor invasion compared to the tumors derived from mAst expressing PDGFR α -wt (Figure 24K and N, compared to H). Higher magnification images of PDGFR α -R627, PDGFR α -F731/42, and PDGFR α -F720 mutants (Figure 24I, J and L) further illustrated that these mutations significantly negated the enhanced tumorigenicity conferred by PDGFR α activation, leading to the formation of tumors similar in volume and invasiveness to those seen in GFP-expressing mAst tumors (Figure 9B and G).

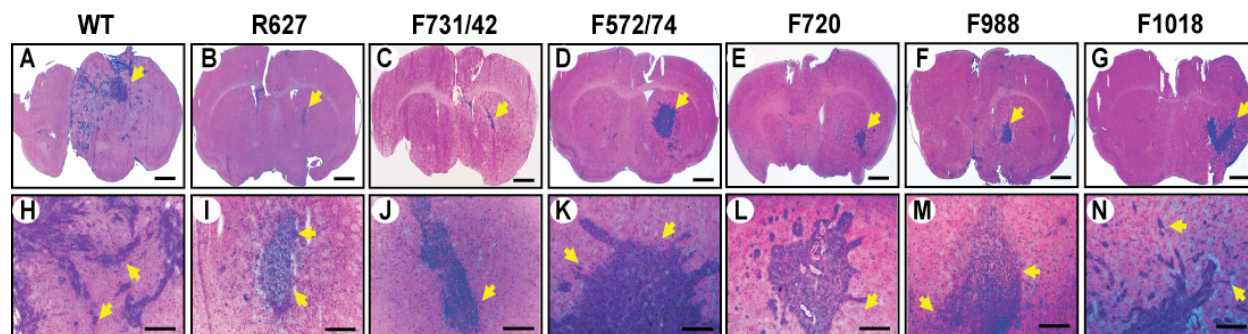


Figure 24. Impacts of individual mutations of PDGFR α in mAst on brain tumorigenesis.

(A) to (N), Representative H&E staining images of various brain sections from two independent experiments with at least 5 mice per group with similar results. Mice received either types of cells displayed similar tumor onset and survival time as described in text for mice in Figure 1. Brains were harvested 25-30 days post-transplantation for A ; 30-35 days for B, C, D and G; and 35-40 days for E and F. Bar, A to G, 1 mm, H to N 200 μ m. Arrows, tumors or invading cells.

Moreover, PDGFR α -F731/42 and PDGFR α -F720 tumors showed a significantly decreased cell proliferation (Figure 25A and B) and increased apoptosis (Figure 26A and B), whereas PDGFR α -F572/74, PDGFR α -F988, and PDGFR α -F1018 tumors exhibited moderate or minimal impacts on cell proliferation and survival compared to PDGFR α -wt tumors. Conversely, retention of any one of the five signaling modules (Y731/42, Y572/74, Y720, Y988, and Y1018 PDGFR α mutants) (74) was insufficient to rescue the abolished tumorigenesis in the brain (data not shown). Taken together, these data indicate that ablation of PDGFR α association with SHP-2 or PI3K abrogates tumorigenicity of *Ink4a/Arf*^{-/-} mAst expressing PDGFR α , whereas individual association of PI3K, SHP-2, SFK, or PLC γ with the RTK was insufficient to elicit the full spectrum of tumor-promoting effects of PDGFR α .

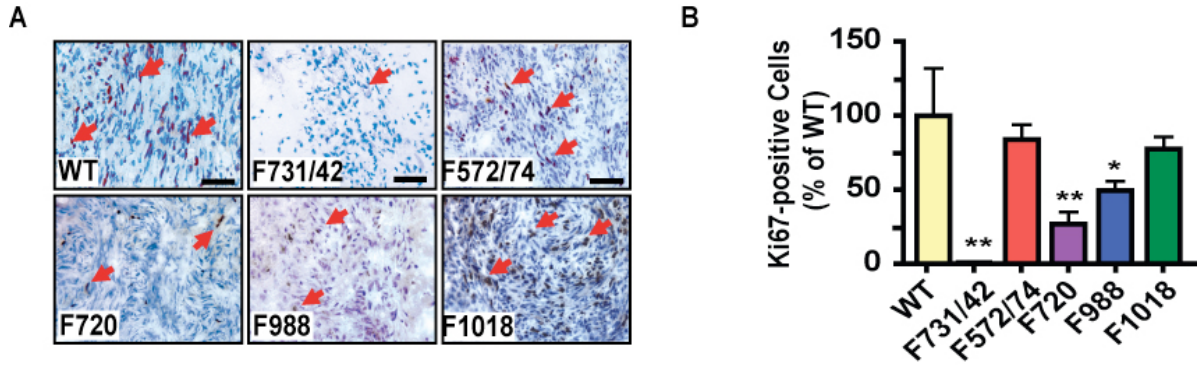


Figure 25. Impacts of individual mutations of PDGFR α in mAst on *in vivo* proliferation in the mouse brain.

(A) Ki-67 staining of brain sections, bar, 50 μ m. Red arrows, Ki-67-positive cells. (B) Quantification of Ki-67 staining. Data are presented as mean \pm s.d. *, $P < 0.01$; **, $P < 0.001$.

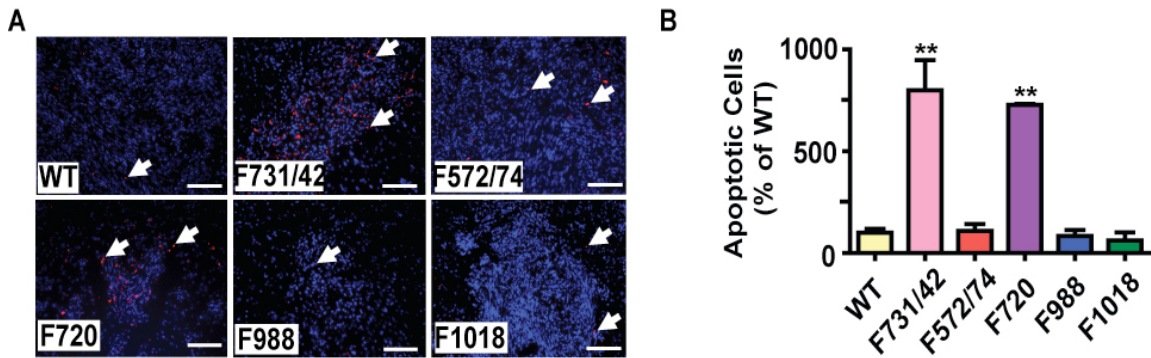


Figure 26. Impacts of individual mutations of PDGFR α in mAst on *in vivo* apoptosis in the mouse brain.

(A) (TUNEL staining images, bar, 100 μ m. (B) Quantification of TUNEL staining. Data are presented as mean \pm s.d. **, $P < 0.001$.

3.3.3 Pharmacological inhibition of SHP-2 or PI3K abrogates PDGF-promoted tumorigenesis of *Ink4a/Arf*^{-/-} mouse astrocytes or human glioma cells

We further investigated whether inhibition of SHP-2 and PI3K activities by pharmacological approaches suppresses tumorigenicity of PDGFR α /-A expressing *Ink4a/Arf*^{-/-} mAst and LN444 cells. To this end, we exploited several pharmacological inhibitors against PI3K (LY294002), SHP-2 (PHPS-1 and NSC87877) (275), and SFK (SU6656 and PP2). As shown in Figure 7, LY294002 inhibits PDGF-A-induced phosphorylation of Akt at 10 μ M in mAst and 5 μ M in LN444 glioma cells, whereas Erk1/2 phosphorylation was unaffected by LY294002 treatment in both types of cells (Figure 27A and 28A). Of note, a modest decrease in p-Erk1/2 level in mAst treated with 20 μ M LY294002 was observed (Figure 27A). At a concentration of 100 μ M (275), both PHPS-1 and NSC87877 significantly inhibited p-Erk1/2, a direct downstream target of SHP-2, in mAst and LN444 cells (Figure 27B and 28B). Next, we examined the impact of the pharmacological interventions of these signaling enzymes on *in-vitro* cell transformation and found that 10 μ M LY294002 that had no effect on Erk1/2 activation suppressed soft agar growth of PDGFR α -expressing mAst stimulated by PDGF-A (Figure 27D) and PDGF-A-expressing LN444 cells (Figure 28C). Similarly, 100 μ M of either PHPS-1 or NSC87877 ablated PDGFR α -stimulated anchorage-independent growth in soft agar, but only had minimal effect on the cell survival and caspase-3 activation of both PDGFR α /-A-expressing mAst and LN444 cells in culture (Figure 29). Additionally, the MEK inhibitor PD98059 at 10 μ M that suppressed PDGF-A-induced p-Erk1/2 in mAst (Figure 27C) also inhibited soft agar growth of these cells (Figure 27D), validating Erk1/2 as a mediator of PDGFR α -SHP-2 signaling. In contrast, two SFK inhibitors, 5 μ M SU6656 and PP2, also showed a modest impact on tumorigenesis of these cells

(Figure 27D and 28C). Taken together, these data demonstrate that the PDGFR α -enhanced tumorigenicity of *Ink4a/Arf*-deficient mAst and human glioma cells requires intact SHP-2 and PI3K enzymatic activities.

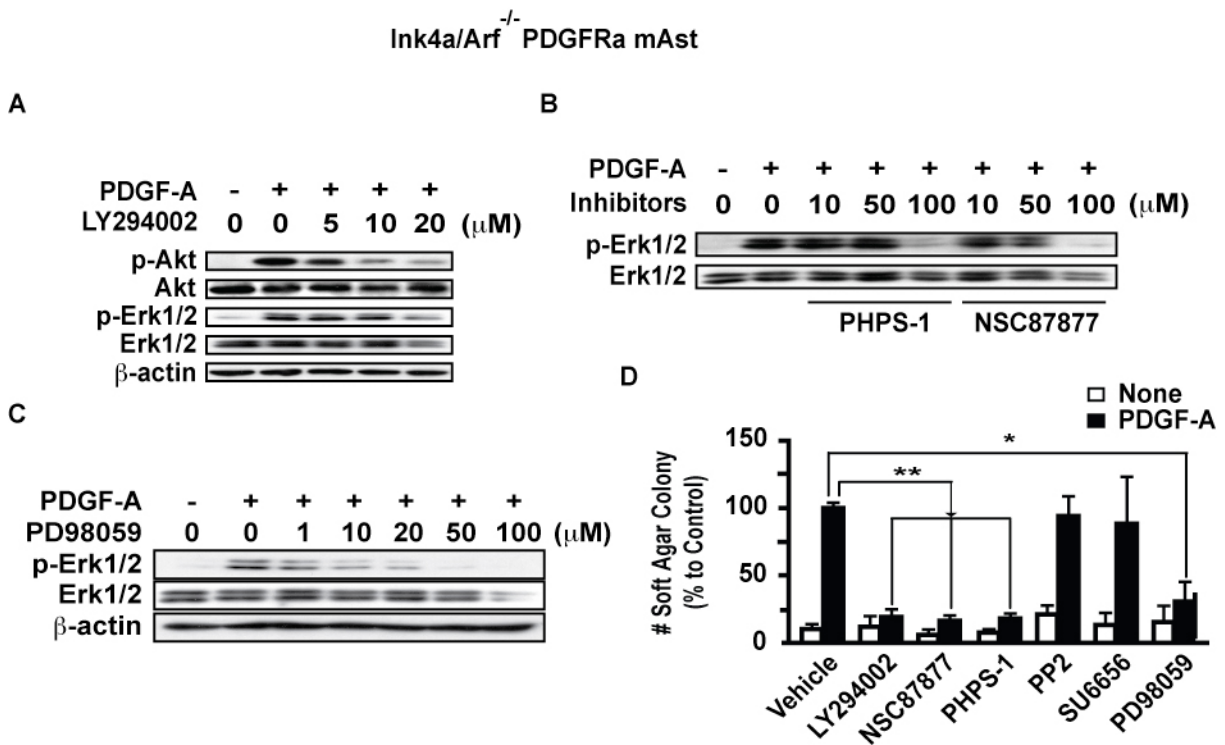


Figure 27. Inhibition of PI3K or SHP-2 activity suppresses PDGFR α -stimulated signaling and cell transformation in *Ink4a/Arf*^{-/-} mAst.

Inhibitors of PI3K (LY294002), SHP-2 (PHPS-1 and NSC87877), and MEK (PD98059), but not SFK (SU6656 and PP2) abrogate cell transformation of PDGFR α -overexpressing *Ink4a/Arf*^{-/-} mAst. (A) to (C) *Ink4a/Arf*^{-/-} mAst expressing PDGFR α were serum-starved for 24 hours followed by incubation with various inhibitors at indicated concentrations for an additional 24 hours. Cells were then stimulated with 50 ng/ml PDGF-A for 5 min before IB analyses. Total Erk1/2 or Akt and β -actin proteins were used as loading controls. (D) Quantification of soft agar assays. Cells were grown in triplicates in soft agar with or without LY294002 (10 μ M), PHPS-1 (100 μ M), NSC87877 (100 μ M), PP2 (5 μ M), SU6656 (5 μ M), or PD98059 (10 μ M). Data are presented as mean \pm s.d. *, $P < 0.001$; **, $P < 0.0001$.

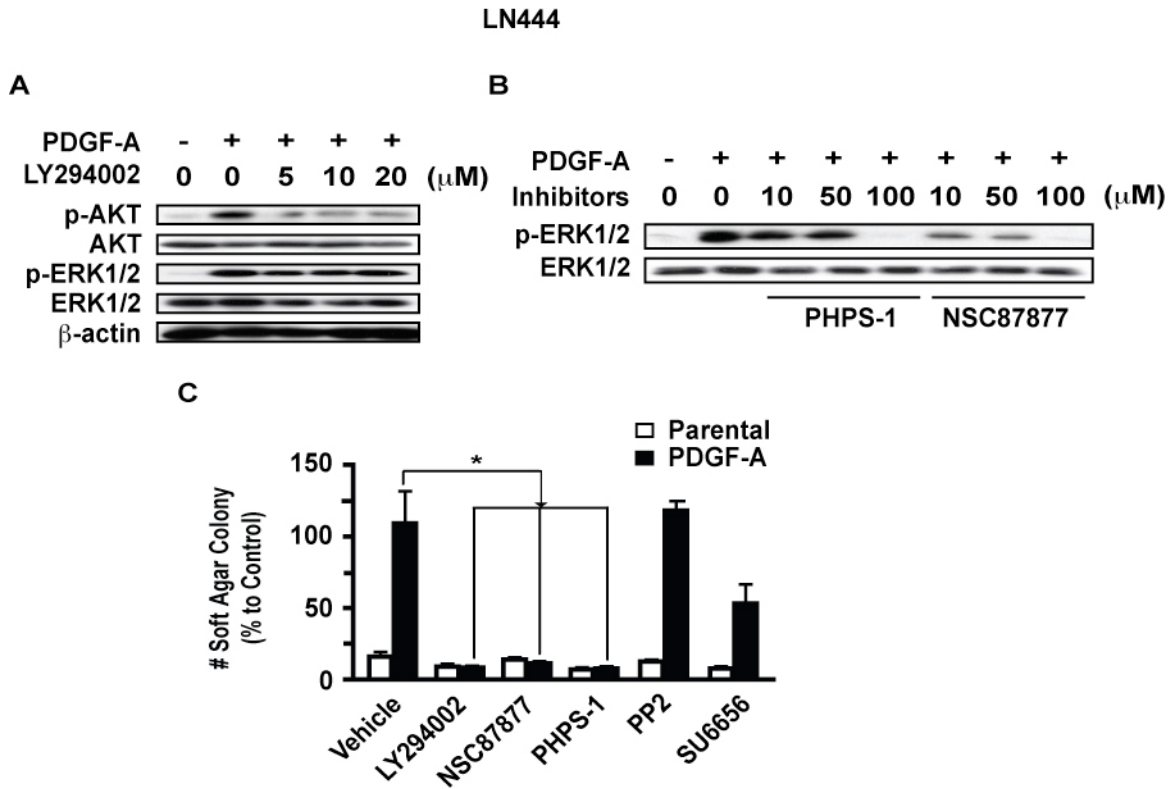


Figure 28. Inhibition of PI3K or SHP-2 activities suppresses PDGFR α -stimulated signaling and cell transformation in LN444 cells.

PI3K and SHP-2 inhibitors suppress PDGF-A-promoted soft agar growth of *INK4A/ARF*-deficient LN444 glioma cells. (A) and (B) IB analysis. Corresponding total proteins or β -actin were used as loading controls. (C) Soft agar assays. Concentrations of the inhibitors and experimental conditions were identical to those in Figure 29D. Data are presented as mean \pm s.d. *, $P < 0.01$.

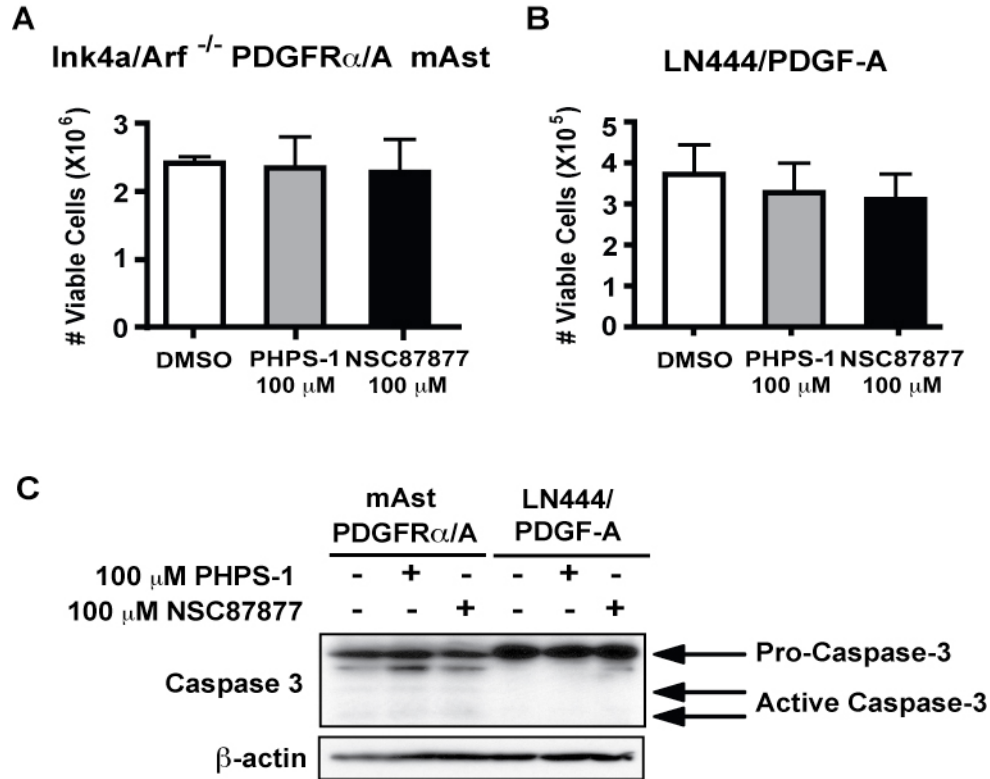


Figure 29. Effects of SHP-2 inhibitors on *Ink4a/Arf*^{-/-} mAst and LN444 cell viability

(A) The same number of PDGFR α /PDGF-A-coexpressing *Ink4a/Arf*^{-/-} mAst or LN444 cells was separately cultured in the presence of DMSO, 100 μM PHPS-1 or NSC87877 for 48 hours. Trypan Blue exclusion assay was then performed to determine cell viability. No significant difference was found between inhibitor- and DMSO-treated groups of both types of cells. Data are presented as mean \pm s.d. (B) PDGFR α /PDGF-A-coexpressing *Ink4a/Arf*^{-/-} mAst or LN444 cells were separately cultured in the presence or absence of 100 μM PHPS-1 or NSC87877 for 48 hours. Cells were then lysed for IB analysis using an anti-caspase-3 antibody. No detectable caspase-3 cleavage was seen in both types of cells. β -actin was used as a loading control.

3.3.4 SHP-2 ablation disrupts PI3K/AKT activation by interfering with PI3K association with PDGFR α

We then examined the impact of SHP-2 inhibitors, PHPS-1 and NSC87877, and PDGFR α -F720 on the PI3K-signaling. As shown in Figure 23B and 30A, PDGFR α -F720 mutant and SHP-2 inhibitors significantly decreased PDGF-A-stimulated p-Akt in PDGFR α -expressing mAst. A near complete knockdown of SHP-2 by siRNAs markedly reduced the stimulated p-Akt levels in these cells, possibly through interruption of the association between PI3K (p85 subunit) and PDGFR α (Figure 30B).

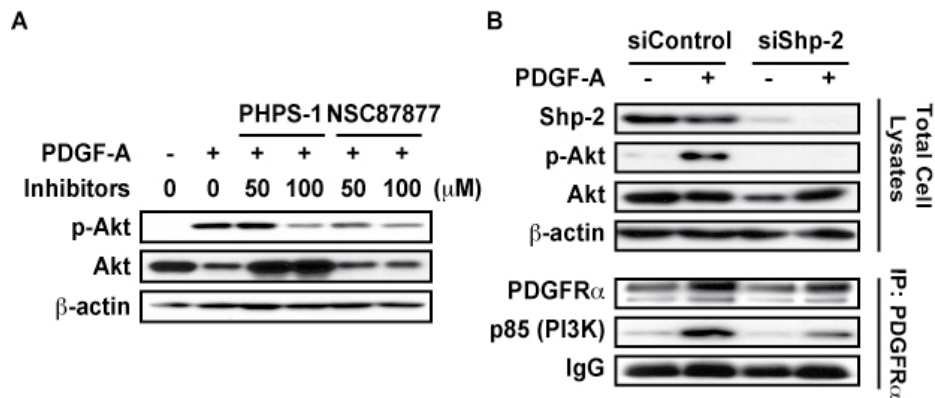


Figure 30. SHP-2 recruits PI3K to activate AKT pathway and is important for PDGF-A-stimulated growth.

(A) IB analyses of serum-starved *Ink4a/Arf*^{-/-} PDGFR α -expressing mAst were treated with SHP-2 inhibitors PHPS-1 or NSC87877 for 24 hours followed by 50 ng/ml PDGF-A for 5 min. (B) IP-IB analysis of PDGFR α -overexpressing mAst that were transfected with SHP-2 siRNA for 48 hours, serum-starved for an additional 24 hours followed by PDGF-A stimulation. Corresponding total proteins, β -actin, or total pulled-down IgG were used as loading controls.

However, a previous study showed that PDGFR α -F720 mutation did not result in a decrease in PI3K association with the RTK in mouse fibroblasts (74). Similarly, when SHP-2 was knocked down in NIH3T3 cells, a minimal impact of SHP-2 inhibition on PDGF-A-induced PI3K association and Akt phosphorylation was observed in these fibroblasts (Figure 31A), suggesting that the impact of SHP-2 on PI3K association with the RTK and p-Akt in astrocytes and glioma cells was specific. To examine whether the effect of SHP-2 knockdown on p-Akt signaling was specific to PDGFR α signaling, we knocked down SHP-2 by siRNAs in EGFRvIII-expressing *Ink4a/Arf*^{-/-} mAst (PTEN wt), LN444, and U87MG (both PTEN mutant) cells. We observed a reduction or a modest impact of p-AKT level in LN444/EGFRvIII and U87MG/EGFRvIII cells, respectively (Figure 31B), suggesting that SHP-2 also regulates PI3K/AKT activation in other RTK signaling. However, Akt phosphorylation was absent in *Ink4a/Arf*^{-/-} EGFRvIII mAst, possibly due to the presence of WT Pten in these cells. Together, we have demonstrated that SHP-2 regulates PI3K binding to the PDGFR α and the downstream AKT phosphorylation, and this regulation is likely also present in other RTK signaling such as EGFR signaling but is cell type-specific.

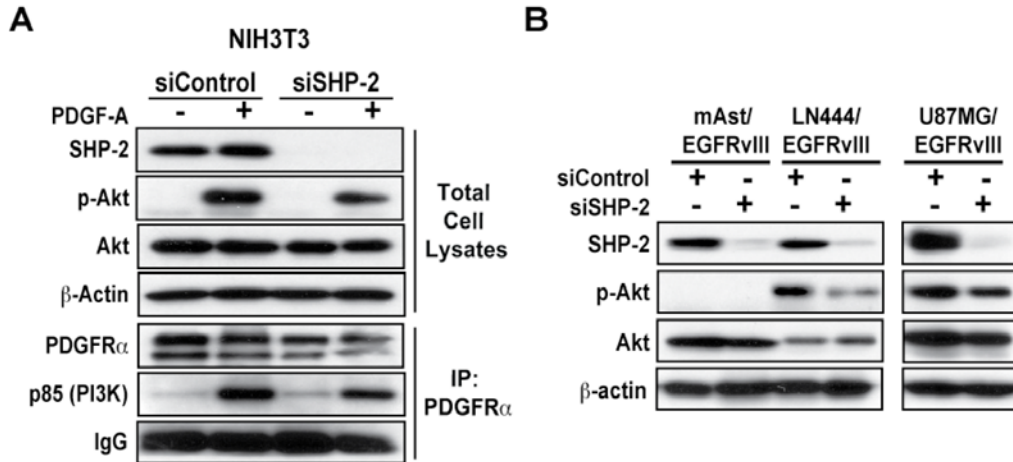


Figure 31. The impacts of SHP-2 knockdown in NIH3T3, *Ink4a/Arf*^{-/-} EGFRvIII mAst, LN444/EGFRvIII, and U87MG/EGFRvIII cells.

(A) Association of PI3K to PDGFR α and downstream Akt phosphorylation in NIH3T3 cells were only moderately affected by SHP-2 knockdown. IB analysis of NIH3T3 mouse fibroblasts that were transfected with control or SHP-2 siRNA for 48 hours, serum-starved for an additional 24 hours followed by 50 ng/ml PDGF-A stimulation. Various whole-cell lysates or immunoprecipitates pulled down by an anti-PDGFR α antibody were subjected to IB analysis using indicated antibodies. Corresponding total proteins, β -actin, or total pulled-down IgG were used as loading controls for induced protein phosphorylation (272) or associations (IP followed by IB). (B) *Ink4a/Arf*^{-/-} EGFRvIII mAst, LN444/EGFRvIII, and U87MG/EGFRvIII cells were transfected with control or SHP-2 siRNA for 48 hours, and then lysed for IB analysis using indicated antibodies. β -actin was used as a loading control.

3.3.5 SHP-2 ablation attenuates the enhanced anchorage-independent growth of PDGFR α -overexpressing cells which can be rescued by constitutively active PI3K signaling

We further determined the impact of the ablation of SHP-2 on cell transformation. Strikingly, stable knockdown of SHP-2 by shRNAs markedly reduced PDGFR α -promoted soft agar growth of mAst (Figure 32).

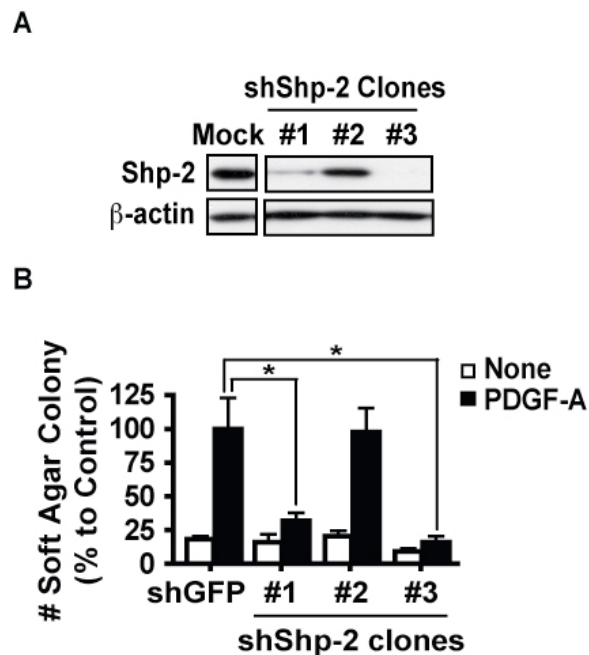


Figure 32. SHP-2 knockdown suppresses PDGF-A-stimulated soft agar growth of Ink4a/Arf^{-/-} mAst overexpressing PDGFR α .

(A) IB analysis showing SHP-2 knockdown by different shRNA clones with distinct knockdown efficiencies.

(B) Clones that induce significant reduction in SHP-2 expression (clones 1 and 3) lead to decreased tumor cell growth in soft agar. Data are presented as mean \pm s.d. *, $P < 0.01$, Student's *t* test.

Since in clinical glioblastomas, activating PI3K mutations are mostly observed in specimens with no *PDGFRA* aberrations (10, 11), we introduced a constitutively active PI3K p110 subunit (p110 α -CAAX) into *Ink4a/Arf*^{-/-} mAst that either expressed PDGFR α -F720 or a SHP-2 shRNA (Figure 33A). In both cell lines, we observed a rescue effect of p110 α -CAAX in soft agar colony formation (Figure 33B), suggesting that PI3K/AKT acts downstream to SHP-2 in PDGFR α -overexpressing gliomas, and that activating PI3K mutations in clinical gliomas might be able to bypass SHP-2 activation to promote tumorigenesis. Taken together, our results suggest that SHP-2 regulates the PI3K/AKT/mTOR-signaling emanating from PDGFR α activation and this regulation is important for PDGF-A-stimulated cell transformation.

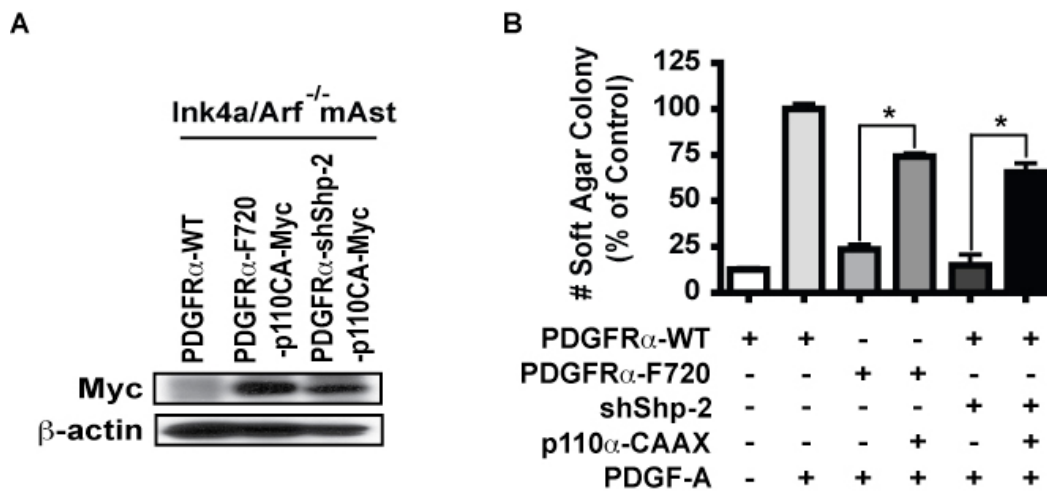


Figure 33. Constitutively activated PI3K rescued the inhibitory effect of SHP-2 inhibition on blocking PDGFR α -mediated cell transformation.

(A) IB analysis of expression of p110 α -CAAX. (B) Soft agar assays. Data are presented as mean \pm SEM. *, $P < 0.0001$. For IB analysis, β -actin was used as a loading control.

3.3.6 SHP-2 ablation disrupts mTORC1/S6K activation and mTOR inhibitor rapamycin treatment suppresses growth of PDGFR α - or EGFRvIII-overexpressing cells

Next, we tested whether signaling downstream to Akt was affected by SHP-2 inhibition. We found that SHP-2 inhibitors (Figure 34A), PDGFR α -F720 mutations (Figure 34B), or SHP-2 siRNA knockdown (Figure 34C) significantly impaired PDGF-A-stimulated phosphorylation of S6 kinase (p-S6K) downstream to the mTOR pathway. These results suggest that PDGFR α -promoted tumorigenesis necessitates an intact SHP-2 activity that regulates the PI3K/AKT/mTOR/S6K pathway.

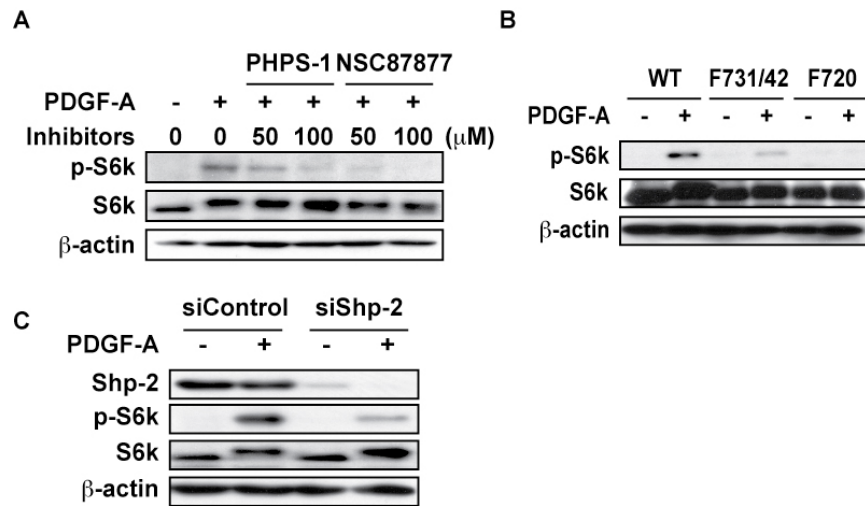


Figure 34. SHP-2 is required for activation of mTOR/S6K pathway stimulated by PDGF-A in PDGFR α -overexpressing mAst.

(A) IB analyses of serum-starved *Ink4a/Arf*^{-/-} PDGFR α -expressing mAst that were treated with SHP-2 inhibitors PHPS-1 or NSC87877 for 24 hours followed by 50 ng/ml PDGF-A for 5 min. (B) IB analysis of phospho-S6 kinase levels of various mAst stimulated by PDGF-A. (C) IB analysis of PDGFR α -overexpressing mAst that were transfected with SHP-2 siRNA for 48 hours, serum-starved for an additional 24 hours followed by PDGF-A stimulation.

Since PDGF-A-induced cell transformation requires an intact SHP-2 to activate PI3K/AKT/mTOR/S6K pathway, it was of interest to examine whether mTOR inhibitors under intensive clinical testing were able to suppress the PDGF-promoted tumorigenesis. As shown in Figure 36, treatment with a mTOR complex 1 (mTORC1) inhibitor rapamycin led to a dose-dependent decrease in soft agar colonies formed by PDGF-A-stimulated *Ink4a/Arf*^{-/-} mAst expressing PDGFR α or LN444 cells (Figure 35A and B), compared to their respective DMSO-treated controls. Similarly, rapamycin was able to effectively suppress the cell transformation capacity conferred by EGFRvIII expression in these cells (Figure 36), further suggesting the importance of downstream mTOR/S6K pathway in PDGF- or EGFR-mediated tumorigenesis.

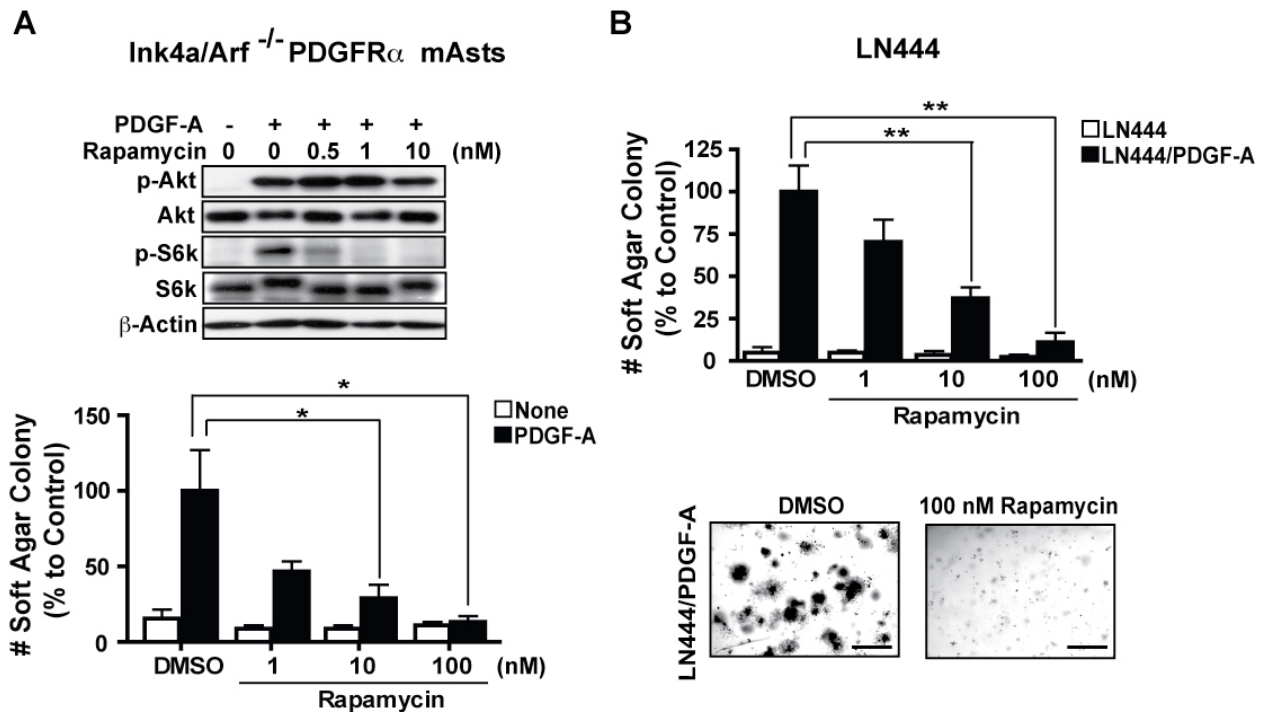


Figure 35. Rapamycin inhibits PDGFR α -promoted cell transformation.

(A) *Upper panel*, IB analysis of whole-cell lysates from serum-starved PDGFR α -expressing *Ink4a/Arf*^{-/-} mAst that were pre-incubated in the presence or absence of rapamycin at indicated concentrations for 24 hours

followed by stimulation with or without PDGF-A for 5 min. Corresponding total proteins or β -actin were used as loading controls for induced protein phosphorylation. *Lower panel*, bar graph, quantification of soft agar assays. Cells were grown in triplicates in soft agar with or without rapamycin at indicated concentrations. PDGF-A-expressing mAst in 10% of total cells were included as a source of PDGF-AA in these experiments. (B) Soft agar assay of LN444 and LN444/PDGF-A glioma cells treated with indicated concentration of rapamycin. *Upper panel*, bar graph, quantification of the soft agar assay. *Lower panel*, representative images of LN444/PDGF-A cells treated with DMSO control or 100 nM rapamycin. Data are presented as percentage to the controls in mean \pm s.d. and are representative of two independent experiments. *, $P < 0.05$; **, $P < 0.01$, Student's *t* test.

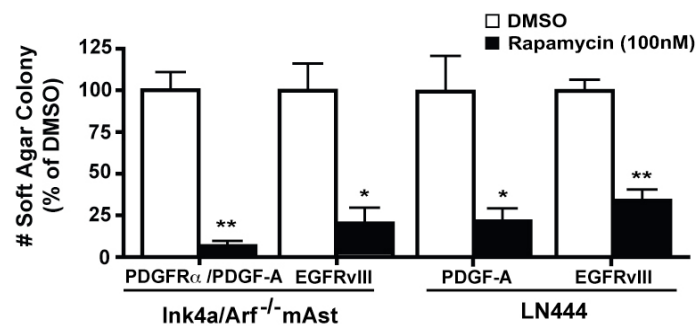


Figure 36. Rapamycin inhibits EGFRvIII-promoted cell transformation.

Soft agar assay of PDGFR α /PDGF-A- or EGFRvIII-expressing *Ink4a/Arf*^{-/-} mAst or LN444 cells treated with 100 nM rapamycin. Cells were grown in triplicates in soft agar with or without rapamycin at indicated concentrations. Data are presented as percentage to the controls in mean \pm s.d. and are representative of two independent experiments. *, $P < 0.005$; **, $P < 0.001$, Student's *t* test.

Previous studies suggested that the limited efficacy of rapamycin in clinical use was due to the capacity of rapamycin to potentiate PI3K/Akt signaling (276). However, we did not observe an increase of p-Akt level in both *Ink4a/Arf*-deficient mAst and LN444 cells treated with rapamycin up to 72 hours (Figure 37).

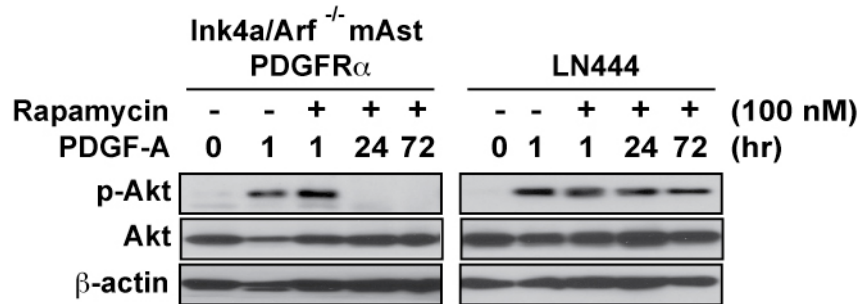


Figure 37. Rapamycin treatment does not lead to feedback AKT activation in PDGF-A-stimulated cells.

IB analysis of whole-cell lysates from serum-starved PDGFR α -expressing *Ink4a/Arf*^{-/-} mAst that were pre-incubated in the presence or absence of 100nM rapamycin for 24 hours followed by stimulation with PDGF-A for the indicated times. Total Akt or β -actin was used as loading controls for induced protein phosphorylation.

3.4 SUMMARY AND CONCLUSION

In summary, we have defined the key signaling pathways that are required for PDGFR α -mediated gliomagenesis in the background of *Ink4a/Arf* deletion (Figure 38). When the tyrosine phosphorylation sites for PI3K binding were mutated to phenylalanine, PDGFR α lost the capacity to transform mAsts, both *in vitro* in soft agar and *in vivo* in the mouse brain. Unexpectedly, association between PDGFR α and one of the downstream effector phosphotyrosine phosphatase SHP-2 was also required for maximal tumorigenic potential seen in cells overexpressing the WT receptor. Soft agar colony formation experiments using various pharmacological inhibitors further confirmed the importance of PI3K and SHP-2 activities in PDGF-induced growth. IP/IB experiments showed that SHP-2 association with PDGFR α is required for PI3K/Akt/mTOR pathway activation, further demonstrating a mechanism that SHP-2 can modulate the PDGFR α signaling during the formation of gliomas (Figure 38). As in the PDGFR α -expressing cells, SHP-2 also regulated Akt activation in some EGFRvIII-expressing human glioma cells, suggesting that SHP-2 may be an important signaling molecule where different RTKs signaling pathways converge. Thus we identified SHP-2 to be a potential target for therapeutic intervention for patients with malignant gliomas.

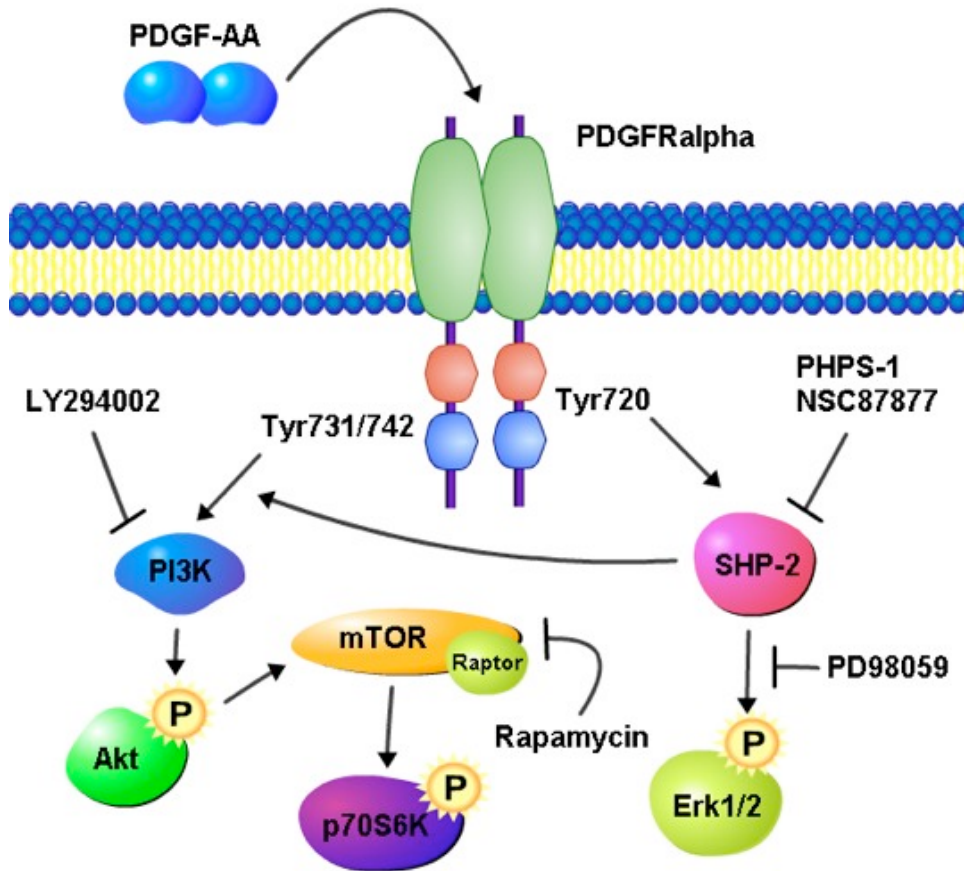


Figure 38. SHP-2-regulated PI3K/AKT/mTOR pathway in the PDGFR α /PDGF-A-mediated gliomagenesis.

PDGF-AA homodimer binding triggers PDGFR α dimerization and autophosphorylation in the cytoplasmic domain. Recruitment of downstream signaling effectors PI3K and SHP-2 is mediated by phosphorylated Tyr 731/742 and Tyr 720, respectively. In addition, in this study we demonstrate that SHP-2 activity is required for the binding between PI3K and pTyr 731/742 of the receptor, and the downstream AKT and mTOR/p70S6K phosphorylation/activation. Inhibitors that suppress SHP-2 phosphatase activity (PHPS-1 and NSC87877) or SHP-2 downstream MEK/MAPK pathway (PD98059) were able to impact on the activation of PI3K pathway as well, indicating SHP-2 activity is important for this regulation. Finally, the SHP-2 inhibitors, MEK inhibitor, PI3K inhibitor LY294002, and mTORC1 inhibitor rapamycin were shown to suppress PDGF-induced tumorigenesis, and the constitutively active PI3K was capable of rescuing the anti-tumor effect of SHP-2 ablation, suggesting this network of signaling interactions are crucial to gliomagenesis promoted by PDGF over-activation.

4.0 PDGFRA/PDGF-A EXPRESSION IN CLINICAL GLIOMA TISSUES IS CONCOMITANT WITH ACTIVATION OF SHP-2 AND PI3K/AKT/MTOR SIGNALING PATHWAYS

4.1 INTRODUCTION AND RATIONALE

We have identified in our mouse model that SHP-2 is required for optimal PI3K/Akt/mTOR activation downstream to PDGFR α , and activation of both SHP-2 and PI3K was required for maximal tumorigenesis induced by PDGFR α overexpression. To further demonstrate that SHP-2 and PI3K activation is present in the PDGFR α /PDGF-A-expressing clinical glioma specimens, we attempted to exploit IHC and IB analyses to characterize the glioma tissues of two separate cohorts.

4.2 MATERIALS AND METHODS

4.2.1 Antibodies

The following antibodies were used in this study: rabbit anti-PDGFR α (sc-338, IHC, 1:50), rabbit anti-PDGF-A (sc-128, IHC, 1:50), and goat anti- β -actin (sc-1616, 1:500) antibodies were from Santa Cruz Biotechnology Inc., Santa Cruz, CA; mouse anti-phospho-Akt (Ser473, #4051, 1:1000), rabbit anti-phospho-Akt (Ser473, #4060, IHC, 1:50), rabbit anti-phospho-S6 (Ser235/236, #4858, 1:2000 for IB; 1:50 for IHC), and rabbit anti-phospho-SHP-2 (Tyr542, #3751, 1:1000 for IB; 1:50 for IHC) antibodies were from Cell Signaling Technology, Danvers, MA; All secondary antibodies were from Vector Laboratories (Burlingame, CA) or Jackson ImmunoResearch Laboratories (West Grove, PA). All other reagents were from Invitrogen, Sigma-Aldrich, or Fisher Scientific.

4.2.2 Histology and IHC of Clinical Human Glioma Tissues

Studies using human tissues were reviewed and approved by the Institutional Review Board involving Human Subjects of the University of Pittsburgh (Pittsburgh, PA, USA). The specimens were de-identified human tissues thus no informed consent was required. A total of 158 paraffin-embedded thin sections of primary human glioma specimens were utilized including 87 WHO grade IV GBM, 34 grade III anaplastic astrocytoma (AA), oligodendroglioma (AO) or oligoastrocytoma (AOA) and 37 grade II oligodendroglioma (OD)

and diffuse astrocytoma (DA). Thin sections of human glioma specimens were analyzed by IHC using indicated antibodies. Briefly, the 5- μ m human tissue sections were deparaffinized in xylene followed by rehydration in graded ethanol. After washing with Tris-buffered saline (TBS), the antigen was retrieved by boiling the sections in a citrate buffer (pH 6.0) twice for 5 min. Tissues were blocked by AquaBlock (East Coast Biologics Inc.) for 1 hour at room temperature. Afterwards, tissue sections were then incubated with a primary antibody overnight at 4°C, and blocked by Peroxidase Blocking Reagent (DAKO) for 10 minutes, followed by incubation with a biotinylated secondary antibody for 30 min at room temperature. After washed in PBS, stained tissue sections were visualized by diaminobenzidine chromophore and H₂O₂ followed by hematoxylin counterstaining. Sections were then dehydrated by graded ethanol, and mounted with Permount Solution (5).

4.2.3 Immunoblotting

The IB analysis on the lysates of snap-frozen human GBM tissues was performed as described in **2.2.6** (Page 54) of this dissertation.

4.3 RESULTS

4.3.1 Analysis of PDGFR α /PDGF-A, SHP-2, and PI3K/AKT/mTOR pathway activation status by immunohistochemistry on paraffin-embedded human glioma tissues.

To determine whether PDGF-A and PDGFR α are co-expressed and whether there is a link of overexpression of PDGF-A and PDGFR α and activation of the SHP-2 and the PI3K/AKT/mTOR signaling in clinical glioma specimens, we performed IHC staining on a total of 158 paraffin-embedded primary human glioma specimens using anti-PDGFR α , anti-PDGF-A, anti-p-SHP-2 Tyr542, anti-p-AKT Ser473, and anti-p-S6 Ser235/236 antibodies. PDGFR α proteins were detected at medium to high levels in 17 out of 87 GBMs (WHO grade IV tumors) and 9 out of 71 grade II and III tumors. Among these PDGFR α -positive gliomas, PDGF-A is often co-expressed in the same population of tumor cells (Figure 39B and C, and Table 4). Significantly, phosphorylation of SHP-2 Y542 (p-SHP-2, required for its activation) (277), AKT (p-AKT), and ribosomal S6 subunit (p-S6) was also often detected on sister sections of the same tumor in many of the PDGF-A/PDGFR α -positive glioma specimens (Figure 39 B to F, and Table 4), suggesting a link of activation of PDGF-A/PDGFR α to stimulation of SHP-2, AKT, and mTOR in clinical glioblastoma specimens.

To evaluate the expression of various proteins in the clinical glioma specimens, we employed a set of grading criteria for IHC analysis. As shown in Table 4, in all IHC analyses, tumors that harbor low or no signals in less than 1% of tumor cells were graded as “+ / -”; low signals in around 1-10% of tumor cells as “+”; moderate signals in less than 10-25% as “++”; moderate signals in around 25-50% of the tumor cells as “+++”; and strong signals in 50-75% of

the tumor cells as “++++.” Representative images for each of these categories are shown in Figure 40. Grading of all IHC-stained tumor specimens was independently assessed by two different individuals in the laboratory. The final grading was then determined by comparison and discussion of the scores evaluated by these individuals.

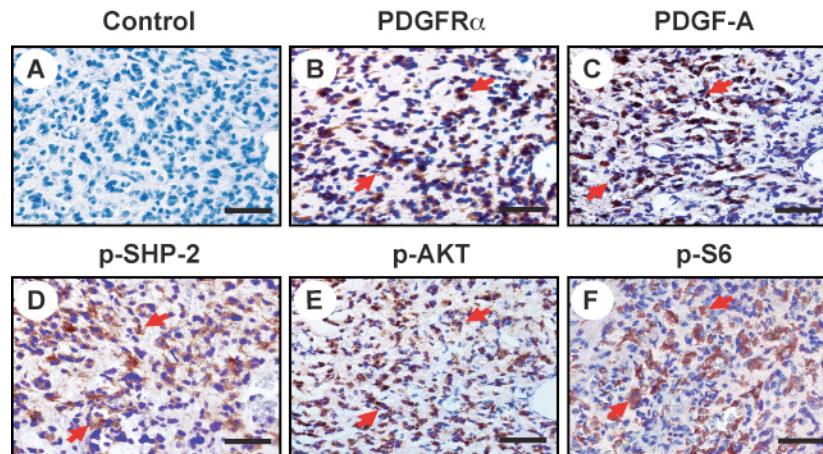


Figure 39. PDGFR α and PDGF-A are co-expressed in clinical glioma specimens with activated SHP-2 and PI3K/AKT/mTOR pathways.

(A) to (F), Images of IHC staining on a representative human GBM specimens, J212 (sister sections), using anti-PDGFR α (B), anti-PDGF-A (C), anti-p-SHP-2 (Y542) (D), anti-p-AKT (E), and anti-p-S6 (F) antibodies.

(A) No primary antibody. Arrows, positive staining of indicated proteins. Bars, 50 μ m.

Table 4. Summary of Immunohistochemical Analyses on Clinical Human Glioma Tissues

Number	Grade	Histology	PDGFR α	PDGF-A	p-Akt	p-S6	p-SHP-2
J7	4	Glioblastoma	++	++	-	-	-
J10	3	Anaplastic Astrocytoma	++	++	+	+	+
J16	3	Anaplastic Oligodendroglioma	+++	+++	++	+	+
J44	2	Diffuse Astrocytoma	+++	++++	++++	+++	++
J57	2	Diffuse Astrocytoma	++	++	+	+	+
J69	4	Glioblastoma	+++	+++	+	++	++
J72	4	Glioblastoma	++	+++	+++	+++	+++
J80	4	Glioblastoma	++	++	+	++	-
J84	4	Glioblastoma	+++	+++	+	+	+
J94	2	Oligodendroglioma	++	++	++	-	-
J152	4	Glioblastoma	+	++	+	+ / -	++
J156	4	Glioblastoma	+	+	+	++	+
J158	4	Glioblastoma	+++	++	+++	+	++
J159	4	Glioblastoma	+++	+ / -	+++	+	++
J161	4	Glioblastoma	++	+	++	++	++
J163	4	Glioblastoma	++	+++	++	+++	+
J165	3	Anaplastic Astrocytoma	++	++	++	++	-
J171	3	Anaplastic Oligodendroglioma	+++	++	++	++	++++
J182	1	Pilocytic Astrocytoma	+ / -	+ / -	-	-	+
J183	1	Pilocytic Astrocytoma	+ / -	+ / -	+	++	+
J196	3	Anaplastic Astrocytoma	+++	++	+++	++	++++
J200	3	Anaplastic Oligodendroglioma	++	+ / -	++	+	-
J211	4	Glioblastoma	+	+	+	+	+
J212	4	Glioblastoma	+++	++	++	+++	+
J216	4	Glioblastoma	+	++	++	++	++
J233	4	Glioblastoma	+	+ / -	-	-	-
J235	4	Glioblastoma	+	++	+	++	+
JKU01	4	Glioblastoma	+ / -	++	+ / -	+	+
JKU02	4	Glioblastoma	++	+ / -	+ / -	+ / -	+ / -
JKU03	4	Glioblastoma	++	+ / -	+	+	+
JKU04	4	Glioblastoma	++	+	+	+	++
JKU05	4	Glioblastoma	++	++	++	+	+
JKU06	3	Anaplastic Astrocytoma	+++	++++	+	+ / -	++
JKU07	4	Glioblastoma	++	++	+	+ / -	++
JKU08	4	Glioblastoma	+++	++	+	+	+
JKU09	4	Glioblastoma	+	+++	+	+	+
JKU10	4	Glioblastoma	++	+++	++	+	+

++++ Strong signals in most tumor cells (50~75%)
 +++ Moderate signals in most tumor cells (25~50%)
 ++ Moderate signals in some tumor cells (10~25%)
 + Low signals in few tumor cells (1~10%)
 + / - Low or no signals in few tumor cells (<1%)
 - No detectable signals in all tumor cells (0%)

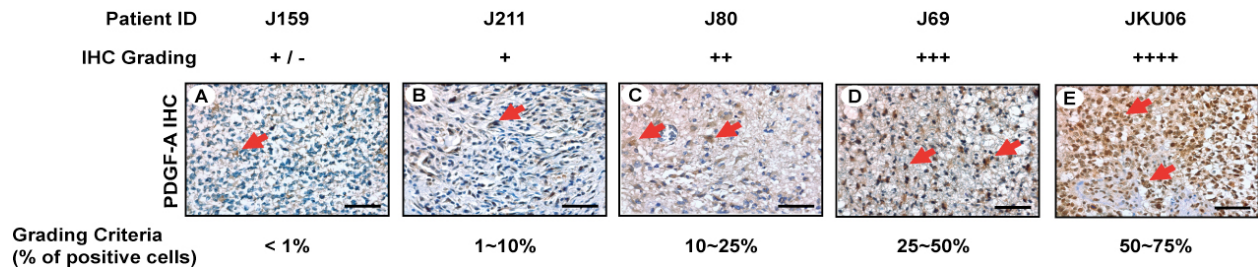


Figure 40. Representative images of PDGF-A IHC staining showing grading of clinical glioma tissues according to PDGF-A positivity.

Images of IHC staining on representative human GBM specimens graded as (A) “+ / -”: Low or no signals in few tumor cells (< 1%); (B) “+”: Low signals in few tumor cells (1~10%); (C) “++”: Moderate signals in some tumor cells (10~25%); (D) “+++”: Moderate signals in most tumor cells (25~50%); (E) “++++”: Strong signals in most tumor cells (50~75%). Arrows, positive staining of PDGF-A proteins. Bars, 50 μ m.

4.3.2 Analysis of PDGFR α /PDGF-A, SHP-2, and PI3K/AKT/mTOR pathway activation status by immunoblotting using snap-frozen human glioma tissues.

To validate these IHC data, we performed IB analyses on a separate cohort of a total of 20 snap-frozen clinical GBM specimens. As shown in Figure 41, PDGFR α is expressed at high levels in 7 out of 20 GBM samples, 5 of which expressed PDGF-A proteins, suggesting an autocrine PDGFR α signaling in these tumors. In 4 out of these 5 PDGF-A/PDGFR α -positive tumors, p-AKT, p-SHP-2 and p-S6 were also detected. Of note, expression of PDGF-A, p-AKT, p-SHP-2 and p-S6 at various levels in other tumor samples likely reflects the impact of heterogeneous gene alterations such as mutations of *PTEN*, *TP53* and overexpression of EGFR/EGFRvIII and c-MET that affect the expression or activation (phosphorylation) of these proteins in clinical

glioblastomas. Taken together, these results establish a link of PDGF-A/PDGFR α expression with activation of SHP-2, PI3K/AKT/mTOR signaling in clinical glioblastoma samples.

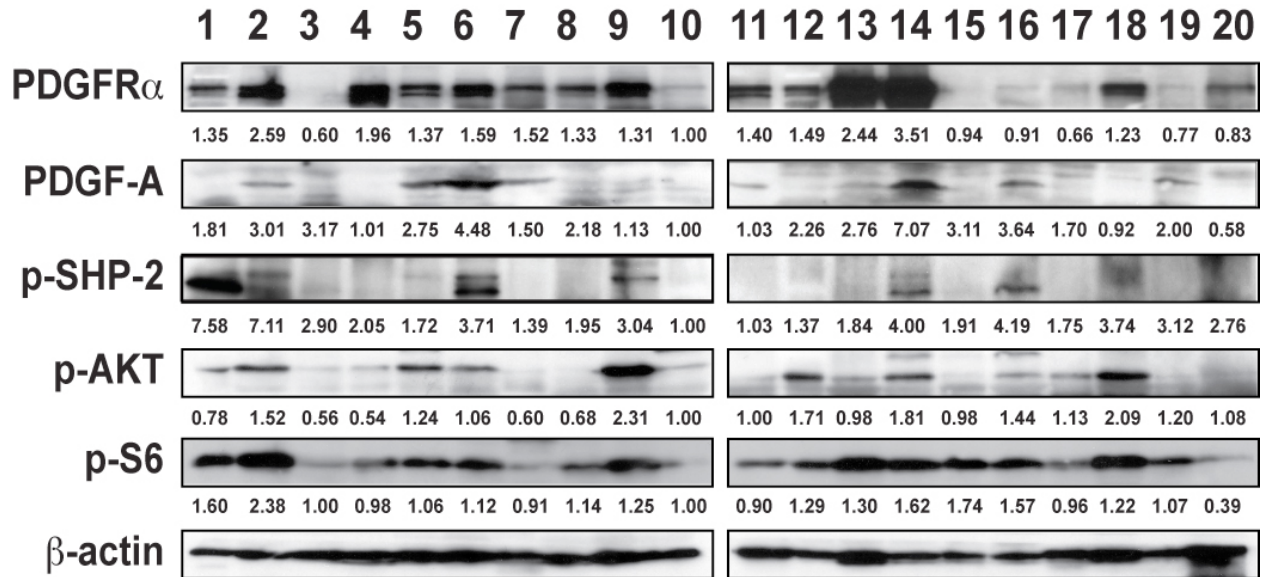


Figure 41. PDGFR α and PDGF-A are co-expressed in clinical glioma specimens with activated SHP-2 and PI3K/AKT/mTOR pathways.

IB analysis of tissue lysates of a separate cohort of 20 human GBM snap-frozen specimens using indicated antibodies. β -actin was used as a loading control. The band intensity was determined by Adobe Photoshop CS3 Version 10.0.1 software. The mean intensity of each tumor sample was then normalized according to the corresponding β -actin levels and compared to that of GBM #10.

4.4 SUMMARY AND CONCLUSION

We have characterized PDGFR α expression and its downstream pathway activation using IHC staining in a cohort of 158 grade II-IV human glioma specimens. We found that around 15% of the samples in our collection show medium to high expression of the receptor, many of which also concomitantly express PDGF-A chain. Interestingly, 90% of the PDGFR α -positive tumors also harbor activation of PI3K/Akt pathway as determined by p-Akt expression, while 80% show phosphorylation of p70 S6 ribosomal subunit downstream to the mTOR pathway. Our IB analyses on a separate cohort of 20 human GBM samples further confirmed these results. Although a causal link between activation of PI3K/Akt/mTOR and PDGF-induced glioma formation requires the use of animal models or *in vitro* cultured tumor-derived cell lines, we provide evidence that there is co-occurrence of PI3K/Akt/mTOR activation and PDGFR/PDGF-A autocrine in human glioma tissues.

5.0 GENERATION OF GENETICALLY MODIFIED MICE USING THE SLEEPING BEAUTY TRANSPOSON SYSTEM—A POTENTIAL PLATFORM FOR PRE-CLINICAL TESTING OF PDGF/SHP-2 TARGETED THERAPIES

5.1 INTRODUCTION AND RATIONALE

5.1.1 Animal Model Systems For Malignant Gliomas

Since PDGF-targeted therapies have been largely disappointing to date, development of animal models of malignant gliomas that can re-capitulate the human tumor progression, histology, and genetic alterations is urgent. Most of the current mouse models of spontaneous gliomas involve generation of germ-line transgenic GEMs (162) or the use of viral vectors delivering genes of interest into the mouse brain (164-167). However, the production and the subsequent characterization of GEMs or viral vectors can take a long time and is often expensive. Moreover, the viral capacity for DNA cargos is limited; the stability of the vectors may be compromised by reverse transcription; and the preferential insertion of viral vectors into actively transcribed sequences may increase the chance of undesired mutagenesis.

5.1.2 Sleeping Beauty Awakens!

In an effort to develop a non-viral, time- and cost-efficient method to generate spontaneous mouse models of malignant gliomas, Dr. John R. Ohlfest at University of Minnesota (Minneapolis, MN) has exploited an ancient transposon system to deliver various oncogenes into the mouse brain, and successfully generated *de novo* brain tumor GEM models by using several different combinations of oncogene/shRNA expression (174). This ancient transposon system, called *Sleeping Beauty* (SB), was so-named since it was first isolated from salmonid fish as a dormant “junk DNA” with accumulated mutations. The SB transposon, together with the transposase gene that is responsible for its transposition in the genome, was later “resurrected” by site-directed mutagenesis to remove the inactivating mutations, and was shown to be capable of jumping via cut-and-paste in fish, mouse, and human cells (175). It thus represents the first transposon system isolated from the vertebrate animals. Since its discovery, the SB system has been developed as a novel tool both in cancer gene discovery (278, 279) and in gene therapy (280, 281), for SB is able to transpose randomly throughout the genome by insertional mutagenesis and its expression is relatively stable compared with traditional non-viral, episomal DNA plasmids used for gene therapies.

The SB transposase recognizes and binds the inverted direct repeats flanking the DNA sequence of interest, excises and inserts it into a new location within a TA dinucleotide in the targeted genomic sequence. The long-term stable *in vivo* expression of the SB-mediated transposons in the genome suggests that SB system is a candidate for generating animal models of various cancers. Combined with transgenic or knockout mice, SB system can be used to study the cooperation between different oncogene expression and loss of tumor suppressors in cancers.

For example, SB transposase-mediated expression of an activated *NRAS* can cooperate with loss of *Arf* to generate liver cancers (282). Additionally, the use of tissue-specific promoter-driven expression of the SB transposase can restrict the transposition in specific types of cells, further improving the power of this system to model various human diseases including cancers (176). We have here recently established the SB system in our lab. We plan to exploit this system to model PDGF-driven gliomagenesis in various types of mice including BALB/c, C57BL/6, p53^{-/-}, and likely the Ink4a/*Arf*^{-/-} mice. We expect that a combinational use of this system with various existing knockout/transgenic mice will elucidate the pathogenesis of gliomas and facilitate pre-clinical assessments of various targeted therapies for this cancer. Therefore the ancient *Sleeping Beauty* transposon system has awakened in the field of cancer research.

5.2 MATERIALS AND METHODS

5.2.1 Animal Care and Mating

All animal experiments were approved by Institutional Animal Care and Use Committee (IACUC) of University of Pittsburgh, Pittsburgh, PA. C57BL/6 mice were purchased from The Jackson Laboratory. Breeding pairs were setup in one pair per cage and females checked for their pregnancy everyday until they gave birth. Neonates with ages < 48 hours were used for experiments.

5.2.2 SB DNA Plasmid Vectors

The generation of pT2/Luc//PGK-SB13, pT/CMV-SV40-LgT, pT/CAGGS-NRAS-V12 vectors were described previously (174). PT2/CMV-PDGFR α was created by excising the CMV-PDGFR α from pcDNA3/PDGFR α as an Nru I/Not I fragment and ligating into the pT2 vector between the Bgl II and Not I sites as a blunt end/Not I fragment. PT2/MSCV was created by excising the MScV 5'-LTR and 3'-LTR from pMSCV-PGK-GFP vector (a kind gift from Dr. Tao Cheng at University of Pittsburgh, Pittsburgh, PA) as a Bgl II/Not I and Nco I/Hind III fragments, respectively, and ligating them into the pT2 vector between the same restriction sites. The pT2/MSCV/PDGF-A vector was then generated by excising the PDGF-A cDNA from pMXI-PDGF-A vector as an Eco RI fragment and ligating into the Eco RI site of the pT2/MSCV vector. Plasmids were purified using EndoFree Plasmid Maxi Kit (Qiagen, cat#: 12362) and stored in 0.1% TE buffer (pH8.0) at -80 °C.

5.2.3 Intracranial SB DNA Injection Using Polyethylenimine (PEI) *In-vivo* Transfection

The DNA plasmids used for stereotactic injection were prepared using an *in vivo*-jetPEI reagent (Polyplus Transfection) according to manufacturer's instructions. Briefly, SB plasmids pT2/Luc//PGK-SB13, pT/CMV-SV40-LgT, and pT/CAGGS-NRASV12 (0.1, 0.2, and 0.2 μ g per mouse) were diluted in half the volume of the total to be injected (1 μ l per mouse) in 5% dextrose. The *in vivo*-jetPEI reagent was diluted in a separate half volume of the total in 5% dextrose. After 5 min incubation of both mixtures, PEI reagent was added into the DNA solution. The cocktail was then incubated at room temperature for another 15 min before used directly for

intracranial injection. The amount of PEI reagent to be used was calculated as μl of PEI (150mM) used = $\frac{(\mu\text{gDNA} \times 3) \times N/P}{150}$. To achieve an N/P ratio of 7, 0.21 μl of PEI was used with 0.5 μg of DNA plasmids per neonate. The final DNA concentration in the DNA/PEI mixture to be injected was 0.5 $\mu\text{g}/\mu\text{l}$.

Stereotactic injection of SB DNA/PEI mixtures into neonatal mice was performed as previously described (174). Briefly, neonatal C57BL/6 mice (24~48 hours after birth) were placed on ice for 3-5 min to induce hypothermia anesthesia. Mice were then secured on a dry ice/ethanol-cooled neonatal mouse adaptor (Stoelting, cat. #51625). A 10 μl syringe with a 30-gauge needle (Hamilton) attached to the Quintessential Stereotactic Injector system (Stoelting, cat. #53311) and a Digital Three Axis Manipulator Arm (Stoelting, cat. #51904) were used to inject the DNA/PEI mixtures at a flow rate of 0.5 $\mu\text{l}/\text{min}$ for 2 min into the right lateral ventricle at a coordinate of 0.8 mm lateral, 1.5 mm anterior to the lambda, and 1.5 mm under the dura. After the injection, the needle was gently pulled out 0.5 mm and left for an extra 1 min before gently pulled out of the brain. The neonates were then placed under a heat lamp to recover from anesthesia and transferred back into the cage with the female mouse before returned to their housing area.

5.2.4 Bioluminescence Detection and Histology

In vivo luciferase detection was performed as previously described (174). Briefly, 48 hours after the injection, neonatal mice were placed in a 6-well plate and transferred to the bioluminescence facility. Mice were then injected i.p. with 50 μl of D-Luciferin Firefly (33 mg/ml; Caliper Life

Sciences, cat. #XR-1001) per mouse. Neonates were then imaged using Xenogen IVIS-200 Optical *In vivo* Imaging System (Xenogen corp., Alameda, CA) and analyzed using Living Imaging Software Version 4.1 (Caliper Life Sciences, Hopkinton, MA). Adult mice of age of 20 days were weaned and monitored for luciferase expression 1-2 times every 10 days until signs of tumor burdens. For luciferase imaging in the adult mice, mice were placed in an isoflurane chamber to induce anesthesia, and were then injected i.p. with 150 μ l of D-Luciferin. After 5 min, mice were imaged using the Xenogen IVIS-200 Imaging System. When neuropathological symptoms developed due to tumor burdens in the brain, the mice were euthanized. Brains of mice were then removed, embedded in Optimum Cutting Temperature (OCT) compound (Tissue-Tek) at -80°C , and cryo-sectioned at 5- μm thickness. Sections of brains were stored at -80°C until histological analysis. The following antibodies were used in IHC of this study: a rat anti-mouse CD31 (#550274, IHC, 1:1000) antibody was from BD Biosciences, San Jose, CA; a rabbit anti-Ki67 antigen (NCL-Ki67p, IHC, 1:200) antibody was from Leica Microsystems Inc., Bannockburn, IL.

5.3 RESULTS

5.3.1 Monitoring real-time tumor growth by luciferase bioluminescence

In order to establish a time- and cost-efficient glioma model that can more accurately recapitulate human tumors in our lab, in collaboration with Dr. Hideho Okada at University of Pittsburgh Cancer Institute (Pittsburgh, PA), we have established the SB-mediated spontaneous glioma formation model in our lab. It has been reported previously that spontaneous gliomas formed near the ventricles after the mice were injected with vectors encoding SB transposase and transposons carrying SV40-LgT and hyper-active human NRAS-G12V (G-to-V mutation in glycine residue 12 of the *NRAS* gene) expression (174). We thus first utilized this combination of oncogenes in our preliminary testing of the SB model. As shown in Figure 42, representative of two of the experiments using NRAS-G12V and SV40-LgT combination, we showed that median survival of mice is around 65 days, with some mice dying as early as 30-40 days and the others up to 80-90 days post-injection. Since the co-injected SB transposase vector contains a firefly luciferase gene, we can monitor the real-time tumor development by using bioluminescence imaging. We first confirmed whether the *in vivo* transfection of SB vectors was successful by imaging the neonatal mice 48 hours post-injection. As shown in Figure 43A, successful transfection is evident with strong luciferase signals in the brain of mice. All the luciferase-negative neonates (less than 10%) were euthanized and excluded from the study. The remaining neonates were kept in the same cage with the mother until around 20 days of age. After weaning, the mice were monitored closely for tumor formation by luciferase imaging 1-2 times every 10 days. As shown in Figure 43B, Mouse 2 represents one of the mice that developed luciferase-

positive tumors as early as 30 days (“early-progression” tumor). They often showed high morbidity by day 40 and prompted us to sacrifice them. Some of the mice, however, did not develop detectable luciferase expression until 40-50 days post-injection (“late-progression” tumors). As shown in Figure 43B, Mouse 1 showed luciferase expression around 46 days and Mouse 3 around 54 days post-injection, both of which did not show apparent neuropathological symptoms by the time of tumor development.

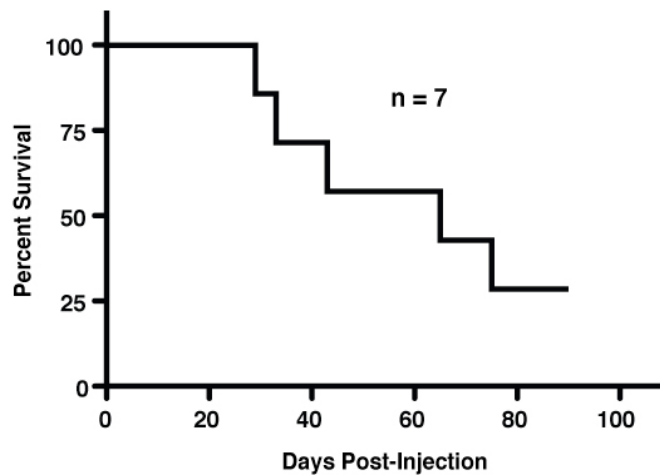


Figure 42. Kaplan-Meier survival curve for mice injected with SB transposase and NRAS/SV40-LgT-encoding transposons.

Survival analyses were performed on 7 SB-injected mice from two independent experiments. The median survival time was 65 days post-injection. Two mice survived up to 90 days with no signs of tumor burden prior to sacrifice.

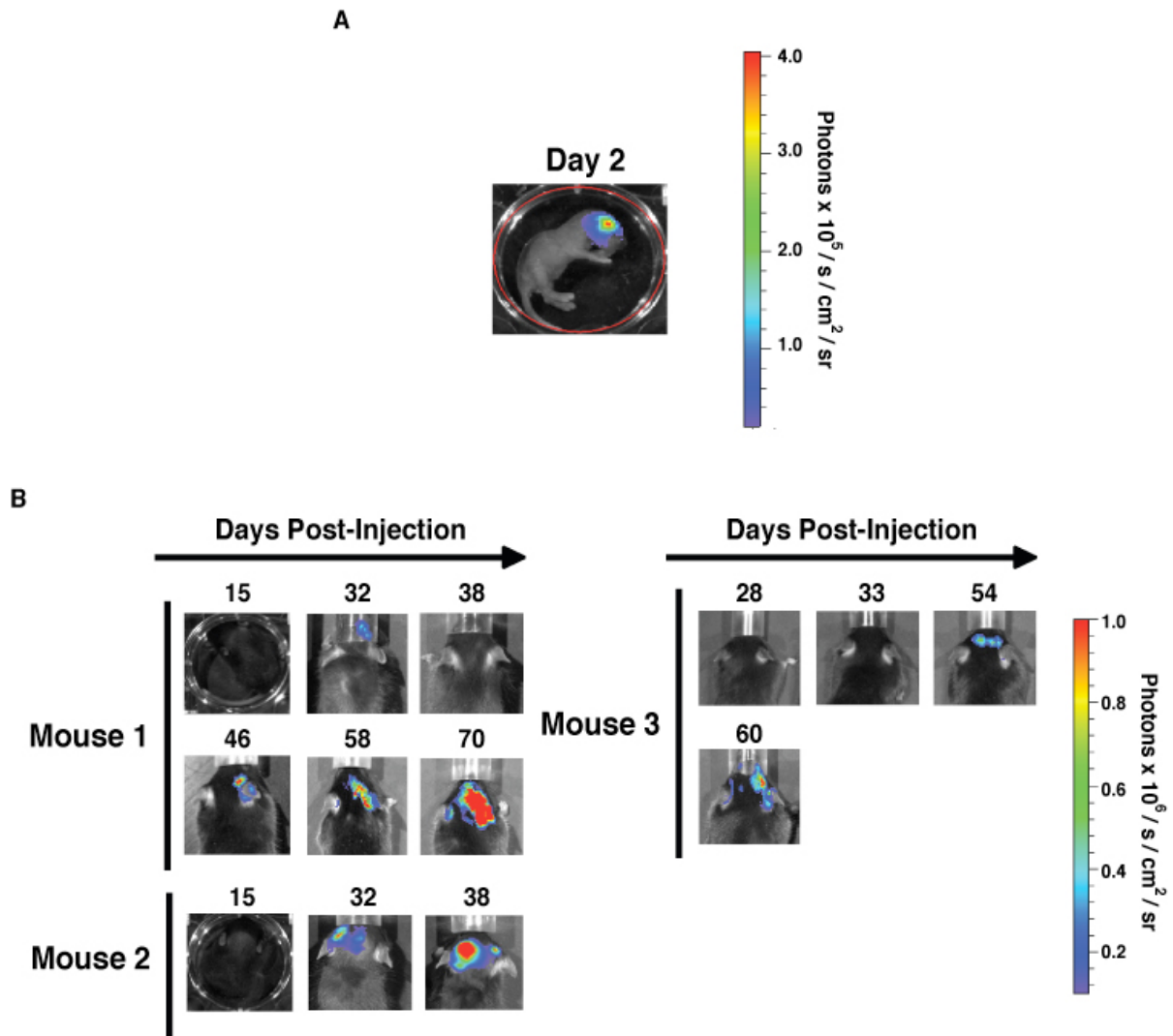


Figure 43. Luciferase imaging for mice injected with SB transposase and NRAS/SV40-LgT-encoding transposons.

(A) On day 2 post-injection, neonates were placed in a 6-well tissue culture plate and subjected to luciferase imaging as described in the Materials and Methods section. Mice with low or undetectable bioluminescence signals were euthanized and excluded from the study. (B) Luciferase images of representative SB-induced mice at different time points were shown. In some mice, the tumor progressed faster (Mouse 2; “early-progression” group) than the others (Mouse 1 and 3; “late-progression” group).

It has been noted that a higher injection volume (2 μ l) resulted in development of hydrocephalus, which is evident with an enlarged skull and accumulation of cerebrospinal fluid in the ventricular space (174). This complication seemed to occur more frequently in C57BL/6 mice than other strains of mice due to different genetic susceptibility (174). We constantly observed hydrocephalus in over 70% of the mice that were injected with 2 μ l of the DNA/PEI mixture, as early as 25 days post-injection. These mice often presented with neuropathological symptoms followed by death within 1-2 weeks and thus were excluded from the survival analyses. In order to avoid this complication, we reduced the injection volume but kept the same DNA concentration by injecting a total volume of 1 μ l with 0.5 μ g DNA per mouse. In these experiments, hydrocephalus became less prevalent and occurred only in < 25% of the cases. In one of the experiments, among the five mice that received 1 μ l of DNA/PEI mixtures, one died 3 days after weaning with no signs of tumor or hydrocephalus development. One developed mild hydrocephalus with high luciferase signal in the brain (Mouse 6) (Table 5). Subsequent histological analysis revealed that a grade III/IV tumor formed in the left ventricle, reminiscent of the observation in the previous report showing that hydrocephalic brain frequently harbored multifocal tumors in both lateral ventricles (174). Of the three remaining mice, one started to show luciferase expression in the brain 50 days post-injection and developed a grade III/IV tumor 60 days confirmed by histological assessment (Mouse 3). The other two mice showed no signs of tumor up to 90 days and were thus excluded from the study (Mouse 4 and 5). Overall, injection with 1 μ l of the DNA/PEI complex gave a significantly lower incidence of developing hydrocephalus but also came with a price of reduced tumor penetrance in C57BL/6 mice. Taken together, we have successfully generated SB-induced spontaneous glioma mouse models with

around 60% penetrance and were able to monitor real-time tumor progression through bioluminescence imaging.

5.3.2 Histological analyses of SB tumors reveal characteristics corresponding to those observed in human gliomas

Previous report showed that mice that received SB transposase-mediated NRAS and SV40-LgT expression developed spontaneous gliomas after 3-4 weeks and the tumor diagnosis often corresponds to WHO grade III and IV (174). A subsequent report using SB-induced expression of *NRASV12* and *shp53* also showed tumor histology corresponding to different grades of human gliomas (283). In this experiment, Fujita and colleagues demonstrated that SB-induced gliomas at 21 days post-injection resembled human grade II diffuse fibrillary astrocytomas, while 60-day tumors showed additional features such as pleomorphic nuclei and active mitoses, thus resembling WHO grade III gliomas (283). We observed differential tumor progression rates among SB-induced gliomas. As shown in Figure 43B, some of the mice developed tumors as early as 30 days whereas the others did not show detectable luciferase signal until 50 days post-injection. The mice with “early-progression” tumors often developed hydrocephalus around 30-40 days post-injection. This observation was reminiscent of a previous report, in which researchers generated spontaneous gliomas by injecting PDGF-B-encoding retrovirus into lateral ventricle of E14 mice and observed a group of “early-affected” mice showed high incidence of hydrocephalus and differential tumor histology, as compared to “late-affected” mice (167).

When the brains with SB-induced tumors were harvested and assessed for the presence of features of human tumors, both early- and late-progression tumors showed neuro-pathological

characteristics of high-grade gliomas, including high cellularity, cell infiltration into normal brain parenchyma, nuclear atypia, brisk mitotic activity, focal necrosis, and high Ki67 positivity (Figure 44, 45 and Table 5). We also found that one of the “early-progression” tumors (Mouse 6) contained multi-nuclear tumor cells characteristic of giant cell GBMs in humans (3). However, we were not able to confirm the presence of microvascular proliferation in all tumor specimens analyzed. In order to assess the endothelial cell proliferation of the SB-induced tumors, we performed IHC staining with an anti-platelet endothelial cell adhesion molecule 1 (PECAM-1/CD31) antibody on tumor sections from different mice. The intensity of CD31 staining in glioma tissues has been linked to degree of angiogenesis (259) and glioma tumor grades (284). As shown in Figure 45, both “early-“ and “late-progression” SB-induced tumors displayed active endothelial proliferation (Figure 45E-G), as compared to normal brain control (Figure 45A). Based on the histological and immunological features of these SB-induced tumors, we concluded that these spontaneous mouse gliomas resemble WHO grade III/IV gliomas in humans (Table 5). Taken together, we have demonstrated that SB-induced spontaneous gliomas displayed similar characteristics to human gliomas both histologically and immunohistochemically and thus this model is a promising tool for pre-clinical testing of various standard or targeted therapies, including the development of anti-PDGFR α /SHP-2 treatments.

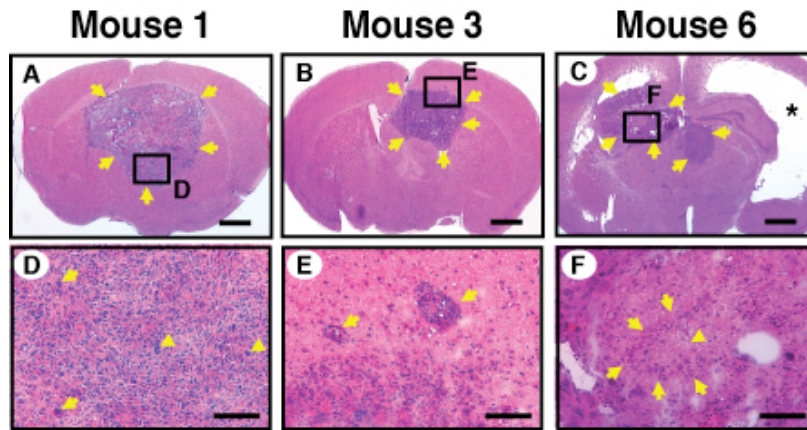


Figure 44. SB-induced spontaneous gliomas exhibit characteristics of human gliomas.

Representative H&E staining images were shown for Mouse 1 (A), 3 (B), and 6 (C). Yellow arrows demarcate the tumors of each mouse. Detailed histological characteristics of SB-induced mice are summarized in Table 5. (D), (E), (F) are enlarged images of the boxed regions indicated in (A), (B), and (C), respectively. Tumor cells in (D) show high anaplasia, pleomorphic nuclei (arrows), active mitotic activity (arrowheads), and poorly differentiated glial cells. (E) shows infiltration of tumor cells into the surrounding brain parenchyma (arrows). (F) Prominent pseudopalisading cells (arrows) surrounding an area of focal necrosis (arrowhead), a typical feature of human GBMs. Scale bars, 1 mm for panels A-C; 100 μ m for D-F.

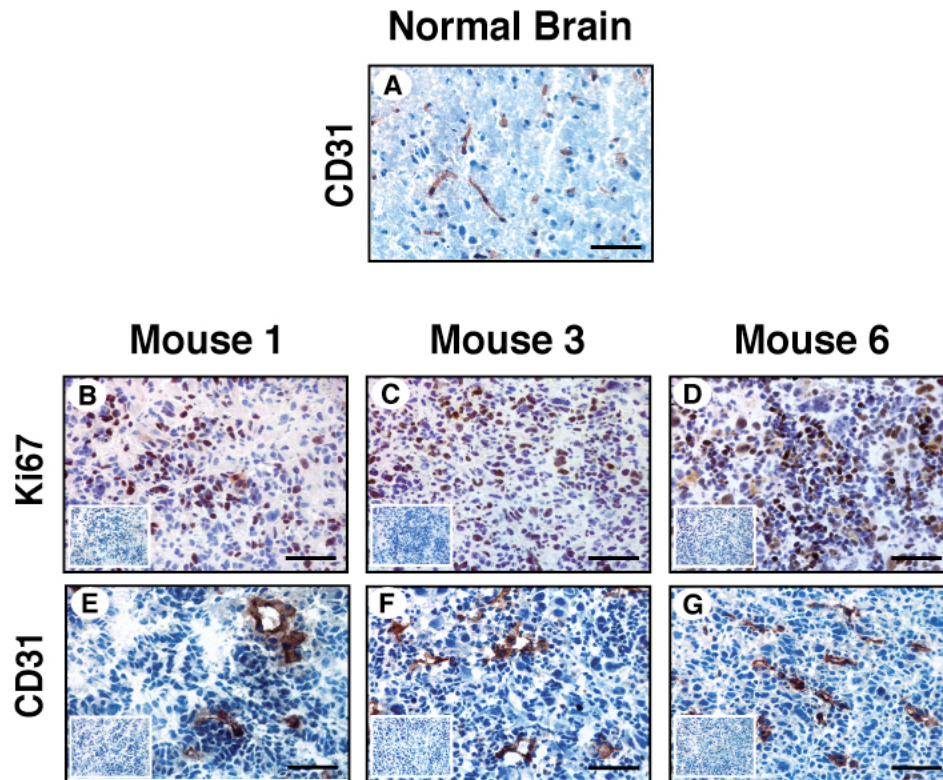


Figure 45. SB-induced spontaneous gliomas showed high positivity for Ki67 and CD31 staining.

(A) CD31 staining of normal mouse brain. (B)-(D) Representative Ki67 IHC staining images on frozen sections of Mouse 1 (B), 3 (C), and 6 (D). Representative CD31 IHC staining images on frozen sections of Mouse 1 (E), 3 (F), and 6 (G). Insets, corresponding negative controls for each image. Scale bars, 50 μ m.

Table 5. Histological and immunohistochemical analyses of SB-induced gliomas.

Mouse#	Surv	Size	Ki67	CD31	CD	DI	PN	MT	FN	Grade
1	75	L	+++	+++	+++	+++	+++	+++	++	III / IV
2	43	M	ND	ND	+	+	+	+ / -	-	II
3	65	M	+++	+++	+++	++	+++	+++	+	III / IV
4	90	N	NA	NA	NA	NA	NA	NA	NA	NA
5	90	N	NA	NA	NA	NA	NA	NA	NA	NA
6	33	M	++	+++	++	++	+++	++	++	III / IV

Abbreviations: Surv: survival time (days post-injection); L, large; M, medium; S, small; N, no tumor found; ND, not determined; NA, non-applicable; CD, cell density; DI diffuse infiltration; PN, pleomorphic nuclei; MT, mitosis; FN, focal necrosis. The sizes of tumors were estimated using these criteria: small, < 1 mm in diameter; medium, 1-3 mm; large, > 3 mm. The tumors were graded based on the presence of histological features found in human gliomas.

5.4 SUMMARY AND CONCLUSION

By using the SB transposon system, we have successfully generated NRAS- and SV40-LgT-mediated spontaneous glioma mouse model. We were able to track the *in vivo* tumor growth via bioluminescence imaging, and to assess the resulted tumors based on their resemblance to the neuro-pathological features of clinical human gliomas. With the pT2/CMV-PDGFR α and pT2/MSCV/PDGF-A vectors now available in our lab, generation of SB-mediated, PDGF-induced spontaneous gliomas and the subsequent pre-clinical testing of various targeted therapies on these mice will ensue.

6.0 DISCUSSION AND FUTURE DIRECTIONS

6.1 DISCUSSION

In this dissertation, we report that PDGFR α and/or PDGF-A overexpression is able to drive gliomagenesis of *Ink4a/Arf*-deficient mAst and human glioma LN444 and LN443 cells. Re-introduction of p16INK4a but not p19ARF into *Ink4a/Arf*-null mAst suppresses PDGFR α -promoted tumor growth. In the absence of PI3K or SHP-2 signaling, PDGFR α fails to enhance tumorigenesis in the brain of mice. Additionally, we establish a link between activation of SHP-2 and the PI3K/AKT/mTOR signaling in PDGFR α -stimulated tumorigenesis *in vitro*, in mice, and in clinical glioblastoma specimens. Therefore, our data demonstrate that co-alteration of the RTK PDGFR α and tumor suppressor p16INK4a is required for gliomagenesis and that SHP-2 is a critical linker between the PI3K/ AKT /mTOR pathway and PDGFR α in the formation of gliomas.

A unique feature of this study is that specific activation of PDGFR α signaling *in vivo* by PDGF-A, a ligand that only binds to PDGFR α but not PDGFR β (71) as an autocrine loop significantly enhanced the tumorigenesis of *Ink4a/Arf*-deficient mAst and human glioma cells in the brain. Early studies of clinical glioma specimens showed that PDGF-A and PDGFR α are overexpressed in tumor cells while PDGF-B and PDGFR β are expressed in hyperplastic capillaries, suggesting both autocrine and paracrine loops for PDGF/PDGFR activation in

gliomas (127). In neonate and adult mice, expression of PDGF-B induces *de novo* gliomas from GFAP-positive astrocytes and nestin-expressing glial progenitor cells through activation of PDGFR α and PDGFR β in the brain of both WT and *Ink4a/Arf*-deficient animals (165, 270). Moreover, in WT *Ink4a/Arf* mice, infusion of PDGF-A proteins into the lateral ventricle stimulated tumor-like growth of PDGFR α -positive NSC in the SVZ in the brain (104). Importantly, data of the cancer genome atlas (10) and other studies revealed that PDGFR α is overexpressed and amplified, and often co-expressed with PDGF-A in clinical glioblastoma samples (10, 12, 130). Our results not only functionally validated these studies but also further demonstrated the significance of specific activation of PDGFR α signaling by PDGF-A in cooperation with loss of p16INK4a but not p19ARF in promoting gliomagenesis. We found that when PDGFR α signaling is activated in *Ink4a/Arf*^{-/-} mAst or human glioma cells, mice that received these cells developed significantly larger and highly invasive tumors in the brain. In contrast, no enhancement of tumorigenesis was found in mice that received glioma cells with PDGFR α and an intact *CDKN2A* locus (267). Together, our studies indicate that PDGFR α activation together with *Ink4a/Arf* loss results in enhanced tumor growth of both mAst and human glioma cells in the brain.

Tumor suppressor P16INK4A is frequently mutated in clinical glioblastomas (11, 12, 245). In mice, loss of p16INK4a and p19ARF was shown to be indispensable in facilitating tumorigenesis (42). *Ink4a/Arf*-deficient mice were viable and developed spontaneous tumors at early ages, but without detectable tumors in the brain (42, 45). Further studies showed that *Ink4a/Arf* loss cooperates with oncogenic K-Ras, EGFRvIII or PDGF-B expression in promoting gliomagenesis in the brain (45, 164, 165, 255, 270). However, compared to p16INK4a loss that contributes to tumor initiation from mAst, p19ARF deficiency was shown to display a more

pronounced impact on cell transformation and gliomagenesis (44, 168). Our data corroborates and also differs with these studies. We showed that re-expression of p16INK4a but not p19ARF in PDGFR α -expressing *Ink4a/Arf*^{-/-} mAst inhibited tumorigenesis. Inhibition of CDK4/6, the direct target of p16INK4a by a specific inhibitor (268) in *Ink4a/Arf*^{-/-} mAst and glioma cells attenuated PDGF-A stimulation of soft agar growth, suggesting CDK4/6/p-RB signaling is required for PDGFR α -induced tumorigenesis. On the contrary, although p53 was functional in *Ink4a/Arf*^{-/-} PDGFR α -expressing mAst, p19ARF was unable to suppress soft agar growth of these cells. Since p19ARF de-represses p53 signaling while PI3K/Akt activates p53 E3 ubiquitin ligase Mdm2 (285), it is plausible that the robust PI3K/Akt activation in PDGFR α -overexpressing cells triggers Mdm2-mediated p53 degradation and thereby renders tumorigenic mAst resistant to p19ARF inhibition (269). It is also likely that loss of p19ARF is required for survival of glioma cells under certain condition such as treatment of DNA damage-inducing agent CDDP (Figure 21). At least during the initiation or maintenance of cell transformation, p19ARF loss appears to be dispensable (44, 168), since knockdown of *INK4A* alone in *INK4A/ARF*-wt LN319 glioma cells restored PDGFR α stimulation of anchorage-independent growth in soft agar. Taken together, these data suggest that p16INK4a loss plays a predominant role in PDGFR α -promoted gliomagenesis.

The third important aspect in this study is that we functionally assigned signal modules of PDGFR α in promoting gliomagenesis and tumor invasion in the brain of mice. Previous studies by uncoupling individual signaling pathways from PDGFR α using a series of F-to-Y mutants revealed unequal contributions of each signaling pathway emanating from PDGFR α activation (71, 75, 76). Our *in vivo* and biochemical data corroborate these reports. When compared with PDGFR α -wt overexpression, loss of intrinsic tyrosine kinase activity (R627) of the RTK or

binding capacity to PI3K (F731/42) or SHP-2 (F720) abrogated PDGFR α -promoted gliomagenesis, thus signifying the central roles of PI3K and SHP-2 signaling in PDGFR α function. However, while disruption of PDGFR α association with SFKs (F572/74) or PLC γ (F1018) only had a moderate impact on tumor formation in the brain, significant inhibition of tumor cell infiltration in the brain was seen in these tumors, as compared to the PDGFR α -wt tumors, thus validating the role of SFKs and PLC γ in mediating PDGFR α -stimulated cell invasion (74). Moreover, a separate set of experiments with individual “add-back panel” mutants (Y731/42, Y572/74, Y720, Y988, and Y1018) could not fully restore PDGFR α -promoted tumorigenesis in the brain (data not shown), consistent with the previous findings using an identical set of PDGFR α “add-back panel” mutants (74). It is plausible that similar to this previous *in vitro* study (74), in which retention of a combination of two or three add-back signaling modules with comparable level of total RTK protein in PDGFR α -wt-expressing cells was able to restore PDGFR α -mediated biological responses, co-activation of PI3K (Y731/42)- and SHP-2 (Y720)-mediated signaling may be required for the full spectrum of wt PDGFR α -promoted gliomagenesis in the brain.

The most novel finding in this study is the emergence of SHP-2 as an essential mediator in PDGFR α -promoted gliomagenesis. SHP-2 (encoded by *PTPN11* gene) is a protein tyrosine phosphatase (PTP) identified as a *bona fide* proto-oncogene that activates Ras-MAPK-signaling through a yet-to-be-defined mechanism (286). Additionally, the role of SHP-2 in mediating PDGFR α signaling has not been clear (69, 71, 76). In human cancers including GBMs, mutations of SHP-2 or its binding partners have been reported, leading to sustained Ras-MAPK signaling (287, 288). Recent automated signaling network-based analysis on the TCGA genomic data has designated *PTPN11* as one of the six “Linker” genes, which are statistically enriched for

connections to various GBM altered genes, thus suggesting a critical role for SHP-2/*PTPN11* in modulation of downstream biological signaling in gliomagenesis (289). Our data not only establish the critical role of SHP-2 in mediating PDGFR α activation for glioma formation but also functionally validate this hypothesis. We showed that inhibition of SHP-2 function by removal of its binding module in PDGFR α (F720 mutant), gene knockdown or pharmacological inhibitors significantly impaired PDGFR α stimulation of tumorigenesis *in vivo* and *in vitro* and its downstream signaling effectors, Erk1/2 and PI3K/Akt/mTOR in *Ink4a/Arf*-deficient mAst and glioma cells. Significantly, re-expression of a constitutively active p110, the catalytic subunit of PI3K, rescued the inhibition of SHP-2 in *Ink4a/Arf*-deficient mAst. In EGFRvIII-expressing U87MG glioma cells, SHP-2 regulates activities of ERK/2 and CDC2 that modulates cell cycle progression, but has a minimal effect on AKT activation (275). On the contrary, we found that knockdown of SHP-2 not only attenuated PDGFR α stimulation of Erk1/2 activity but also impaired PI3K/Akt/mTOR activity in *Ink4a/Arf*-deficient mAst and human glioma cells. The impact of inhibition of SHP-2 on PI3K/Akt signaling seems specific in astrocytic tumors since we did not observe an inhibition of PDGF-A stimulation of p-Akt or PI3K association with PDGFR α in SHP-2 knocking down NIH3T3 fibroblasts. On the other hand, a MEK inhibitor PD98059 also reduced the tumorigenicity of *Ink4a/Arf*-deficient mAst, indicating that SHP-2-mediated PDGFR α signaling requires not only PI3K/Akt but also Erk1/2 activation in gliomagenesis. Additionally, SHP-2 was found to either positively or negatively regulate PI3K/AKT activity (287). However, in our model systems, SHP-2 is required for full activation of PI3K/Akt/mTOR and inhibition of mTOR by rapamycin markedly suppressed PDGFR α -promoted tumorigenesis. These data are significant since a recent proteomic study revealed that mTOR signaling is predominantly activated in “*PDGFRA* co-cluster” glioblastomas (143), thus

corroborating our observations. However, since phosphorylation of Akt Ser473 occurs both upstream and downstream to mTOR complex 2 (mTORC2) signaling, our data do not rule out the role of mTORC2 in PDGFR α -activated signaling. Lastly, our data also demonstrated the importance of activation of PI3K/mTOR signaling by SHP-2 in PDGFR α - or EGFRvIII-promoted tumorigenesis. Taken together, our findings suggest SHP-2 as a critical modulator that regulates PDGFR α -mediated PI3K/AKT/mTOR activities in the development of malignant glioblastomas.

To better understand the tumorigenesis processes in human brain and predict responses to therapeutic interventions such as PDGF/SHP-2/PI3K inhibition, it is necessary to develop animal models that re-capitulate the histology, progression, and microenvironment of the human malignant gliomas. We have demonstrated in this dissertation that we are able to generate a mouse model that developed malignant brain gliomas that displayed several neuro-pathological features found in clinical human gliomas, by using *Sleeping Beauty* Transposon-driven NRAS and SV40 Large T antigen expression (174). The differential tumor incidences and survival time among these mice likely resulted from different transfection efficiency, different targeted insertion sites within the genome, or distinct types of cells targeted. We observed that mice developing hydrocephalus tended to develop tumors with markedly different histopathological features than those in mice without hydrocephalus. To decrease the incidence of hydrocephalus, we reduced the injection volume from 2 μ l to 1 μ l and observed a significant decrease of hydrocephalus in the injected mice. However, the penetrance of tumor development in these mice still needs to be improved (~60%). We are currently in the process of testing SB-induced tumor model in other strains of mice such as BALB/c mice with a newly improved animal protocol, which was reported to show a more favorable penetrance than did C57BL/6 mice (174).

We anticipate that the use of SB system in PDGF-induced gliomagenesis will help to better understand gliomas induced by aberrant activation of PDGF signaling and further provide a platform for pre-clinical testing of newly developed drugs targeting this molecular pathway. However, cautions should be taken when using mouse as a model system. The marked differences between mouse and human could compromise the use of these models in predicting human tumor responses to various therapeutic interventions. On the other hand, the tumors generated from xenografting of human glioma tissues into immuno-deficient mice are expected to intrinsically resemble human tumors more than do those derived from the mouse cells. However, several caveats exist in the xenograft mouse models. The xenograft tumors lack the interactions with functional immune systems and tumor microenvironment (e.g. the normal human brain cells and vasculatures). Several approaches to generate “humanized” tumor microenvironments have been proposed (179). This might be achieved by transgenic expression of human tumor microenvironment-specific genes in the mouse brain, or by introducing stem cells that can generate human-like stromal or perivascular cells. Interestingly, mouse HSCs have been shown to generate endothelial cells and pericytes that support glioma cell angiogenesis in the mouse brain (290, 291). The feasibility of generating human vasculatures in the mouse brain (a “humanized mouse brain”) using stem cell technology or transgenic approach for understanding of tumor pathogenesis and prediction of anti-tumor drug responses thus warrants further investigations. For these reasons, perhaps a model that incorporates spontaneous tumor induction by SB or other types of vectors with the use of “humanized mouse brains” will ultimately overcome the limitations presented by the current animal models.

In summary, this dissertation provides molecular insights into the mechanisms by which *PDGFRA* amplification together with loss of *INK4A/ARF* promotes gliomagenesis in the brain.

Our data identified SHP-2, as well as PI3K, as a pivotal mediator of PDGFR α signaling in glioma formation. These results have direct clinical relevance since we not only establish a model system to demonstrate the co-operative role of *PDGFRA* overexpression and *INK4A/ARF* loss in clinical glioblastomas, but also provide functional evidence to validate genomic analyses demonstrating that SHP-2/*PTPN11* is an essential “Linker” among glioma altered genes (289); secondly, activated mTOR signaling is predominantly found within the subclass of glioblastomas with abnormal PDGFR α signaling (143); and thirdly, activating PI3K mutations (*PIK3CA* and *PIK3R1*) occur mostly in clinical glioblastomas without *PDGFRA* aberrations (11). Given that the clinical experiences of most of the targeted therapies developed to date are disappointing, identifying and targeting molecules that are robust in the face of network interactions between different genetic aberrations may prove more effective (292); SHP-2/*PTPN11* thus represents one of these candidates. Consequently, our results strongly suggest SHP-2/*PTPN11* as a potential target for treatments of human glioblastomas with *PDGFRA* overexpression.

6.2 FUTURE DIRECTIONS

In order to develop a time- and cost-efficient mouse model for spontaneous glioma formation, we have collaborated with Dr. John R. Ohlfest at University of Minnesota and Dr. Okada Hideho at University of Pittsburgh and successfully generated spontaneous gliomas in C57BL/6 mice that received SB transposon-mediated NRASV12 and SV40 Large T antigen expression. In addition, vectors that encoding PDGF-B (pT2/EF1aRU5-mPDGFB) and EGFRvIII (pT3.5/CMV-EGFRvIII) were also obtained from Dr. Ohlfest and Dr. Okada, respectively.

Moreover, we have generated SB plasmid DNA constructs encoding PDGFR α (pT2/CMV-PDGFR α) and PDGF-A (pT2/MSCV-PDGFA). In order to assess the contributions of various genetic alterations to glioma formation, we will introduce the SB-mediated expression of PDGFs or EGFRvIII into several available transgenic/knock-out mice such as Ink4a/Arf^{-/-} (42), PTEN^{-/-} (293) (in collaboration with Dr. Ronald A. Depinho at Harvard Medical School), and p53^{-/-} (294) (in collaboration with Dr. Lin Zhang at University of Pittsburgh) mice. We will then perform transcriptome analyses to determine whether tumors generated from these combinations of genetic aberrations harbor expression of signature genes found in the four subtypes of human GBMs within TCGA dataset (11). For example, we expect the combination of PDGF overexpression and p53 deletion in these mice will result in formation of gliomas resembling the Proneural subtype of GBMs, whereas introduction of EGFRvIII expression into PTEN-deficient mice could lead to development of tumors comparable to the Classical subtype of human GBMs.

After identifying various mouse tumors that resemble human subtype of GBMs, we will treat the mice with these gliomas with various targeted pharmacological inhibitors, such as SHP-2 inhibitors PHPS-1 and NSC87877 (described in Chapter 3) and determine whether these tumors are sensitive to SHP-2 inhibition by these inhibitors. Bioluminescence imaging will be performed to monitor the tumor growth before and after the treatments; histological and immunohistochemical analyses will also be used to assess the neuropathological features present in these tumors (as described in Chapter 5 of this dissertation). Other treatment modalities will also be exploited in treating these mice, such as a novel fully human monoclonal PDGFR α neutralizing antibody, IMC-3G3 (249, 250, 295, 296) (obtained from Eli Lilly and Company, Indianapolis, IN). We expect to observe an initial regression of tumors after treatment of either SHP-2 inhibitors or the PDGFR α neutralizing antibody. However, we will deliberately keep

certain number of groups of mice up to 2 years in order to determine whether tumor recurrences will occur. After the tumor recurrence, subsequent transcriptome analyses will be performed to determine the presence of signature genetic changes that may indicate a shift of tumor subtypes within these recurrent tumors as compared to the primary tumors. We expect that mice treated with SHP-2 inhibitors will be less likely to suffer from tumor recurrence since we hypothesize that SHP-2 ablation leads to elimination of multiple oncogenic signaling pathways involved in all GBM subtypes and thus significantly reduces the possibility that alternative signaling pathways will be activated after the treatment.

We will also isolate tumors cells from these SB-induced gliomas in the mouse brain, using methods described by the previous report (174). Briefly, we will performed FACS cell sorting by expression of GFP (encoded by SB vectors) or the putative glioma stem cell marker CD133 by utilizing a CD133/2 (clone 293C3, Miltenyi Biotec Inc, Auburn, CA) antibody conjugated with allophycocyanin (APC). We will then determine the tumorigenicity of secondary tumors generated from implantation of these sorted cells to assess whether CD133-positive population of tumor cells represent the real CSCs in various tumors that resemble the four subtypes of human GBMs. We will also identify the integration sites of SB transposons within genomes of these sorted cells, as described in the previous report (174), to determine whether off-target disruptions of certain genes are required for generation of the tumors observed in these mice. We expect that the CD133-positive CSCs isolated from tumors that resemble various human GBM subtypes will display differential tumorigenic potentials. The CSCs isolated from Proneural-like tumors are the most likely to be highly tumorigenic compared with those from other subtypes, since Proneural human GBMs express genes characteristic of early CNS development and thus it is possible that initiation/maintenance of these tumors may re-capitulate

the process in normal CNS development. That is, the cell of origin of the Proneural GBMs is likely the neural stem/glial progenitor cells (such as CD133-positive cells) that generate various cells in the normal CNS. For this reason, we expect that compared with CD133-negative population, CD133-positive cells isolated from SB-induced Proneural-like tumors will be more tumorigenic after re-implantation into the mouse brain.

Lastly, it is also of interest to determine whether the putative CD133-positive CSCs are responsible for the tumor recurrence after various PDGF-targeted therapies in the mice with SB-mediated Proneural-like tumors. We will treat the mice with Proneural-like tumors with PDGF- or SHP-2-targeted therapies in combination with various differentiating agents such as all-trans retinoic acid (ATRA) to eliminate the CD133-positive CSC population in the tumor mass (297). In these experiments, immunohistochemistry with antibodies against various neural cells, such as nestin, GFAP, NG2, Olig2, and O4, will be performed on tumors before and after the ATRA treatment to confirm the differentiating effects of ATRA on the tumors. Mice will also be monitored for tumor recurrence for up to 2 years by bioluminescence imaging. We expect ATRA will be able to decrease the CD133-positive CSC population and increase the number of differentiated cells such as GFAP- or O4-positive glial cells in the tumors. Additionally, we expect by differentiating the CSCs, we will be able to render the tumor more sensitive to PDGF- or SHP-2-targeted treatments and decrease the possibility of tumor relapse.

7.0 BIBLIOGRAPHY

1. CBTRUS. 2010 CBTRUS Statistical Report: Primary Brain and Central Nervous System Tumors Diagnosed in the United States in 2004-2006 2010;
2. Furnari, FB, et al. Malignant astrocytic glioma: genetics, biology, and paths to treatment. *Genes Dev.* 2007;21(21):2683-2710.
3. Louis, DN, International Agency for Research on Cancer., and World Health Organization. 2007. *WHO classification of tumours of the central nervous system.* Lyon: International Agency for Research on Cancer. 309 p. pp.
4. Wen, PY, and Kesari, S. Malignant gliomas in adults. *N Engl J Med.* 2008;359(5):492-507.
5. Stupp, R, et al. Radiotherapy plus concomitant and adjuvant temozolomide for glioblastoma. *N Engl J Med.* 2005;352(10):987-996.
6. Ohgaki, H, and Kleihues, P. Genetic pathways to primary and secondary glioblastoma. *Am J Pathol.* 2007;170(5):1445-1453.
7. Ohgaki, H, and Kleihues, P. Genetic alterations and signaling pathways in the evolution of gliomas. *Cancer Sci.* 2009;100(12):2235-2241.
8. Keisner, SV, and Shah, SR. Pazopanib: the newest tyrosine kinase inhibitor for the treatment of advanced or metastatic renal cell carcinoma. *Drugs.* 2011;71(4):443-454.
9. Ressler, S, Bartkova, J, Niederegger, H, Bartek, J, Scharffetter-Kochanek, K, Jansen-Durr, P, and Wlaschek, M. p16INK4A is a robust in vivo biomarker of cellular aging in human skin. *Aging Cell.* 2006;5(5):379-389.
10. TCGA. Comprehensive genomic characterization defines human glioblastoma genes and core pathways. *Nature.* 2008;455(7216):1061-1068.

11. Verhaak, RG, et al. Integrated genomic analysis identifies clinically relevant subtypes of glioblastoma characterized by abnormalities in PDGFRA, IDH1, EGFR, and NF1. *Cancer Cell*. 2010;17(1):98-110.
12. Parsons, DW, et al. An integrated genomic analysis of human glioblastoma multiforme. *Science*. 2008;321(5897):1807-1812.
13. Yan, H, et al. IDH1 and IDH2 mutations in gliomas. *N Engl J Med*. 2009;360(8):765-773.
14. Dang, L, et al. Cancer-associated IDH1 mutations produce 2-hydroxyglutarate. *Nature*. 2009;462(7274):739-744.
15. Nounshmehr, H, et al. Identification of a CpG island methylator phenotype that defines a distinct subgroup of glioma. *Cancer Cell*. 2010;17(5):510-522.
16. Xu, W, et al. Oncometabolite 2-hydroxyglutarate is a competitive inhibitor of alpha-ketoglutarate-dependent dioxygenases. *Cancer Cell*. 2011;19(1):17-30.
17. Reardon, DA, Rich, JN, Friedman, HS, and Bigner, DD. Recent advances in the treatment of malignant astrocytoma. *J Clin Oncol*. 2006;24(8):1253-1265.
18. Mladkova, N, and Chakravarti, A. Molecular profiling in glioblastoma: prelude to personalized treatment. *Curr Oncol Rep*. 2009;11(1):53-61.
19. Purow, B, and Schiff, D. Advances in the genetics of glioblastoma: are we reaching critical mass? *Nat Rev Neurol*. 2009;5(8):419-426.
20. Sherr, CJ, and Roberts, JM. CDK inhibitors: positive and negative regulators of G1-phase progression. *Genes Dev*. 1999;13(12):1501-1512.
21. Canepa, ET, Scassa, ME, Ceruti, JM, Marazita, MC, Carcagno, AL, Sirkin, PF, and Ogara, MF. INK4 proteins, a family of mammalian CDK inhibitors with novel biological functions. *IUBMB Life*. 2007;59(7):419-426.
22. Quelle, DE, Zindy, F, Ashmun, RA, and Sherr, CJ. Alternative reading frames of the INK4a tumor suppressor gene encode two unrelated proteins capable of inducing cell cycle arrest. *Cell*. 1995;83(6):993-1000.

23. Kamijo, T, Zindy, F, Roussel, MF, Quelle, DE, Downing, JR, Ashmun, RA, Grosveld, G, and Sherr, CJ. Tumor suppression at the mouse INK4a locus mediated by the alternative reading frame product p19ARF. *Cell*. 1997;91(5):649-659.
24. Sherr, CJ. Divorcing ARF and p53: an unsettled case. *Nat Rev Cancer*. 2006;6(9):663-673.
25. Pomerantz, J, et al. The Ink4a tumor suppressor gene product, p19Arf, interacts with MDM2 and neutralizes MDM2's inhibition of p53. *Cell*. 1998;92(6):713-723.
26. Sherr, CJ. The INK4a/ARF network in tumour suppression. *Nat Rev Mol Cell Biol*. 2001;2(10):731-737.
27. Collado, M, Blasco, MA, and Serrano, M. Cellular senescence in cancer and aging. *Cell*. 2007;130(2):223-233.
28. Zindy, F, Quelle, DE, Roussel, MF, and Sherr, CJ. Expression of the p16INK4a tumor suppressor versus other INK4 family members during mouse development and aging. *Oncogene*. 1997;15(2):203-211.
29. Krishnamurthy, J, Torrice, C, Ramsey, MR, Kovalev, GI, Al-Regaiey, K, Su, L, and Sharpless, NE. Ink4a/Arf expression is a biomarker of aging. *J Clin Invest*. 2004;114(9):1299-1307.
30. Chkhotua, AB, Gabusi, E, Altimari, A, D'Errico, A, Yakubovich, M, Vienken, J, Stefoni, S, Chieco, P, Yussim, A, and Grigioni, WF. Increased expression of p16(INK4a) and p27(Kip1) cyclin-dependent kinase inhibitor genes in aging human kidney and chronic allograft nephropathy. *Am J Kidney Dis*. 2003;41(6):1303-1313.
31. Rossi, DJ, Jamieson, CH, and Weissman, IL. Stems cells and the pathways to aging and cancer. *Cell*. 2008;132(4):681-696.
32. Molofsky, AV, Slutsky, SG, Joseph, NM, He, S, Pardal, R, Krishnamurthy, J, Sharpless, NE, and Morrison, SJ. Increasing p16INK4a expression decreases forebrain progenitors and neurogenesis during ageing. *Nature*. 2006;443(7110):448-452.
33. Bruggeman, SW, et al. Ink4a and Arf differentially affect cell proliferation and neural stem cell self-renewal in Bmi1-deficient mice. *Genes Dev*. 2005;19(12):1438-1443.

34. Park, IK, Qian, D, Kiel, M, Becker, MW, Pihalja, M, Weissman, IL, Morrison, SJ, and Clarke, MF. Bmi-1 is required for maintenance of adult self-renewing haematopoietic stem cells. *Nature*. 2003;423(6937):302-305.
35. Janzen, V, Forkert, R, Fleming, HE, Saito, Y, Waring, MT, Dombkowski, DM, Cheng, T, DePinho, RA, Sharpless, NE, and Scadden, DT. Stem-cell ageing modified by the cyclin-dependent kinase inhibitor p16INK4a. *Nature*. 2006;443(7110):421-426.
36. Matheu, A, Pantoja, C, Efeyan, A, Criado, LM, Martin-Caballero, J, Flores, JM, Klatt, P, and Serrano, M. Increased gene dosage of Ink4a/Arf results in cancer resistance and normal aging. *Genes Dev*. 2004;18(22):2736-2746.
37. Matheu, A, Maraver, A, and Serrano, M. The Arf/p53 pathway in cancer and aging. *Cancer Res*. 2008;68(15):6031-6034.
38. Kamb, A, Gruis, NA, Weaver-Feldhaus, J, Liu, Q, Harshman, K, Tavtigian, SV, Stockert, E, Day, RS, 3rd, Johnson, BE, and Skolnick, MH. A cell cycle regulator potentially involved in genesis of many tumor types. *Science*. 1994;264(5157):436-440.
39. Nobori, T, Miura, K, Wu, DJ, Lois, A, Takabayashi, K, and Carson, DA. Deletions of the cyclin-dependent kinase-4 inhibitor gene in multiple human cancers. *Nature*. 1994;368(6473):753-756.
40. Okamoto, A, et al. Mutations and altered expression of p16INK4 in human cancer. *Proc Natl Acad Sci U S A*. 1994;91(23):11045-11049.
41. Hirama, T, and Koeffler, HP. Role of the cyclin-dependent kinase inhibitors in the development of cancer. *Blood*. 1995;86(3):841-854.
42. Serrano, M, Lee, H, Chin, L, Cordon-Cardo, C, Beach, D, and DePinho, RA. Role of the INK4a locus in tumor suppression and cell mortality. *Cell*. 1996;85(1):27-37.
43. Sharpless, NE, Bardeesy, N, Lee, KH, Carrasco, D, Castrillon, DH, Aguirre, AJ, Wu, EA, Horner, JW, and DePinho, RA. Loss of p16Ink4a with retention of p19Arf predisposes mice to tumorigenesis. *Nature*. 2001;413(6851):86-91.
44. Sharpless, NE, Ramsey, MR, Balasubramanian, P, Castrillon, DH, and DePinho, RA. The differential impact of p16(INK4a) or p19(ARF) deficiency on cell growth and tumorigenesis. *Oncogene*. 2004;23(2):379-385.

45. Bachoo, RM, et al. Epidermal growth factor receptor and Ink4a/Arf: convergent mechanisms governing terminal differentiation and transformation along the neural stem cell to astrocyte axis. *Cancer Cell*. 2002;1(3):269-277.
46. Holland, EC, Hively, WP, DePinho, RA, and Varmus, HE. A constitutively active epidermal growth factor receptor cooperates with disruption of G1 cell-cycle arrest pathways to induce glioma-like lesions in mice. *Genes Dev*. 1998;12(23):3675-3685.
47. Uhrbom, L, Dai, C, Celestino, JC, Rosenblum, MK, Fuller, GN, and Holland, EC. Ink4a-Arf loss cooperates with KRas activation in astrocytes and neural progenitors to generate glioblastomas of various morphologies depending on activated Akt. *Cancer Res*. 2002;62(19):5551-5558.
48. Arap, W, Nishikawa, R, Furnari, FB, Cavenee, WK, and Huang, HJ. Replacement of the p16/CDKN2 gene suppresses human glioma cell growth. *Cancer Res*. 1995;55(6):1351-1354.
49. Uhrbom, L, Nister, M, and Westermarck, B. Induction of senescence in human malignant glioma cells by p16INK4A. *Oncogene*. 1997;15(5):505-514.
50. Ichimura, K, Bolin, MB, Goike, HM, Schmidt, EE, Moshref, A, and Collins, VP. Deregulation of the p14ARF/MDM2/p53 pathway is a prerequisite for human astrocytic gliomas with G1-S transition control gene abnormalities. *Cancer Res*. 2000;60(2):417-424.
51. Fulci, G, Labuhn, M, Maier, D, Lachat, Y, Hausmann, O, Hegi, ME, Janzer, RC, Merlo, A, and Van Meir, EG. p53 gene mutation and ink4a-arf deletion appear to be two mutually exclusive events in human glioblastoma. *Oncogene*. 2000;19(33):3816-3822.
52. Jen, J, Harper, JW, Bigner, SH, Bigner, DD, Papadopoulos, N, Markowitz, S, Willson, JK, Kinzler, KW, and Vogelstein, B. Deletion of p16 and p15 genes in brain tumors. *Cancer Res*. 1994;54(24):6353-6358.
53. Merlo, A, Herman, JG, Mao, L, Lee, DJ, Gabrielson, E, Burger, PC, Baylin, SB, and Sidransky, D. 5' CpG island methylation is associated with transcriptional silencing of the tumour suppressor p16/CDKN2/MTS1 in human cancers. *Nat Med*. 1995;1(7):686-692.
54. Fueyo, J, Gomez-Manzano, C, Bruner, JM, Saito, Y, Zhang, B, Zhang, W, Levin, VA, Yung, WK, and Kyritsis, AP. Hypermethylation of the CpG island of p16/CDKN2 correlates with gene inactivation in gliomas. *Oncogene*. 1996;13(8):1615-1619.

55. Arap, W, Knudsen, ES, Wang, JY, Cavenee, WK, and Huang, HJ. Point mutations can inactivate in vitro and in vivo activities of p16(INK4a)/CDKN2A in human glioma. *Oncogene*. 1997;14(5):603-609.
56. Ross, R, Glomset, J, Kariya, B, and Harker, L. A platelet-dependent serum factor that stimulates the proliferation of arterial smooth muscle cells in vitro. *Proc Natl Acad Sci U S A*. 1974;71(4):1207-1210.
57. Kohler, N, and Lipton, A. Platelets as a source of fibroblast growth-promoting activity. *Exp Cell Res*. 1974;87(2):297-301.
58. Ross, R, and Vogel, A. The platelet-derived growth factor. *Cell*. 1978;14(2):203-210.
59. Westermark, B, and Wasteson, A. A platelet factor stimulating human normal glial cells. *Exp Cell Res*. 1976;98(1):170-174.
60. Heldin, CH, Westermark, B, and Wasteson, A. Platelet-derived growth factor: purification and partial characterization. *Proc Natl Acad Sci U S A*. 1979;76(8):3722-3726.
61. Heldin, CH, Westermark, B, and Wasteson, A. Specific receptors for platelet-derived growth factor on cells derived from connective tissue and glia. *Proc Natl Acad Sci U S A*. 1981;78(6):3664-3668.
62. Heldin, CH, and Westermark, B. Mechanism of action and in vivo role of platelet-derived growth factor. *Physiol Rev*. 1999;79(4):1283-1316.
63. Betsholtz, C, et al. cDNA sequence and chromosomal localization of human platelet-derived growth factor A-chain and its expression in tumour cell lines. *Nature*. 1986;320(6064):695-699.
64. Collins, T, Bonthron, DT, and Orkin, SH. Alternative RNA splicing affects function of encoded platelet-derived growth factor A chain. *Nature*. 1987;328(6131):621-624.
65. Fredriksson, L, Li, H, and Eriksson, U. The PDGF family: four gene products form five dimeric isoforms. *Cytokine Growth Factor Rev*. 2004;15(4):197-204.

66. Andrae, J, Gallini, R, and Betsholtz, C. Role of platelet-derived growth factors in physiology and medicine. *Genes Dev.* 2008;22(10):1276-1312.
67. Heldin, CH, Backstrom, G, Ostman, A, Hammacher, A, Ronnstrand, L, Rubin, K, Nister, M, and Westermark, B. Binding of different dimeric forms of PDGF to human fibroblasts: evidence for two separate receptor types. *Embo J.* 1988;7(5):1387-1393.
68. Kelly, JD, Haldeman, BA, Grant, FJ, Murray, MJ, Seifert, RA, Bowen-Pope, DF, Cooper, JA, and Kazlauskas, A. Platelet-derived growth factor (PDGF) stimulates PDGF receptor subunit dimerization and intersubunit trans-phosphorylation. *J Biol Chem.* 1991;266(14):8987-8992.
69. Heldin, CH, Ostman, A, and Ronnstrand, L. Signal transduction via platelet-derived growth factor receptors. *Biochim Biophys Acta.* 1998;1378(1):F79-113.
70. Klinghoffer, RA, Hamilton, TG, Hoch, R, and Soriano, P. An allelic series at the PDGFalphaR locus indicates unequal contributions of distinct signaling pathways during development. *Dev Cell.* 2002;2(1):103-113.
71. Tallquist, M, and Kazlauskas, A. PDGF signaling in cells and mice. *Cytokine Growth Factor Rev.* 2004;15(4):205-213.
72. Klinghoffer, RA, Mueting-Nelsen, PF, Faerman, A, Shani, M, and Soriano, P. The two PDGF receptors maintain conserved signaling in vivo despite divergent embryological functions. *Mol Cell.* 2001;7(2):343-354.
73. Hamilton, TG, Klinghoffer, RA, Corrin, PD, and Soriano, P. Evolutionary divergence of platelet-derived growth factor alpha receptor signaling mechanisms. *Mol Cell Biol.* 2003;23(11):4013-4025.
74. Rosenkranz, S, DeMali, KA, Gelderloos, JA, Bazenet, C, and Kazlauskas, A. Identification of the receptor-associated signaling enzymes that are required for platelet-derived growth factor-AA-dependent chemotaxis and DNA synthesis. *J Biol Chem.* 1999;274(40):28335-28343.
75. Van Stry, M, Kazlauskas, A, Schreiber, SL, and Symes, K. Distinct effectors of platelet-derived growth factor receptor-alpha signaling are required for cell survival during embryogenesis. *Proc Natl Acad Sci U S A.* 2005;102(23):8233-8238.

76. Betsholtz, C. Insight into the physiological functions of PDGF through genetic studies in mice. *Cytokine Growth Factor Rev.* 2004;15(4):215-228.
77. Popovici, C, Isnardon, D, Birnbaum, D, and Roubin, R. Caenorhabditis elegans receptors related to mammalian vascular endothelial growth factor receptors are expressed in neural cells. *Neurosci Lett.* 2002;329(1):116-120.
78. Learte, AR, Forero, MG, and Hidalgo, A. Gliatrophic and gliatropic roles of PVF/PVR signaling during axon guidance. *Glia.* 2008;56(2):164-176.
79. Valenzuela, CF, Kazlauskas, A, and Weiner, JL. Roles of platelet-derived growth factor in the developing and mature nervous systems. *Brain Res Brain Res Rev.* 1997;24(1):77-89.
80. Raff, MC, Miller, RH, and Noble, M. A glial progenitor cell that develops in vitro into an astrocyte or an oligodendrocyte depending on culture medium. *Nature.* 1983;303(5916):390-396.
81. Pringle, NP, and Richardson, WD. A singularity of PDGF alpha-receptor expression in the dorsoventral axis of the neural tube may define the origin of the oligodendrocyte lineage. *Development.* 1993;117(2):525-533.
82. Richardson, WD, Pringle, N, Mosley, MJ, Westermarck, B, and Dubois-Dalcq, M. A role for platelet-derived growth factor in normal gliogenesis in the central nervous system. *Cell.* 1988;53(2):309-319.
83. Noble, M, Murray, K, Stroobant, P, Waterfield, MD, and Riddle, P. Platelet-derived growth factor promotes division and motility and inhibits premature differentiation of the oligodendrocyte/type-2 astrocyte progenitor cell. *Nature.* 1988;333(6173):560-562.
84. Raff, MC, Lillien, LE, Richardson, WD, Burne, JF, and Noble, MD. Platelet-derived growth factor from astrocytes drives the clock that times oligodendrocyte development in culture. *Nature.* 1988;333(6173):562-565.
85. Yeh, HJ, Ruit, KG, Wang, YX, Parks, WC, Snider, WD, and Deuel, TF. PDGF A-chain gene is expressed by mammalian neurons during development and in maturity. *Cell.* 1991;64(1):209-216.

86. Fruttiger, M, et al. Defective oligodendrocyte development and severe hypomyelination in PDGF-A knockout mice. *Development*. 1999;126(3):457-467.
87. Calver, AR, Hall, AC, Yu, WP, Walsh, FS, Heath, JK, Betsholtz, C, and Richardson, WD. Oligodendrocyte population dynamics and the role of PDGF in vivo. *Neuron*. 1998;20(5):869-882.
88. McKinnon, RD, Waldron, S, and Kiel, ME. PDGF alpha-receptor signal strength controls an RTK rheostat that integrates phosphoinositol 3'-kinase and phospholipase Cgamma pathways during oligodendrocyte maturation. *J Neurosci*. 2005;25(14):3499-3508.
89. Armstrong, RC, Harvath, L, and Dubois-Dalcq, ME. Type 1 astrocytes and oligodendrocyte-type 2 astrocyte glial progenitors migrate toward distinct molecules. *J Neurosci Res*. 1990;27(3):400-407.
90. Barres, BA, Hart, IK, Coles, HS, Burne, JF, Voyvodic, JT, Richardson, WD, and Raff, MC. Cell death and control of cell survival in the oligodendrocyte lineage. *Cell*. 1992;70(1):31-46.
91. Woodruff, RH, Fruttiger, M, Richardson, WD, and Franklin, RJ. Platelet-derived growth factor regulates oligodendrocyte progenitor numbers in adult CNS and their response following CNS demyelination. *Mol Cell Neurosci*. 2004;25(2):252-262.
92. Baron, W, Shattil, SJ, and French-Constant, C. The oligodendrocyte precursor mitogen PDGF stimulates proliferation by activation of alpha(v)beta3 integrins. *Embo J*. 2002;21(8):1957-1966.
93. Nishiyama, A, Lin, XH, Giese, N, Heldin, CH, and Stallcup, WB. Interaction between NG2 proteoglycan and PDGF alpha-receptor on O2A progenitor cells is required for optimal response to PDGF. *J Neurosci Res*. 1996;43(3):315-330.
94. van Heyningen, P, Calver, AR, and Richardson, WD. Control of progenitor cell number by mitogen supply and demand. *Curr Biol*. 2001;11(4):232-241.
95. Redwine, JM, and Armstrong, RC. In vivo proliferation of oligodendrocyte progenitors expressing PDGFalphaR during early remyelination. *J Neurobiol*. 1998;37(3):413-428.
96. Soriano, P. The PDGF alpha receptor is required for neural crest cell development and for normal patterning of the somites. *Development*. 1997;124(14):2691-2700.

97. Murtie, JC, Zhou, YX, Le, TQ, Vana, AC, and Armstrong, RC. PDGF and FGF2 pathways regulate distinct oligodendrocyte lineage responses in experimental demyelination with spontaneous remyelination. *Neurobiol Dis.* 2005;19(1-2):171-182.
98. Hu, JG, Fu, SL, Wang, YX, Li, Y, Jiang, XY, Wang, XF, Qiu, MS, Lu, PH, and Xu, XM. Platelet-derived growth factor-AA mediates oligodendrocyte lineage differentiation through activation of extracellular signal-regulated kinase signaling pathway. *Neuroscience.* 2008;151(1):138-147.
99. Appolloni, I, Calzolari, F, Tutucci, E, Caviglia, S, Terrile, M, Corte, G, and Malatesta, P. PDGF-B induces a homogeneous class of oligodendrogliomas from embryonic neural progenitors. *Int J Cancer.* 2009;124(10):2251-2259.
100. Bogler, O, Wren, D, Barnett, SC, Land, H, and Noble, M. Cooperation between two growth factors promotes extended self-renewal and inhibits differentiation of oligodendrocyte-type-2 astrocyte (O-2A) progenitor cells. *Proc Natl Acad Sci U S A.* 1990;87(16):6368-6372.
101. Frost, EE, Nielsen, JA, Le, TQ, and Armstrong, RC. PDGF and FGF2 regulate oligodendrocyte progenitor responses to demyelination. *J Neurobiol.* 2003;54(3):457-472.
102. Wolswijk, G, and Noble, M. Cooperation between PDGF and FGF converts slowly dividing O-2Aadult progenitor cells to rapidly dividing cells with characteristics of O-2Aperinatal progenitor cells. *J Cell Biol.* 1992;118(4):889-900.
103. Kondo, T, and Raff, M. Oligodendrocyte precursor cells reprogrammed to become multipotential CNS stem cells. *Science.* 2000;289(5485):1754-1757.
104. Jackson, EL, Garcia-Verdugo, JM, Gil-Perotin, S, Roy, M, Quinones-Hinojosa, A, VandenBerg, S, and Alvarez-Buylla, A. PDGFR alpha-positive B cells are neural stem cells in the adult SVZ that form glioma-like growths in response to increased PDGF signaling. *Neuron.* 2006;51(2):187-199.
105. Lu, QR, Sun, T, Zhu, Z, Ma, N, Garcia, M, Stiles, CD, and Rowitch, DH. Common developmental requirement for Olig function indicates a motor neuron/oligodendrocyte connection. *Cell.* 2002;109(1):75-86.

106. Lu, QR, Yuk, D, Alberta, JA, Zhu, Z, Pawlitzky, I, Chan, J, McMahon, AP, Stiles, CD, and Rowitch, DH. Sonic hedgehog--regulated oligodendrocyte lineage genes encoding bHLH proteins in the mammalian central nervous system. *Neuron*. 2000;25(2):317-329.
107. Zhou, Q, Wang, S, and Anderson, DJ. Identification of a novel family of oligodendrocyte lineage-specific basic helix-loop-helix transcription factors. *Neuron*. 2000;25(2):331-343.
108. Finzsch, M, Stolt, CC, Lommes, P, and Wegner, M. Sox9 and Sox10 influence survival and migration of oligodendrocyte precursors in the spinal cord by regulating PDGF receptor alpha expression. *Development*. 2008;135(4):637-646.
109. Chojnacki, A, and Weiss, S. Isolation of a novel platelet-derived growth factor-responsive precursor from the embryonic ventral forebrain. *J Neurosci*. 2004;24(48):10888-10899.
110. Hamada, T, Ui-Tei, K, and Miyata, Y. A novel gene derived from developing spinal cords, SCDGF, is a unique member of the PDGF/VEGF family. *FEBS Lett*. 2000;475(2):97-102.
111. Hamada, T, Ui-Tei, K, Imaki, J, Takahashi, F, Onodera, H, Mishima, T, and Miyata, Y. The expression of SCDGF/PDGF-C/fallotein and SCDGF-B/PDGF-D in the rat central nervous system. *Mech Dev*. 2002;112(1-2):161-164.
112. Aase, K, Abramsson, A, Karlsson, L, Betsholtz, C, and Eriksson, U. Expression analysis of PDGF-C in adult and developing mouse tissues. *Mech Dev*. 2002;110(1-2):187-191.
113. Ding, H, Wu, X, Kim, I, Tam, PP, Koh, GY, and Nagy, A. The mouse *Pdgfc* gene: dynamic expression in embryonic tissues during organogenesis. *Mech Dev*. 2000;96(2):209-213.
114. Ding, H, et al. A specific requirement for PDGF-C in palate formation and PDGFR-alpha signaling. *Nat Genet*. 2004;36(10):1111-1116.
115. Reigstad, LJ, Varhaug, JE, and Lillehaug, JR. Structural and functional specificities of PDGF-C and PDGF-D, the novel members of the platelet-derived growth factors family. *Febs J*. 2005;272(22):5723-5741.
116. Waterfield, MD, Scrace, GT, Whittle, N, Stroobant, P, Johnsson, A, Wasteson, A, Westermark, B, Heldin, CH, Huang, JS, and Deuel, TF. Platelet-derived growth factor is

- structurally related to the putative transforming protein p28^{sis} of simian sarcoma virus. *Nature*. 1983;304(5921):35-39.
117. Doolittle, RF, Hunkapiller, MW, Hood, LE, Devare, SG, Robbins, KC, Aaronson, SA, and Antoniades, HN. Simian sarcoma virus onc gene, v-sis, is derived from the gene (or genes) encoding a platelet-derived growth factor. *Science*. 1983;221(4607):275-277.
 118. Nister, M, Heldin, CH, Wasteson, A, and Westermark, B. A platelet-derived growth factor analog produced by a human clonal glioma cell line. *Ann N Y Acad Sci*. 1982;397(25-33).
 119. Betsholtz, C, Heldin, CH, Nister, M, Ek, B, Wasteson, A, and Westermark, B. Synthesis of a PDGF-like growth factor in human glioma and sarcoma cells suggests the expression of the cellular homologue to the transforming protein of simian sarcoma virus. *Biochem Biophys Res Commun*. 1983;117(1):176-182.
 120. Nister, M, Heldin, CH, Wasteson, A, and Westermark, B. A glioma-derived analog to platelet-derived growth factor: demonstration of receptor competing activity and immunological crossreactivity. *Proc Natl Acad Sci U S A*. 1984;81(3):926-930.
 121. Heldin, CH, Johnsson, A, Wennergren, S, Wernstedt, C, Betsholtz, C, and Westermark, B. A human osteosarcoma cell line secretes a growth factor structurally related to a homodimer of PDGF A-chains. *Nature*. 1986;319(6053):511-514.
 122. Hammacher, A, Nister, M, Westermark, B, and Heldin, CH. A human glioma cell line secretes three structurally and functionally different dimeric forms of platelet-derived growth factor. *Eur J Biochem*. 1988;176(1):179-186.
 123. Nister, M, Hammacher, A, Mellstrom, K, Siegbahn, A, Ronnstrand, L, Westermark, B, and Heldin, CH. A glioma-derived PDGF A chain homodimer has different functional activities from a PDGF AB heterodimer purified from human platelets. *Cell*. 1988;52(6):791-799.
 124. Nister, M, Libermann, TA, Betsholtz, C, Pettersson, M, Claesson-Welsh, L, Heldin, CH, Schlessinger, J, and Westermark, B. Expression of messenger RNAs for platelet-derived growth factor and transforming growth factor-alpha and their receptors in human malignant glioma cell lines. *Cancer Res*. 1988;48(14):3910-3918.
 125. Harsh, GR, Keating, MT, Escobedo, JA, and Williams, LT. Platelet derived growth factor (PDGF) autocrine components in human tumor cell lines. *J Neurooncol*. 1990;8(1):1-12.

126. Hermansson, M, Nister, M, Betsholtz, C, Heldin, CH, Westermark, B, and Funa, K. Endothelial cell hyperplasia in human glioblastoma: coexpression of mRNA for platelet-derived growth factor (PDGF) B chain and PDGF receptor suggests autocrine growth stimulation. *Proc Natl Acad Sci U S A*. 1988;85(20):7748-7752.
127. Hermanson, M, Funa, K, Hartman, M, Claesson-Welsh, L, Heldin, CH, Westermark, B, and Nister, M. Platelet-derived growth factor and its receptors in human glioma tissue: expression of messenger RNA and protein suggests the presence of autocrine and paracrine loops. *Cancer Res*. 1992;52(11):3213-3219.
128. Plate, KH, Breier, G, Farrell, CL, and Risau, W. Platelet-derived growth factor receptor-beta is induced during tumor development and upregulated during tumor progression in endothelial cells in human gliomas. *Lab Invest*. 1992;67(4):529-534.
129. Maxwell, M, Naber, SP, Wolfe, HJ, Galanopoulos, T, Hedley-Whyte, ET, Black, PM, and Antoniades, HN. Coexpression of platelet-derived growth factor (PDGF) and PDGF-receptor genes by primary human astrocytomas may contribute to their development and maintenance. *J Clin Invest*. 1990;86(1):131-140.
130. Martinho, O, et al. Expression, mutation and copy number analysis of platelet-derived growth factor receptor A (PDGFRA) and its ligand PDGFA in gliomas. *Br J Cancer*. 2009;101(6):973-982.
131. Hermanson, M, et al. Association of loss of heterozygosity on chromosome 17p with high platelet-derived growth factor alpha receptor expression in human malignant gliomas. *Cancer Res*. 1996;56(1):164-171.
132. Smith, JS, Wang, XY, Qian, J, Hosek, SM, Scheithauer, BW, Jenkins, RB, and James, CD. Amplification of the platelet-derived growth factor receptor-A (PDGFRA) gene occurs in oligodendrogliomas with grade IV anaplastic features. *J Neuropathol Exp Neurol*. 2000;59(6):495-503.
133. Fleming, TP, Saxena, A, Clark, WC, Robertson, JT, Oldfield, EH, Aaronson, SA, and Ali, IU. Amplification and/or overexpression of platelet-derived growth factor receptors and epidermal growth factor receptor in human glial tumors. *Cancer Res*. 1992;52(16):4550-4553.
134. Varela, M, Ranuncolo, SM, Morand, A, Lastiri, J, De Kier Joffe, EB, Puricelli, LI, and Pallotta, MG. EGF-R and PDGF-R, but not bcl-2, overexpression predict overall survival in patients with low-grade astrocytomas. *J Surg Oncol*. 2004;86(1):34-40.

135. Mapstone, T, McMichael, M, and Goldthwait, D. Expression of platelet-derived growth factors, transforming growth factors, and the ros gene in a variety of primary human brain tumors. *Neurosurgery*. 1991;28(2):216-222.
136. Majumdar, K, Radotra, BD, Vasishta, RK, and Pathak, A. Platelet-derived growth factor expression correlates with tumor grade and proliferative activity in human oligodendrogliomas. *Surg Neurol*. 2009;72(1):54-60.
137. Shih, AH, Dai, C, Hu, X, Rosenblum, MK, Koutcher, JA, and Holland, EC. Dose-dependent effects of platelet-derived growth factor-B on glial tumorigenesis. *Cancer Res*. 2004;64(14):4783-4789.
138. Liang, Y, et al. Gene expression profiling reveals molecularly and clinically distinct subtypes of glioblastoma multiforme. *Proc Natl Acad Sci U S A*. 2005;102(16):5814-5819.
139. Phillips, HS, et al. Molecular subclasses of high-grade glioma predict prognosis, delineate a pattern of disease progression, and resemble stages in neurogenesis. *Cancer Cell*. 2006;9(3):157-173.
140. Kotliarov, Y, et al. High-resolution global genomic survey of 178 gliomas reveals novel regions of copy number alteration and allelic imbalances. *Cancer Res*. 2006;66(19):9428-9436.
141. Maher, EA, et al. Marked genomic differences characterize primary and secondary glioblastoma subtypes and identify two distinct molecular and clinical secondary glioblastoma entities. *Cancer Res*. 2006;66(23):11502-11513.
142. Yin, D, et al. High-resolution genomic copy number profiling of glioblastoma multiforme by single nucleotide polymorphism DNA microarray. *Mol Cancer Res*. 2009;7(5):665-677.
143. Brennan, C, Momota, H, Hambardzumyan, D, Ozawa, T, Tandon, A, Pedraza, A, and Holland, E. Glioblastoma subclasses can be defined by activity among signal transduction pathways and associated genomic alterations. *PLoS One*. 2009;4(11):e7752.
144. Sugawa, N, Ekstrand, AJ, James, CD, and Collins, VP. Identical splicing of aberrant epidermal growth factor receptor transcripts from amplified rearranged genes in human glioblastomas. *Proc Natl Acad Sci U S A*. 1990;87(21):8602-8606.

145. Frederick, L, Wang, XY, Eley, G, and James, CD. Diversity and frequency of epidermal growth factor receptor mutations in human glioblastomas. *Cancer Res.* 2000;60(5):1383-1387.
146. Kumabe, T, Sohma, Y, Kayama, T, Yoshimoto, T, and Yamamoto, T. Amplification of alpha-platelet-derived growth factor receptor gene lacking an exon coding for a portion of the extracellular region in a primary brain tumor of glial origin. *Oncogene.* 1992;7(4):627-633.
147. Rand, V, et al. Sequence survey of receptor tyrosine kinases reveals mutations in glioblastomas. *Proc Natl Acad Sci U S A.* 2005;102(40):14344-14349.
148. Ozawa, T, et al. PDGFRA gene rearrangements are frequent genetic events in PDGFRA-amplified glioblastomas. *Genes Dev.* 2010;24(19):2205-2218.
149. Clarke, ID, and Dirks, PB. A human brain tumor-derived PDGFR-alpha deletion mutant is transforming. *Oncogene.* 2003;22(5):722-733.
150. Liu, KW, et al. SHP-2/PTPN11 mediates gliomagenesis driven by PDGFRA and INK4A/ARF aberrations in mice and humans. *J Clin Invest.* 2011;121(3):905-917.
151. Lokker, NA, Sullivan, CM, Hollenbach, SJ, Israel, MA, and Giese, NA. Platelet-derived growth factor (PDGF) autocrine signaling regulates survival and mitogenic pathways in glioblastoma cells: evidence that the novel PDGF-C and PDGF-D ligands may play a role in the development of brain tumors. *Cancer Res.* 2002;62(13):3729-3735.
152. LaRochelle, WJ, et al. Platelet-derived growth factor D: tumorigenicity in mice and dysregulated expression in human cancer. *Cancer Res.* 2002;62(9):2468-2473.
153. Crawford, Y, Kasman, I, Yu, L, Zhong, C, Wu, X, Modrusan, Z, Kaminker, J, and Ferrara, N. PDGF-C mediates the angiogenic and tumorigenic properties of fibroblasts associated with tumors refractory to anti-VEGF treatment. *Cancer Cell.* 2009;15(1):21-34.
154. di Tomaso, E, et al. Glioblastoma recurrence after cediranib therapy in patients: lack of "rebound" revascularization as mode of escape. *Cancer Res.* 2011;71(1):19-28.

155. di Tomaso, E, London, N, Fuja, D, Logie, J, Tyrrell, JA, Kamoun, W, Munn, LL, and Jain, RK. PDGF-C induces maturation of blood vessels in a model of glioblastoma and attenuates the response to anti-VEGF treatment. *PLoS One*. 2009;4(4):e5123.
156. Gondi, CS, Veeravalli, KK, Gorantla, B, Dinh, DH, Fassett, D, Klopfenstein, JD, Gujrati, M, and Rao, JS. Human umbilical cord blood stem cells show PDGF-D-dependent glioma cell tropism in vitro and in vivo. *Neuro Oncol*. 2010;12(5):453-465.
157. Weiss, WA, et al. Neuropathology of genetically engineered mice: consensus report and recommendations from an international forum. *Oncogene*. 2002;21(49):7453-7463.
158. Weissenberger, J, Steinbach, JP, Malin, G, Spada, S, Rulicke, T, and Aguzzi, A. Development and malignant progression of astrocytomas in GFAP-v-src transgenic mice. *Oncogene*. 1997;14(17):2005-2013.
159. Ding, H, Roncari, L, Shannon, P, Wu, X, Lau, N, Karaskova, J, Gutmann, DH, Squire, JA, Nagy, A, and Guha, A. Astrocyte-specific expression of activated p21-ras results in malignant astrocytoma formation in a transgenic mouse model of human gliomas. *Cancer Res*. 2001;61(9):3826-3836.
160. Reilly, KM, Loisel, DA, Bronson, RT, McLaughlin, ME, and Jacks, T. Nf1;Trp53 mutant mice develop glioblastoma with evidence of strain-specific effects. *Nat Genet*. 2000;26(1):109-113.
161. Zhu, Y, Guignard, F, Zhao, D, Liu, L, Burns, DK, Mason, RP, Messing, A, and Parada, LF. Early inactivation of p53 tumor suppressor gene cooperating with NF1 loss induces malignant astrocytoma. *Cancer Cell*. 2005;8(2):119-130.
162. Hede, SM, Hansson, I, Afink, GB, Eriksson, A, Nazarenko, I, Andrae, J, Genove, G, Westermarck, B, and Nister, M. GFAP promoter driven transgenic expression of PDGFB in the mouse brain leads to glioblastoma in a Trp53 null background. *Glia*. 2009;57(11):1143-1153.
163. Nazarenko, I, Hedren, A, Sjodin, H, Orrego, A, Andrae, J, Afink, GB, Nister, M, and Lindstrom, MS. Brain Abnormalities and Glioma-Like Lesions in Mice Overexpressing the Long Isoform of PDGF-A in Astrocytic Cells. *PLoS One*. 2011;6(4):e18303.
164. Uhrbom, L, Hesselager, G, Nister, M, and Westermarck, B. Induction of brain tumors in mice using a recombinant platelet-derived growth factor B-chain retrovirus. *Cancer Res*. 1998;58(23):5275-5279.

165. Dai, C, Celestino, JC, Okada, Y, Louis, DN, Fuller, GN, and Holland, EC. PDGF autocrine stimulation dedifferentiates cultured astrocytes and induces oligodendrogliomas and oligoastrocytomas from neural progenitors and astrocytes in vivo. *Genes Dev.* 2001;15(15):1913-1925.
166. Assanah, M, Lochhead, R, Ogden, A, Bruce, J, Goldman, J, and Canoll, P. Glial progenitors in adult white matter are driven to form malignant gliomas by platelet-derived growth factor-expressing retroviruses. *J Neurosci.* 2006;26(25):6781-6790.
167. Calzolari, F, Appolloni, I, Tutucci, E, Caviglia, S, Terrile, M, Corte, G, and Malatesta, P. Tumor progression and oncogene addiction in a PDGF-B-induced model of gliomagenesis. *Neoplasia.* 2008;10(12):1373-1382, following 1382.
168. Tchougounova, E, Kastemar, M, Brasater, D, Holland, EC, Westermarck, B, and Uhrbom, L. Loss of Arf causes tumor progression of PDGFB-induced oligodendroglioma. *Oncogene.* 2007;26(43):6289-6296.
169. Johansson, FK, Brodd, J, Eklof, C, Ferletta, M, Hesselager, G, Tiger, CF, Uhrbom, L, and Westermarck, B. Identification of candidate cancer-causing genes in mouse brain tumors by retroviral tagging. *Proc Natl Acad Sci U S A.* 2004;101(31):11334-11337.
170. Krum, JM, and Rosenstein, JM. VEGF mRNA and its receptor flt-1 are expressed in reactive astrocytes following neural grafting and tumor cell implantation in the adult CNS. *Exp Neurol.* 1998;154(1):57-65.
171. Chen, Y, Miles, DK, Hoang, T, Shi, J, Hurlock, E, Kernie, SG, and Lu, QR. The basic helix-loop-helix transcription factor olig2 is critical for reactive astrocyte proliferation after cortical injury. *J Neurosci.* 2008;28(43):10983-10989.
172. Hesselager, G, Uhrbom, L, Westermarck, B, and Nister, M. Complementary effects of platelet-derived growth factor autocrine stimulation and p53 or Ink4a-Arf deletion in a mouse glioma model. *Cancer Res.* 2003;63(15):4305-4309.
173. Assanah, MC, Bruce, JN, Suzuki, SO, Chen, A, Goldman, JE, and Canoll, P. PDGF stimulates the massive expansion of glial progenitors in the neonatal forebrain. *Glia.* 2009;57(16):1835-1847.
174. Wiesner, SM, et al. De novo induction of genetically engineered brain tumors in mice using plasmid DNA. *Cancer Res.* 2009;69(2):431-439.

175. Ivics, Z, Hackett, PB, Plasterk, RH, and Izsvak, Z. Molecular reconstruction of Sleeping Beauty, a Tc1-like transposon from fish, and its transposition in human cells. *Cell*. 1997;91(4):501-510.
176. Dupuy, AJ, Rogers, LM, Kim, J, Nannapaneni, K, Starr, TK, Liu, P, Largaespada, DA, Scheetz, TE, Jenkins, NA, and Copeland, NG. A modified sleeping beauty transposon system that can be used to model a wide variety of human cancers in mice. *Cancer Res*. 2009;69(20):8150-8156.
177. Voskoglou-Nomikos, T, Pater, JL, and Seymour, L. Clinical predictive value of the in vitro cell line, human xenograft, and mouse allograft preclinical cancer models. *Clin Cancer Res*. 2003;9(11):4227-4239.
178. Sharma, SV, Haber, DA, and Settleman, J. Cell line-based platforms to evaluate the therapeutic efficacy of candidate anticancer agents. *Nat Rev Cancer*. 2010;10(4):241-253.
179. Rangarajan, A, and Weinberg, RA. Opinion: Comparative biology of mouse versus human cells: modelling human cancer in mice. *Nat Rev Cancer*. 2003;3(12):952-959.
180. van Staveren, WC, Solis, DY, Hebrant, A, Detours, V, Dumont, JE, and Maenhaut, C. Human cancer cell lines: Experimental models for cancer cells in situ? For cancer stem cells? *Biochim Biophys Acta*. 2009;1795(2):92-103.
181. Vargo-Gogola, T, and Rosen, JM. Modelling breast cancer: one size does not fit all. *Nat Rev Cancer*. 2007;7(9):659-672.
182. Dai, C, Lyustikman, Y, Shih, A, Hu, X, Fuller, GN, Rosenblum, M, and Holland, EC. The characteristics of astrocytomas and oligodendrogliomas are caused by two distinct and interchangeable signaling formats. *Neoplasia*. 2005;7(4):397-406.
183. Hu, X, Pandolfi, PP, Li, Y, Koutcher, JA, Rosenblum, M, and Holland, EC. mTOR promotes survival and astrocytic characteristics induced by Pten/AKT signaling in glioblastoma. *Neoplasia*. 2005;7(4):356-368.
184. Paugh, BS, et al. Integrated molecular genetic profiling of pediatric high-grade gliomas reveals key differences with the adult disease. *J Clin Oncol*. 2010;28(18):3061-3068.
185. Pollack, IF, Hamilton, RL, James, CD, Finkelstein, SD, Burnham, J, Yates, AJ, Holmes, EJ, Zhou, T, and Finlay, JL. Rarity of PTEN deletions and EGFR amplification in

- malignant gliomas of childhood: results from the Children's Cancer Group 945 cohort. *J Neurosurg.* 2006;105(5 Suppl):418-424.
186. Takei, H, Yogeswaren, ST, Wong, KK, Mehta, V, Chintagumpala, M, Dauser, RC, Lau, CC, and Adesina, AM. Expression of oligodendroglial differentiation markers in pilocytic astrocytomas identifies two clinical subsets and shows a significant correlation with proliferation index and progression free survival. *J Neurooncol.* 2008;86(2):183-190.
 187. Shoshan, Y, Nishiyama, A, Chang, A, Mork, S, Barnett, GH, Cowell, JK, Trapp, BD, and Staugaitis, SM. Expression of oligodendrocyte progenitor cell antigens by gliomas: implications for the histogenesis of brain tumors. *Proc Natl Acad Sci U S A.* 1999;96(18):10361-10366.
 188. Trojanowski, JQ, Tohyama, T, and Lee, VM. Medulloblastomas and related primitive neuroectodermal brain tumors of childhood recapitulate molecular milestones in the maturation of neuroblasts. *Mol Chem Neuropathol.* 1992;17(2):121-135.
 189. Williams, BP, Park, JK, Alberta, JA, Muhlebach, SG, Hwang, GY, Roberts, TM, and Stiles, CD. A PDGF-regulated immediate early gene response initiates neuronal differentiation in ventricular zone progenitor cells. *Neuron.* 1997;18(4):553-562.
 190. Whelan, HT, Nelson, DB, Strother, D, Przybylski, C, Figge, G, and Mamandi, A. Medulloblastoma cell line secretes platelet-derived growth factor. *Pediatr Neurol.* 1989;5(6):347-352.
 191. Smits, A, van Grieken, D, Hartman, M, Lendahl, U, Funa, K, and Nister, M. Coexpression of platelet-derived growth factor alpha and beta receptors on medulloblastomas and other primitive neuroectodermal tumors is consistent with an immature stem cell and neuronal derivation. *Lab Invest.* 1996;74(1):188-198.
 192. MacDonald, TJ, Brown, KM, LaFleur, B, Peterson, K, Lawlor, C, Chen, Y, Packer, RJ, Cogen, P, and Stephan, DA. Expression profiling of medulloblastoma: PDGFRA and the RAS/MAPK pathway as therapeutic targets for metastatic disease. *Nat Genet.* 2001;29(2):143-152.
 193. Andrae, J, Molander, C, Smits, A, Funa, K, and Nister, M. Platelet-derived growth factor-B and -C and active alpha-receptors in medulloblastoma cells. *Biochem Biophys Res Commun.* 2002;296(3):604-611.

194. Yuan, L, Santi, M, Rushing, EJ, Cornelison, R, and MacDonald, TJ. ERK activation of p21 activated kinase-1 (Pak1) is critical for medulloblastoma cell migration. *Clin Exp Metastasis*. 2010;27(7):481-491.
195. Black, P, Carroll, R, and Glowacka, D. Expression of platelet-derived growth factor transcripts in medulloblastomas and ependymomas. *Pediatr Neurosurg*. 1996;24(2):74-78.
196. Taylor, MD, et al. Radial glia cells are candidate stem cells of ependymoma. *Cancer Cell*. 2005;8(4):323-335.
197. Poppleton, H, and Gilbertson, RJ. Stem cells of ependymoma. *Br J Cancer*. 2007;96(1):6-10.
198. Diers-Fenger, M, Kirchhoff, F, Kettenmann, H, Levine, JM, and Trotter, J. AN2/NG2 protein-expressing glial progenitor cells in the murine CNS: isolation, differentiation, and association with radial glia. *Glia*. 2001;34(3):213-228.
199. Maxwell, M, Galanopoulos, T, Hedley-Whyte, ET, Black, PM, and Antoniades, HN. Human meningiomas co-express platelet-derived growth factor (PDGF) and PDGF-receptor genes and their protein products. *Int J Cancer*. 1990;46(1):16-21.
200. Mauro, A, Di Sapio, A, Mocellini, C, and Schiffer, D. Control of meningioma cell growth by platelet-derived growth factor (PDGF). *J Neurol Sci*. 1995;131(2):135-143.
201. Black, PM, Carroll, R, Glowacka, D, Riley, K, and Dashner, K. Platelet-derived growth factor expression and stimulation in human meningiomas. *J Neurosurg*. 1994;81(3):388-393.
202. Shamah, SM, Alberta, JA, Giannobile, WV, Guha, A, Kwon, YK, Carroll, RS, Black, PM, and Stiles, CD. Detection of activated platelet-derived growth factor receptors in human meningioma. *Cancer Res*. 1997;57(18):4141-4147.
203. Lusi, EA, Chicoine, MR, and Perry, A. High throughput screening of meningioma biomarkers using a tissue microarray. *J Neurooncol*. 2005;73(3):219-223.
204. Kirsch, M, Wilson, JC, and Black, P. Platelet-derived growth factor in human brain tumors. *J Neurooncol*. 1997;35(3):289-301.

205. Johnson, MD, Woodard, A, Kim, P, and Frexes-Steed, M. Evidence for mitogen-associated protein kinase activation and transduction of mitogenic signals by platelet-derived growth factor in human meningioma cells. *J Neurosurg.* 2001;94(2):293-300.
206. Johnson, MD, Okedli, E, Woodard, A, Toms, SA, and Allen, GS. Evidence for phosphatidylinositol 3-kinase-Akt-p7S6K pathway activation and transduction of mitogenic signals by platelet-derived growth factor in meningioma cells. *J Neurosurg.* 2002;97(3):668-675.
207. Suzuki, K, Momota, H, Tonooka, A, Noguchi, H, Yamamoto, K, Wanibuchi, M, Minamida, Y, Hasegawa, T, and Houkin, K. Glioblastoma simultaneously present with adjacent meningioma: case report and review of the literature. *J Neurooncol.* 2010;99(1):147-153.
208. Argyriou, AA, and Kalofonos, HP. Molecularly targeted therapies for malignant gliomas. *Mol Med.* 2009;15(3-4):115-122.
209. Radford, IR. Imatinib. Novartis. *Curr Opin Investig Drugs.* 2002;3(3):492-499.
210. Kilic, T, Alberta, JA, Zdunek, PR, Acar, M, Iannarelli, P, O'Reilly, T, Buchdunger, E, Black, PM, and Stiles, CD. Intracranial inhibition of platelet-derived growth factor-mediated glioblastoma cell growth by an orally active kinase inhibitor of the 2-phenylaminopyrimidine class. *Cancer Res.* 2000;60(18):5143-5150.
211. Servidei, T, Riccardi, A, Sanguinetti, M, Dominici, C, and Riccardi, R. Increased sensitivity to the platelet-derived growth factor (PDGF) receptor inhibitor STI571 in chemoresistant glioma cells is associated with enhanced PDGF-BB-mediated signaling and STI571-induced Akt inactivation. *J Cell Physiol.* 2006;208(1):220-228.
212. Wen, PY, et al. Phase I/II study of imatinib mesylate for recurrent malignant gliomas: North American Brain Tumor Consortium Study 99-08. *Clin Cancer Res.* 2006;12(16):4899-4907.
213. Raymond, E, et al. Phase II study of imatinib in patients with recurrent gliomas of various histologies: a European Organisation for Research and Treatment of Cancer Brain Tumor Group Study. *J Clin Oncol.* 2008;26(28):4659-4665.
214. Razis, E, et al. Phase II study of neoadjuvant imatinib in glioblastoma: evaluation of clinical and molecular effects of the treatment. *Clin Cancer Res.* 2009;15(19):6258-6266.

215. Stommel, JM, et al. Coactivation of receptor tyrosine kinases affects the response of tumor cells to targeted therapies. *Science*. 2007;318(5848):287-290.
216. Pietras, K, Rubin, K, Sjoblom, T, Buchdunger, E, Sjoquist, M, Heldin, CH, and Ostman, A. Inhibition of PDGF receptor signaling in tumor stroma enhances anti-tumor effect of chemotherapy. *Cancer Res*. 2002;62(19):5476-5484.
217. Houghton, PJ, Germain, GS, Harwood, FC, Schuetz, JD, Stewart, CF, Buchdunger, E, and Traxler, P. Imatinib mesylate is a potent inhibitor of the ABCG2 (BCRP) transporter and reverses resistance to topotecan and SN-38 in vitro. *Cancer Res*. 2004;64(7):2333-2337.
218. Bergers, G, Song, S, Meyer-Morse, N, Bergsland, E, and Hanahan, D. Benefits of targeting both pericytes and endothelial cells in the tumor vasculature with kinase inhibitors. *J Clin Invest*. 2003;111(9):1287-1295.
219. Reardon, DA, et al. Phase II study of imatinib mesylate plus hydroxyurea in adults with recurrent glioblastoma multiforme. *J Clin Oncol*. 2005;23(36):9359-9368.
220. Desjardins, A, et al. Phase II study of imatinib mesylate and hydroxyurea for recurrent grade III malignant gliomas. *J Neurooncol*. 2007;83(1):53-60.
221. Reardon, DA, et al. Multicentre phase II studies evaluating imatinib plus hydroxyurea in patients with progressive glioblastoma. *Br J Cancer*. 2009;101(12):1995-2004.
222. Dresemann, G, et al. Imatinib in combination with hydroxyurea versus hydroxyurea alone as oral therapy in patients with progressive pretreated glioblastoma resistant to standard dose temozolomide. *J Neurooncol*. 2010;96(3):393-402.
223. Ren, H, Tan, X, Dong, Y, Giese, A, Chou, TC, Rainov, N, and Yang, B. Differential effect of imatinib and synergism of combination treatment with chemotherapeutic agents in malignant glioma cells. *Basic Clin Pharmacol Toxicol*. 2009;104(3):241-252.
224. Reardon, DA, et al. Safety and pharmacokinetics of dose-intensive imatinib mesylate plus temozolomide: phase 1 trial in adults with malignant glioma. *Neuro Oncol*. 2008;10(3):330-340.
225. Abouantoun, TJ, and MacDonald, TJ. Imatinib blocks migration and invasion of medulloblastoma cells by concurrently inhibiting activation of platelet-derived growth

- factor receptor and transactivation of epidermal growth factor receptor. *Mol Cancer Ther.* 2009;8(5):1137-1147.
226. Pollack, IF, et al. Phase I trial of imatinib in children with newly diagnosed brainstem and recurrent malignant gliomas: a Pediatric Brain Tumor Consortium report. *Neuro Oncol.* 2007;9(2):145-160.
227. Neyns, B, et al. Phase II study of sunitinib malate in patients with recurrent high-grade glioma. *J Neurooncol.* 2010;Epub ahead of print(
228. Batchelor, TT, et al. Phase II study of cediranib, an oral pan-vascular endothelial growth factor receptor tyrosine kinase inhibitor, in patients with recurrent glioblastoma. *J Clin Oncol.* 2010;28(17):2817-2823.
229. Brandes, AA, Stupp, R, Hau, P, Lacombe, D, Gorlia, T, Tosoni, A, Mirimanoff, RO, Kros, JM, and van den Bent, MJ. EORTC study 26041-22041: phase I/II study on concomitant and adjuvant temozolomide (TMZ) and radiotherapy (RT) with PTK787/ZK222584 (PTK/ZK) in newly diagnosed glioblastoma. *Eur J Cancer.* 2010;46(2):348-354.
230. Reardon, DA, Egorin, MJ, Desjardins, A, Vredenburgh, JJ, Beumer, JH, Lagattuta, TF, Gururangan, S, Herndon, JE, 2nd, Salvado, AJ, and Friedman, HS. Phase I pharmacokinetic study of the vascular endothelial growth factor receptor tyrosine kinase inhibitor vatalanib (PTK787) plus imatinib and hydroxyurea for malignant glioma. *Cancer.* 2009;115(10):2188-2198.
231. Hainsworth, JD, Ervin, T, Friedman, E, Priego, V, Murphy, PB, Clark, BL, and Lamar, RE. Concurrent radiotherapy and temozolomide followed by temozolomide and sorafenib in the first-line treatment of patients with glioblastoma multiforme. *Cancer.* 2010;116(15):3663-3669.
232. Reardon, DA, et al. Effect of CYP3A-inducing anti-epileptics on sorafenib exposure: results of a phase II study of sorafenib plus daily temozolomide in adults with recurrent glioblastoma. *J Neurooncol.* 2011;101(1):57-66.
233. Iwamoto, FM, et al. Phase II trial of pazopanib (GW786034), an oral multi-targeted angiogenesis inhibitor, for adults with recurrent glioblastoma (North American Brain Tumor Consortium Study 06-02). *Neuro Oncol.* 2010;12(8):855-861.

234. Mendel, DB, et al. In vivo anti-tumor activity of SU11248, a novel tyrosine kinase inhibitor targeting vascular endothelial growth factor and platelet-derived growth factor receptors: determination of a pharmacokinetic/pharmacodynamic relationship. *Clin Cancer Res.* 2003;9(1):327-337.
235. de Bouard, S, Herlin, P, Christensen, JG, Lemoisson, E, Gauduchon, P, Raymond, E, and Guillamo, JS. Antiangiogenic and anti-invasive effects of sunitinib on experimental human glioblastoma. *Neuro Oncol.* 2007;9(4):412-423.
236. Abouantoun, TJ, Castellino, RC, and MacDonald, TJ. Sunitinib induces PTEN expression and inhibits PDGFR signaling and migration of medulloblastoma cells. *J Neurooncol.* 2011;101(2):215-226.
237. Brastianos, PK, and Batchelor, TT. Vascular endothelial growth factor inhibitors in malignant gliomas. *Target Oncol.* 2010;5(3):167-174.
238. Batchelor, TT, et al. AZD2171, a pan-VEGF receptor tyrosine kinase inhibitor, normalizes tumor vasculature and alleviates edema in glioblastoma patients. *Cancer Cell.* 2007;11(1):83-95.
239. Wood, JM, et al. PTK787/ZK 222584, a novel and potent inhibitor of vascular endothelial growth factor receptor tyrosine kinases, impairs vascular endothelial growth factor-induced responses and tumor growth after oral administration. *Cancer Res.* 2000;60(8):2178-2189.
240. Goldbrunner, RH, Bendszus, M, Wood, J, Kiderlen, M, Sasaki, M, and Tonn, JC. PTK787/ZK222584, an inhibitor of vascular endothelial growth factor receptor tyrosine kinases, decreases glioma growth and vascularization. *Neurosurgery.* 2004;55(2):426-432; discussion 432.
241. Siegelin, MD, Raskett, CM, Gilbert, CA, Ross, AH, and Altieri, DC. Sorafenib exerts anti-glioma activity in vitro and in vivo. *Neurosci Lett.* 2010;478(3):165-170.
242. Yang, F, et al. Sorafenib inhibits signal transducer and activator of transcription 3 signaling associated with growth arrest and apoptosis of medulloblastomas. *Mol Cancer Ther.* 2008;7(11):3519-3526.
243. Yang, F, Brown, C, Buettner, R, Hedvat, M, Starr, R, Scuto, A, Schroeder, A, Jensen, M, and Jove, R. Sorafenib induces growth arrest and apoptosis of human glioblastoma cells

- through the dephosphorylation of signal transducers and activators of transcription 3. *Mol Cancer Ther.* 2010;9(4):953-962.
244. Morris, PG, and Abrey, LE. Novel targeted agents for platelet-derived growth factor receptor and c-KIT in malignant gliomas. *Target Oncol.* 2010;5(3):193-200.
245. Lehky, TJ, Iwamoto, FM, Kreisl, TN, Floeter, MK, and Fine, HA. Neuromuscular junction toxicity with tandutinib induces a myasthenic-like syndrome. *Neurology.* 2011;76(3):236-241.
246. Du, J, et al. Bead-based profiling of tyrosine kinase phosphorylation identifies SRC as a potential target for glioblastoma therapy. *Nat Biotechnol.* 2009;27(1):77-83.
247. Patyna, S, et al. SU14813: a novel multiple receptor tyrosine kinase inhibitor with potent antiangiogenic and anti-tumor activity. *Mol Cancer Ther.* 2006;5(7):1774-1782.
248. Laird, AD, et al. SU6668 is a potent antiangiogenic and anti-tumor agent that induces regression of established tumors. *Cancer Res.* 2000;60(15):4152-4160.
249. Loizos, N, et al. Targeting the platelet-derived growth factor receptor alpha with a neutralizing human monoclonal antibody inhibits the growth of tumor xenografts: implications as a potential therapeutic target. *Mol Cancer Ther.* 2005;4(3):369-379.
250. Shah, GD, Loizos, N, Youssoufian, H, Schwartz, JD, and Rowinsky, EK. Rationale for the development of IMC-3G3, a fully human immunoglobulin G subclass 1 monoclonal antibody targeting the platelet-derived growth factor receptor alpha. *Cancer.* 2010;116(4 Suppl):1018-1026.
251. De Witt Hamer, PC. Small molecule kinase inhibitors in glioblastoma: a systematic review of clinical studies. *Neuro Oncol.* 2010;12(3):304-316.
252. Breedveld, P, Pluim, D, Cipriani, G, Wielinga, P, van Tellingen, O, Schinkel, AH, and Schellens, JH. The effect of Bcrp1 (Abcg2) on the in vivo pharmacokinetics and brain penetration of imatinib mesylate (Gleevec): implications for the use of breast cancer resistance protein and P-glycoprotein inhibitors to enable the brain penetration of imatinib in patients. *Cancer Res.* 2005;65(7):2577-2582.

253. Mukasa, A, Wykosky, J, Ligon, KL, Chin, L, Cavenee, WK, and Furnari, F. Mutant EGFR is required for maintenance of glioma growth in vivo, and its ablation leads to escape from receptor dependence. *Proc Natl Acad Sci U S A*. 2010;107(6):2616-2621.
254. Singh, SK, Clarke, ID, Terasaki, M, Bonn, VE, Hawkins, C, Squire, J, and Dirks, PB. Identification of a cancer stem cell in human brain tumors. *Cancer Res*. 2003;63(18):5821-5828.
255. Hu, X, and Holland, EC. Applications of mouse glioma models in preclinical trials. *Mutat Res*. 2005;576(1-2):54-65.
256. Zhan, Y, Counelis, GJ, and O'Rourke, DM. The protein tyrosine phosphatase SHP-2 is required for EGFRvIII oncogenic transformation in human glioblastoma cells. *Exp Cell Res*. 2009;315(14):2343-2357.
257. Chan, G, Kalaitzidis, D, and Neel, BG. The tyrosine phosphatase Shp2 (PTPN11) in cancer. *Cancer Metastasis Rev*. 2008;27(2):179-192.
258. Tonon, G. From oncogene to network addiction: the new frontier of cancer genomics and therapeutics. *Future Oncol*. 2008;4(4):569-577.
259. Guo, P, Hu, B, Gu, W, Xu, L, Wang, D, Huang, HJ, Cavenee, WK, and Cheng, SY. Platelet-derived growth factor-B enhances glioma angiogenesis by stimulating vascular endothelial growth factor expression in tumor endothelia and by promoting pericyte recruitment. *Am J Pathol*. 2003;162(4):1083-1093.
260. Jarzynka, MJ, Hu, B, Hui, KM, Bar-Joseph, I, Gu, W, Hirose, T, Haney, LB, Ravichandran, KS, Nishikawa, R, and Cheng, SY. ELMO1 and Dock180, a bipartite Rac1 guanine nucleotide exchange factor, promote human glioma cell invasion. *Cancer Res*. 2007;67(15):7203-7211.
261. Sonoda, Y, Kanamori, M, Deen, DF, Cheng, SY, Berger, MS, and Pieper, RO. Overexpression of vascular endothelial growth factor isoforms drives oxygenation and growth but not progression to glioblastoma multiforme in a human model of gliomagenesis. *Cancer Res*. 2003;63(8):1962-1968.
262. Yiin, JJ, Hu, B, Jarzynka, MJ, Feng, H, Liu, KW, Wu, JY, Ma, HI, and Cheng, SY. Slit2 inhibits glioma cell invasion in the brain by suppression of Cdc42 activity. *Neuro Oncol*. 2009;

263. Guo, P, et al. Vascular endothelial growth factor isoforms display distinct activities in promoting tumor angiogenesis at different anatomic sites. *Cancer Res.* 2001;61(23):8569-8577.
264. Yoshida, S, Shimizu, E, Ogura, T, Takada, M, and Sone, S. Stimulatory effect of reconstituted basement membrane components (matrigel) on the colony formation of a panel of human lung cancer cell lines in soft agar. *J Cancer Res Clin Oncol.* 1997;123(6):301-309.
265. Ruan, S, Okcu, MF, Pong, RC, Andreeff, M, Levin, V, Hsieh, JT, and Zhang, W. Attenuation of WAF1/Cip1 expression by an antisense adenovirus expression vector sensitizes glioblastoma cells to apoptosis induced by chemotherapeutic agents 1,3-bis(2-chloroethyl)-1-nitrosourea and cisplatin. *Clin Cancer Res.* 1999;5(1):197-202.
266. Stallcup, WB, and Huang, FJ. A role for the NG2 proteoglycan in glioma progression. *Cell Adh Migr.* 2008;2(3):192-201.
267. Ishii, N, Maier, D, Merlo, A, Tada, M, Sawamura, Y, Diserens, AC, and Van Meir, EG. Frequent co-alterations of TP53, p16/CDKN2A, p14ARF, PTEN tumor suppressor genes in human glioma cell lines. *Brain Pathol.* 1999;9(3):469-479.
268. Wiedemeyer, WR, et al. Pattern of retinoblastoma pathway inactivation dictates response to CDK4/6 inhibition in GBM. *Proc Natl Acad Sci U S A.* 2010;107(25):11501-11506.
269. Fraser, M, Bai, T, and Tsang, BK. Akt promotes cisplatin resistance in human ovarian cancer cells through inhibition of p53 phosphorylation and nuclear function. *Int J Cancer.* 2008;122(3):534-546.
270. Calzolari, F, and Malatesta, P. Recent insights into PDGF-induced gliomagenesis. *Brain Pathol.* 2010;20(3):527-538.
271. Rosenkranz, S, DeMali, KA, Gelderloos, JA, Bazenet, C, and Kazlauskas, A. Identification of the receptor-associated signaling enzymes that are required for platelet-derived growth factor-AA-dependent chemotaxis and DNA synthesis. *J Biol Chem.* 1999;274(40):28335-28343.
272. Van Stry, M, Kazlauskas, A, Schreiber, SL, and Symes, K. Distinct effectors of platelet-derived growth factor receptor-alpha signaling are required for cell survival during embryogenesis. *Proc Natl Acad Sci U S A.* 2005;102(23):8233-8238.

273. Zou, GM, Chan, RJ, Shelley, WC, and Yoder, MC. Reduction of Shp-2 expression by small interfering RNA reduces murine embryonic stem cell-derived in vitro hematopoietic differentiation. *Stem Cells*. 2006;24(3):587-594.
274. Wu, CJ, O'Rourke, DM, Feng, GS, Johnson, GR, Wang, Q, and Greene, MI. The tyrosine phosphatase SHP-2 is required for mediating phosphatidylinositol 3-kinase/Akt activation by growth factors. *Oncogene*. 2001;20(42):6018-6025.
275. Zhan, Y, Counelis, GJ, and O'Rourke, DM. The protein tyrosine phosphatase SHP-2 is required for EGFRvIII oncogenic transformation in human glioblastoma cells. *Exp Cell Res*. 2009;315(14):2343-2357.
276. Abdelnour-Berchtold, E, Cerantola, Y, Roulin, D, Dormond-Meuwly, A, Demartines, N, and Dormond, O. Rapamycin-mediated FOXO1 inactivation reduces the anticancer efficacy of rapamycin. *Anticancer Res*. 2010;30(3):799-804.
277. Lu, W, Gong, D, Bar-Sagi, D, and Cole, PA. Site-specific incorporation of a phosphotyrosine mimetic reveals a role for tyrosine phosphorylation of SHP-2 in cell signaling. *Mol Cell*. 2001;8(4):759-769.
278. Dupuy, AJ, Akagi, K, Largaespada, DA, Copeland, NG, and Jenkins, NA. Mammalian mutagenesis using a highly mobile somatic Sleeping Beauty transposon system. *Nature*. 2005;436(7048):221-226.
279. Collier, LS, Carlson, CM, Ravimohan, S, Dupuy, AJ, and Largaespada, DA. Cancer gene discovery in solid tumours using transposon-based somatic mutagenesis in the mouse. *Nature*. 2005;436(7048):272-276.
280. Wu, A, Oh, S, Ericson, K, Demorest, ZL, Vengco, I, Gharagozlou, S, Chen, W, Low, WC, and Ohlfest, JR. Transposon-based interferon gamma gene transfer overcomes limitations of episomal plasmid for immunogene therapy of glioblastoma. *Cancer Gene Ther*. 2007;14(6):550-560.
281. Ohlfest, JR, et al. Combinatorial antiangiogenic gene therapy by nonviral gene transfer using the sleeping beauty transposon causes tumor regression and improves survival in mice bearing intracranial human glioblastoma. *Mol Ther*. 2005;12(5):778-788.
282. Carlson, CM, Frandsen, JL, Kirchhof, N, McIvor, RS, and Largaespada, DA. Somatic integration of an oncogene-harboring Sleeping Beauty transposon models liver tumor development in the mouse. *Proc Natl Acad Sci U S A*. 2005;102(47):17059-17064.

283. Fujita, M, Kohanbash, G, Fellows-Mayle, W, Hamilton, RL, Komohara, Y, Decker, SA, Ohlfest, JR, and Okada, H. COX-2 Blockade Suppresses Gliomagenesis by Inhibiting Myeloid-Derived Suppressor Cells. *Cancer Res.* 2011;
284. Khattab, AZ, Ahmed, MI, Fouad, MA, and Essa, WA. Significance of p53 and CD31 in astroglomas. *Med Oncol.* 2009;26(1):86-92.
285. Mayo, LD, and Donner, DB. The PTEN, Mdm2, p53 tumor suppressor-oncoprotein network. *Trends Biochem Sci.* 2002;27(9):462-467.
286. Matozaki, T, Murata, Y, Saito, Y, Okazawa, H, and Ohnishi, H. Protein tyrosine phosphatase SHP-2: a proto-oncogene product that promotes Ras activation. *Cancer Sci.* 2009;100(10):1786-1793.
287. Chan, G, Kalaitzidis, D, and Neel, BG. The tyrosine phosphatase Shp2 (PTPN11) in cancer. *Cancer Metastasis Rev.* 2008;27(2):179-192.
288. Navis, AC, van den Eijnden, M, Schepens, JT, Hooft van Huijsduijnen, R, Wesseling, P, and Hendriks, WJ. Protein tyrosine phosphatases in glioma biology. *Acta Neuropathol.* 2010;119(2):157-175.
289. Cerami, E, Demir, E, Schultz, N, Taylor, BS, and Sander, C. Automated network analysis identifies core pathways in glioblastoma. *PLoS One.* 2010;5(2):e8918.
290. Udani, VM, Santarelli, JG, Yung, YC, Wagers, AJ, Cheshier, SH, Weissman, IL, and Tse, V. Hematopoietic stem cells give rise to perivascular endothelial-like cells during brain tumor angiogenesis. *Stem Cells Dev.* 2005;14(5):478-486.
291. Bababeygy, SR, Cheshier, SH, Hou, LC, Higgins, DM, Weissman, IL, and Tse, VC. Hematopoietic stem cell-derived pericytic cells in brain tumor angio-architecture. *Stem Cells Dev.* 2008;17(1):11-18.
292. Ashworth, A, Lord, CJ, and Reis-Filho, JS. Genetic interactions in cancer progression and treatment. *Cell.* 2011;145(1):30-38.
293. Zheng, H, et al. p53 and Pten control neural and glioma stem/progenitor cell renewal and differentiation. *Nature.* 2008;455(7216):1129-1133.

294. Qiu, W, Wu, B, Wang, X, Buchanan, ME, Regueiro, MD, Hartman, DJ, Schoen, RE, Yu, J, and Zhang, L. PUMA-mediated intestinal epithelial apoptosis contributes to ulcerative colitis in humans and mice. *J Clin Invest.* 2011;121(5):1722–1732.
295. Stock, P, Monga, D, Tan, X, Micsenyi, A, Loizos, N, and Monga, SP. Platelet-derived growth factor receptor-alpha: a novel therapeutic target in human hepatocellular cancer. *Mol Cancer Ther.* 2007;6(7):1932-1941.
296. Russell, MR, Liu, Q, and Fatatis, A. Targeting the {alpha} receptor for platelet-derived growth factor as a primary or combination therapy in a preclinical model of prostate cancer skeletal metastasis. *Clin Cancer Res.* 2010;16(20):5002-5010.
297. Karsy, M, Albert, L, Tobias, ME, Murali, R, and Jhanwar-Uniyal, M. All-trans retinoic acid modulates cancer stem cells of glioblastoma multiforme in an MAPK-dependent manner. *Anticancer Res.* 2010;30(12):4915-4920.